Improved QCD Sum Rules for the Nucleon

Diploma Thesis by

Bernhard Langwallner

September 2005

Technische Universität München
Physik-Department
T39 (Prof. Dr. Wolfram Weise)

Contents

Chapter 1

Introduction

Quantum Chromo Dynamics (QCD) is the accepted fundamental theory of strong interactions. It describes the interplay of quarks and gluons which constitute hadronic matter. Since QCD is a non-abelian gauge theory its coupling depends strongly on the momentum scale at which it is probed. Whereas it is small in processes involving high energy or momentum transfer allowing for perturbative treatment (asymptotic freedom), the coupling strength becomes large at typical hadronic scales ($\mu \lesssim 1\,\mathrm{GeV}$). As a consequence, quarks and gluons cannot be observed freely, but only as bound in hadrons. This property of QCD is called confinement.
It is a challenging issue to derive the properties of hadrons from the fundamental theory QCD. However, due to the high complexity of QCD – especially confinement – a straightforward derivation of hadronic observables, such as masses, is not possible. Consequently, various alternative methods have been developped. A successful approach is provided by Chiral Effective Field Theories, where the fundamental degrees of freedom of QCD are exchanged for hadronic degrees of freedom, for which all possible interactions are allowed and parameterized. These parameters have to be determined from experiments.
Another strategy is a sophisticated discretization of QCD on Euclidean space time – Lattice QCD. Because of the huge number of degrees of freedem included in QCD (quarks and gluons of different flavours and colours) the practicable grid sizes are restricted. A way to circumvent the disadvantages of small lattices (i.e. small number of lattice points and big lattice spacing) is to make quark masses unnaturally large. Over the last decades many calculations of the nucleon mass in Lattice QCD have been performed yielding a trend for its dependence on the valence quark mass. This dependence can also be studied by Chiral Perturbation Theory giving an expression for the nucleon mass M_{N} in terms of the pion mass m_π, which is directly related to the quark mass m_q. A third alternative for the prediction of hadronic observables (especially masses) which is more closely related to QCD itself, is the method of QCD sum rules [4]. QCD sum rules rely upon an interpolation between the microscopic world of QCD and the hadronic sector. The central subject of study is the so called correlation function

$$\Pi(q) = i \int d^4x \; e^{iq\cdot x} \langle 0|T\{\eta(x)\bar{\eta}(0)\}|0\rangle$$

which is reminiscent of a hadronic propagator including an interpolating field $\eta(x)$ as a substitute for a hadron wave function. The strategy is to interpret this object in two completely different ways. On the one hand it is identified with a hadronic propagator, and on the other hand the

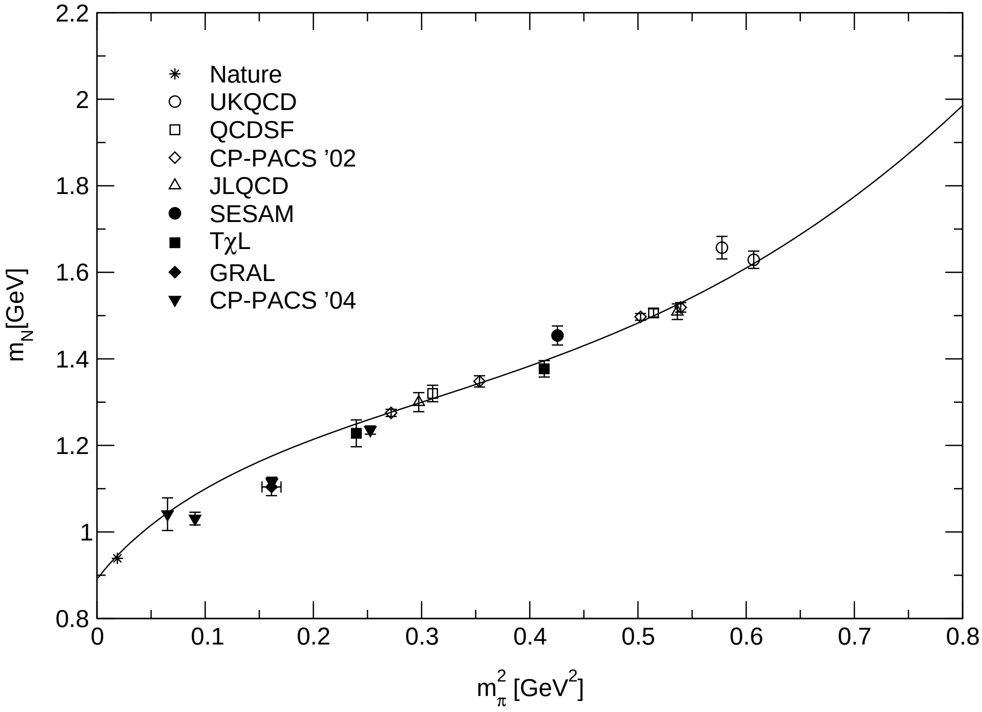

Figure 1.1: The dependence of the nucleon mass on the quark mass from various Lattice QCD calculations and Chiral Perturbation Theory [1] (solid line). Graphic taken from [2]

quark structure of the interpolating field is used to establish contact with quarks, gluons, and the vacuum structure of QCD. An advantage of QCD sum rules is that there are no additional parameters like in Chiral Perturbation Theory. Admittedly, the precision of the results is limited. A famous QCD sum rule result is given by Ioffe's formula for the nucleon mass [5]:

$$M_{\rm N} = -\frac{8\pi^2}{M^2}\langle \bar{q}q\rangle + \ldots \tag{1.1}$$

where M is the so called Borel mass and $\langle \bar{q}q\rangle \approx (-240\,\mathrm{MeV})^3$ is the chiral condensate. Setting $M \approx 1\,\mathrm{GeV}$ one finds $M_{\rm N} \approx 1\,\mathrm{GeV}$. This formula demonstrates the importance of QCD vacuum parameters for hadronic observables.

The aim of this thesis is to extend known nucleon sum rules to the region of higher quark masses like the ones used in present Lattice QCD simulations. The goal is to achieve an independent cross-check to Lattice QCD and Chiral Perturbation Theory without introducing new parameters.

This thesis is structured as follows:

- Chapter 2 reviews some basic facts about QCD. The focus is on chiral symmetry and its spontaneous breaking which leads to a vacuum structure that is crucial for QCD sum rules.
- Chapter 3 introduces the method of QCD sum rules. The fundamental techniques are discussed in some detail leading the way towards the extension to higher quark masses. These techniques are dispersion relations on the hadronic level and the Operator Product Expansion on the quark level.
- In Chapter 4 we set up the main ingredient needed for the derivation of QCD sum rules, which is the so called background field propagator. This propagator is expanded in the quark mass up to order three which should be sufficient for the studied region of quark masses.
- In Chapter 5 the sum rules for the well known nucleon interpolating fields are derived and analysed. A central topic is the method of analysis that is used to get reliable results as well as uncertainties coming from the rather large errors in the QCD input parameters.
- Chapter 6 treats sum rules based on unconventional tensor fields for the nucleon. Compared to the spin-1/2 case, these fields have major advantages. The chapter ends with a combined analysis of the one relible spin-1/2 sum rule and the two convenient tensor sum rules.
- Chapter 7 is dedicated to a detailed treatment of four quark condensates. The prominent but rather vague vacuum saturation hypothesis is discarded and pionic degrees of freedom are explicitly considered.
- The thesis finishes with a summary and outlook. In the Appendix, we derive an efficient machinery for the calculation of special types of Fourier integrals and Borel transforms needed for the derivation of the Operator Product Expansions of the various fields. The last part lists formulas frequently used throughout the calculations.

Chapter 2

Basics of QCD

2.1 The QCD Lagrangian

QCD is a gauge field theory based on a local SU(3) gauge symmetry describing the interaction of massive spin-$\frac{1}{2}$ particles (quarks) with massless spin-1 gauge bosons (gluons). Due to the non-abelian character of SU(3) the gauge bosons interact with each other. The QCD-Lagrangian is

$$\mathscr{L} = \bar{\psi}(iD_\mu\gamma^\mu - \tilde{m})\psi - \frac{1}{2}\mathrm{Tr}\; G_{\mu\nu}G^{\mu\nu} \tag{2.1}$$

where $\tilde{m}$ is the mass matrix, $G_{\mu\nu}$ is the gluonic field strength tensor

$$G_{\mu\nu} = \partial_\mu A_\nu^B t^B - \partial_\nu A_\mu^B t^B + g_s f_{ABC} A_\mu^A A_\nu^B t^C = \frac{i}{g_s}[D_\mu, D_\nu], \tag{2.2}$$

and

$$D_\mu = \partial_\mu - ig_s A_\mu^B t^B$$

the covariant derivative. The matrices $t^B = \lambda^B/2, (B = 1, 2, \dots, 8)$ (λ^B being the Gell-Mann matrices) are the generators of the group SU(3). They satisfy the following relations

$$[t^A, t^B] = if^{ABC}t^C, \qquad \mathrm{Tr}(t^A) = 0, \qquad \mathrm{Tr}(t^A t^B) = \frac{1}{2}\delta_{AB}.$$

The f_{ABC} are the totally antisymmetric structure constants of SU(3). The field ψ unites the fields of the six quark species divided into the light quark sector (u-, d-, and s-quark) and the heavy quark sector (c-, b-, and t-quark). The two lightest quarks are u and d with masses of $m_u \simeq 4\,\mathrm{MeV}$ and $m_d \simeq 8\,\mathrm{MeV}$ (at a renormalization scale of $\sim 1\,\mathrm{GeV}$). In the present thesis, physics including heavier quarks is neglected, so we restrict ourselves to the u- and d-quark. Hence, the field $\psi(x)$ and the mass matrix $\tilde{m}$ reduce to

$$\psi(x) = \begin{pmatrix} u(x) \\ d(x) \end{pmatrix}, \qquad \tilde{m} = \begin{pmatrix} m_u & \\ & m_d \end{pmatrix}$$

Here, $u(x)$ and $d(x)$ are triplets in color space :

$$u(x) = \begin{pmatrix} u_R(x) \\ u_G(x) \\ u_B(x) \end{pmatrix}$$

One fundamental property of QCD is the momentum scale dependence of the coupling strength $\alpha_s = g_s^2/4\pi$. At high energies, $\alpha_s(Q^2)$ is small, allowing for perturbation theory in α_s. This phenomenon is called asymptotic freedom. On the other hand, for $Q^2 \lesssim 1\,\mathrm{GeV}$ α_s strongly increases - perturbative treatment is thus completely impossible. This rise of the coupling constant leads to confinement, the fact that colored quarks and gluons are not visible degrees of freedom. They are bound in color neutral states, the hadrons. In lack of a possibility to solve QCD analytically at low energies, alternative methods have to be found, such as Lattice simulations, chiral perturbation theory or QCD sum rules.

2.2 Symmetries

Apart from the gauge symmetry SU(3) the QCD Lagrangian (2.1) exhibits a global U(1) symmetry $\psi \mapsto e^{i\theta}\psi(x)$. Noether's theorem then yields a conserved quantity: the baryon number

$$B = \frac{1}{3}\int d^3x \psi^\dagger(x)\psi(x).$$

In the limit $m_u, m_d \to 0$, which is a good approximation in most cases, even more symmetries are provided. To extract the most important one, chiral symmetry, we decompose the u-, and d-quark fields into parts with different chirality:

$$\begin{pmatrix} u \\ d \end{pmatrix}_L = \frac{1-\gamma_5}{2}\begin{pmatrix} u \\ d \end{pmatrix}, \qquad \begin{pmatrix} u \\ d \end{pmatrix}_R = \frac{1+\gamma_5}{2}\begin{pmatrix} u \\ d \end{pmatrix}$$

$$\psi = \begin{pmatrix} u \\ d \end{pmatrix} = \begin{pmatrix} u \\ d \end{pmatrix}_L + \begin{pmatrix} u \\ d \end{pmatrix}_R = \psi_L + \psi_R$$

When inserting this decomposition into eq. (2.1) it is observed that only terms involving the mass matrix mix the left- and right-handed parts:

$$\bar\psi(i\not{D} - \tilde m)\psi = \bar\psi_L i\not{D}\psi_L + \bar\psi_R i\not{D}\psi_R - \bar\psi_R\tilde m\psi_L - \bar\psi_L\tilde m\psi_R$$

In the so called chiral limit $\tilde m \to 0$, (2.1) is therefore invariant under separate SU(2) transformations in flavor space

$$\begin{pmatrix} u \\ d \end{pmatrix}_L \mapsto U_L\begin{pmatrix} u \\ d \end{pmatrix}_L, \qquad \begin{pmatrix} u \\ d \end{pmatrix}_R \mapsto U_R\begin{pmatrix} u \\ d \end{pmatrix}_R$$

The Noether currents corresponding to this symmetry are

$$j_L^{\mu k} = \bar\psi_L\gamma^\mu\frac{\tau^k}{2}\psi_L \quad \text{and} \quad j_R^{\mu k} = \bar\psi_R\gamma^\mu\frac{\tau^k}{2}\psi_R$$

where the $\tau^k, k = 1,2,3$ are the Pauli matrices. The vector and axial vector current are defined by certain linear combinations:

$$j_V^{\mu k} = j_L^{\mu k} + j_R^{\mu k} = \bar\psi\gamma^\mu\frac{\tau^k}{2}\psi$$

$$j_A^{\mu k} = j_L^{\mu k} - j_R^{\mu k} = \bar\psi\gamma^\mu\gamma_5\frac{\tau^k}{2}\psi$$

If the symmetry $SU(2)_L\times SU(2)_R$ were realized trivially, all particles would exist in parity doublets. However, the lightest pseudoscalar mesons (negative parity) have much smaller masses than the lightest scalar mesons (positive parity). One concludes that the axial symmetry $SU(2)_A$ related to $j_A^{\mu k}$ is spontaneously broken. Goldstone's theorem states that in a quantum field theory every spontaneously broken global symmetry leads to massless particles with the same quantum numbers as the generators of the broken symmetry. In the case of $SU(2)_A$ these particles are the three pions. Since the chiral symmetry is also broken explicitly due to the finite quark masses, the pions acquire finite masses, too. The same arguments hold when the s-quark is included. The symmetry then is $SU(3)_L\times SU(3)_R$, $SU(3)_A$ being spontaneously broken.

2.3 The Chiral Condensate

Spontaneous chiral symmetry breaking rearranges the vacuum; it is not perturbative like in QED but populated with scalar quark-antiquark pairs, meaning that their density has finite expectation value:

$$\langle 0|\bar{\psi}\psi|0\rangle = \langle 0|\bar{\psi}_L\psi_R + \bar{\psi}_R\psi_L|0\rangle = \langle 0|\bar{u}u + \bar{d}d + \bar{s}s|0\rangle \neq 0. \tag{2.3}$$

The precise definition is given by:

$$\langle 0|\bar{\psi}\psi|0\rangle = -\mathrm{Tr}\lim_{y\to x^+}\langle 0|T\{\psi(x)\bar{\psi}(y)\}|0\rangle.$$

$\langle 0|\bar{\psi}\psi|0\rangle$ is called chiral (or quark) condensate or quark condensate and represents the order parameter for spontaneous chiral symmetry breaking, because $\bar{\psi}\psi = \bar{\psi}_L\psi_R + \bar{\psi}_R\psi_L$ mixes quarks with different chirality.

The chiral condensate is connected to the pion decay constant f_0 in the chiral limit and the quark and pion masses via the Gell-Mann–Oakes-Renner (GOR) relation [3]:

$$m_\pi^2 = -\frac{1}{f_0^2}(m_u + m_d)\langle \bar{u}u + \bar{d}d\rangle + \mathcal{O}(m_{u,d}^2)$$

The presence of $m_{u,d}$ in this equation indicates the amount of explicit chiral symmetry breaking. The pion mass vanishes in the chiral limit $m_{u,d}\to 0$. Small corrections to f_0 yield the physical pion decay constant $f_\pi = 92.4\,\mathrm{MeV} = f_0 + \mathcal{O}(m_{u,d})$. Thus, the GOR relation can be written as:

$$m_\pi^2 = -\frac{1}{f_\pi^2}(m_u + m_d)\langle \bar{u}u + \bar{d}d\rangle + \mathcal{O}(m_{u,d}^2) \tag{2.4}$$

Setting $m_u + m_d \simeq 12\,\mathrm{MeV}$ leads to a quark condensate of $\langle \bar{q}q\rangle \equiv \langle \bar{u}u\rangle = \langle \bar{d}d\rangle \simeq -(239\,\mathrm{MeV})^3$.

2.4 Notations and Conventions

Throughout this thesis we shall use natural units $\hbar = c = 1$. Summation is applied on double indices. For indices and vectors we use the following notations:

- Capital latin letters A, B, C, D denote indices running from 1 to 8, i.e. gluon indices

- Small latin letters a, b, c denote color indices and run from 1 to 3
- Small greek letters $\alpha, \beta, \mu, \nu = 0, 1, 2, 3$ denote Lorentz indices
- Bold face letters $\mathbf{q}, \mathbf{x}, ...$ denote three vectors
- Barred letters $\bar{x}, \bar{q}$ denote Euclidean vectors
- For all operators A, B, ..., $\langle AB \ldots \rangle$ is understood as a vacuum expectation value:

$$\langle AB \ldots \rangle \equiv \langle 0 | AB \ldots | 0 \rangle$$

Chapter 3

QCD Sum Rules

In this section we introduce the technique of QCD sum rules, with particular focus on sum rules for the nucleon. We give a short overview of the strategy behind this technique and address the two major ingredients: dispersion relations and the operator product expansion. Finally, the easiest sum rules for the nucleon which will be extended throughout this thesis, are given as examples.

3.1 Introduction

QCD sum rules were developed by M.A. Shifman, A.I. Vainshtein, and V.I. Zhakarov in [4] for mesons and extended to baryons by Ioffe [5]. In principle, sum rules attempt to interpolate between the two limits of QCD: the quark-gluon sector at high energies and the hadron sector at low energies. The goal is to extract hadronic observables (e.g. masses, coupling constants etc.) from microscopic QCD parameters such as condensates (eq. (2.3)) or quark masses. Since the quark condensate is connected to spontaneous chiral symmetry breaking, its appearance in sum rules can give an indication of the role of the chiral symmetry breaking pattern in the determination of hadronic observables. The central object is the so called correlation function or correlator

$$\Pi(q) = i \int d^4x \; e^{iq\cdot x} \langle 0|T\{\eta(x)\bar{\eta}(0)\}|0\rangle. \tag{3.1}$$

Here $\eta(x)$ is a current built from quark fields and Dirac gamma matrices and $|0\rangle$ is an appropriate ground state (usually vacuum or nuclear matter). The singularities of $\Pi(q)$ for $q^2 > 0$ are associated with hadronic excitations with the quantum numbers of η. An example is the famous current for the nucleon introduced by Ioffe [5]:

$$\eta(x) = \varepsilon_{abc} \left[u^{aT}(x) C \gamma_\mu u^b(x) \right] \gamma_5 \gamma^\mu d^c(x) \tag{3.2}$$

where $a, b, c \in \{\text{red}, \text{green}, \text{blue}\}$ are color indices. The part in parentheses is a diquark which is then coupled to the d-quark. Clearlu, $\Pi(q)$ is a matrix in the case of the nucleon. The ε-tensor is introduced to make the current a color singlet. A possibility to interpolate between the two limits of QCD emerges if one interprets the correlation function in two different ways. On the one hand the field $\eta(x)$ is identified with the nucleon spinor, not resolving the quark structure of η in detail.

What remains resembles the well known fermionic propagator plus a contribution from higher energy excitations in the nucleon channel. This hadronic interpretation will be implemented via dispersion relations.
On the other hand the quark structure of η is used to make contact with the quark-gluon regime. Here, an operator product expansion will be constructed for the time ordered product, which contains QCD parameters. Finally, both versions of the correlator, although valid in extremely different energy regimes, will be equated making use of a Borel transform, assuming that a region of overlap exists. The results are quantitative predictions for spectral properties of the leading particle. The approach works for hadrons of either spin or isospin.

3.2 Physics and Phenomenology of the Correlator

The correlator $\Pi(q)$ describes the propagation of a baryon with the quantum numbers of the field η [6]. To see this, define spectral functions ρ and $\bar{\rho}$ appropriate to the two time orderings in (3.1):

$$\begin{aligned}\rho_{\alpha\beta} &\equiv \frac{1}{2\pi}\int d^4x\; e^{iq\cdot x}\langle 0|\eta_\alpha(x)\bar{\eta}_\beta(0)|0\rangle \\ \bar{\rho}_{\alpha\beta} &\equiv \frac{1}{2\pi}\int d^4x\; e^{iq\cdot x}\langle 0|\bar{\eta}_\beta(0)\eta_\alpha(x)|0\rangle\end{aligned}$$

We assume a dispersion relation for Π (ignoring any subtractions assuring convergence)

$$\Pi_{\alpha\beta}(q) = -\int_{-\infty}^{\infty} dq_0' \left(\frac{\rho_{\alpha\beta}(q')}{q_0 - q_0' + i\varepsilon} + \frac{\bar{\rho}_{\alpha\beta}(q')}{q_0 - q_0' - i\varepsilon}\right) \tag{3.3}$$

and insert a complete set of intermediate states (analogous for $\bar{\rho}$, but with $\delta^{(4)}(q+P_n)$):

$$\rho_{\alpha\beta}(q) = (2\pi)^3 \sum_n \delta^{(4)}(q-P_n)\langle 0|\eta_\alpha(0)|n\rangle\langle n|\bar{\eta}_\beta(0)|0\rangle.$$

So spectral functions measure the intensity at which energy is absorbed from the current at different frequencies. Lorentz covariance and parity invariance give a decomposition for the spectral functions

$$\rho_{\alpha\beta}(q) = \rho_s(q^2)\delta_{\alpha\beta} + \rho_q(q^2)\not{q}_{\alpha\beta} \tag{3.4}$$

which imply a similar decomposition for $\Pi(q)$

$$\Pi(q) = i\int d^4x\; e^{iq\cdot x}\langle 0|T\{\eta(x)\bar{\eta}(0)\}|0\rangle = \Pi_s(q^2)\mathbb{1} + \Pi_q(q^2)\;\not{q} \tag{3.5}$$

$\Pi_s(q^2)$ and $\Pi_q(q^2)$ are called invariant functions. Charge conjugation invariance in vacuum provides the equality of $\rho_i(q^2)$ and $\bar{\rho}_(q^2)$ ($i \in \{s,q\}$) up to a sign. So the integral over energy in (3.3) can be transformed to one over $q'^2 = s$, which gives a dispersion relation for each invariant function

$$\Pi_i(q^2) = \int_0^\infty ds \frac{\rho_i(s)}{s-q^2} + \text{polynomial} \tag{3.6}$$

The spectral form of the correlator can be evaluated by introducing a phenomenological model for the spectral densities ρ_i. It will be decomposed into the part coming from the nucleon pole and the part from the continuum $\rho_i = \rho_i^{\text{pole}} + \rho_i^{\text{cont}}$. The lowest energy contribution comes from the nucleon pole. Therefore we define the matrix element:

$$\langle 0|\eta(0)|N(q)\rangle = \lambda_N u(q) \tag{3.7}$$

where $|N\rangle$ is a nucleon state with four momentum q ($q^2 = M_{\text{N}}^2$) and $u(q)$ is a Dirac spinor for the nucleon. The phenomenological model of the correlator is then constructed inspired by the Feynman propagator

$$\Pi^{\text{phen}}(q) = -\lambda_N^2 \frac{\not{q} + M_{\text{N}}}{q^2 - M_{\text{N}}^2 + i\varepsilon} + \text{continuum}$$

which immediately provides models for the two invariant functions

$$\Pi_s^{\text{phen}}(q^2) = -\lambda_N^2 \frac{M_{\text{N}}}{q^2 - M_{\text{N}}^2 + i\varepsilon} + \text{continuum},$$
$$\Pi_q^{\text{phen}}(q^2) = -\lambda_N^2 \frac{1}{q^2 - M_{\text{N}}^2 + i\varepsilon} + \text{continuum}.$$

For the spectral densities ρ_i this means:

$$\rho_s^{\text{phen}}(s) = \lambda_N^2 M_{\text{N}} \delta(s - M_{\text{N}}^2) + \rho_s^{\text{cont}}(s) \equiv \rho_s^{\text{pole}} + \rho_s^{\text{cont}}(s), \tag{3.8}$$
$$\rho_q^{\text{phen}}(s) = \lambda_N^2 \delta(s - M_{\text{N}}^2) + \rho_q^{\text{cont}}(s) \equiv \rho_q^{\text{pole}} + \rho_q^{\text{cont}}(s). \tag{3.9}$$

The precise form of the continuum distributions ρ_s^{cont} and ρ_s^{cont} is motivated by the microscopic interpretation of the correlation function (3.1) and is given in section 3.5.

3.3 The Background Field Method and Fixed Point Gauge

In calculating QCD sum rules one has to cope with the nontrivial vacuum structure of QCD (chiral condensate etc.). A convenient way of doing this is the so called background field method. The presence of condensates of different type, i.e. quarks and gluons, is parametrized by introducing classical (non-quantized) Grassmann quark fields $\chi_{a\alpha}^q, \bar{\chi}_{b\beta}^q$ and classical gluonic fields $F_{\mu\nu}^A$. For classical fields one has simple Feynman-rules, which are used in evaluating the diagrams needed for the derivation of the sum rules. The main advantage of the background field method is that having introduced these classical fields, the QCD vacuum degenerates to a purely perturbative one in a technical sense, as will be seen in section 3.4.

Since the color degree of freedom is hidden in hadrons, the interpolating fields are colorless, too (see in eq. (3.2)), and the correlator is gauge-invariant. Thus one can use the freedom of gauge to simplify calculations. A prominent and practical gauge is the fixed-point or Fock-Schwinger gauge [7, 8], which was originally invented for use in QED and later extended to QCD in [9, 10, 11]. The gauge condition is given by:

$$x^\mu A_\mu^B(x) = 0$$

The main advantage is that the gluon fields $A^B(x)$ can be expressed directly in terms of the field tensor $G_{\mu\nu}^B(x)$:

$$A_\mu^B(x) = \int_0^1 d\alpha\ \alpha x^\nu G_{\nu\mu}^B(\alpha x)$$

The proof will be given now. Beginning with an obvious identity we get:

$$\begin{aligned} A_\mu^B(y) &= \partial_\mu(y^\nu A_\nu^B(y)) - y^\nu \partial_\mu A_\nu^B(y) \\ &= 0 - y^\nu G_{\mu\nu}^B(y) - y^\nu \partial_\nu A_\mu^B(y) \end{aligned}$$

Setting $y = \alpha x$ and rearranging gives

$$\alpha x^\nu G_{\nu\mu}^B(\alpha x) = A_\mu^B(\alpha x) + \alpha x^\nu \frac{\partial A_\mu^B(\alpha x)}{\partial(\alpha x^\nu)} = \frac{d}{d\alpha}(\alpha A_\mu^B(\alpha x))$$

Integrating shows eq. (3.3). Expanding this equation we arrive at:

$$A_\mu(x) = \frac{1}{2} x^\nu G_{\nu\mu}(0) + \frac{1}{3} x^\lambda x^\nu D_\lambda G_{\nu\mu}(0) + \frac{1}{8} x^\kappa x^\lambda x^\nu D_\kappa D_\lambda G_{\nu\mu}(0) + \dots \tag{3.10}$$

where $G_{\nu\mu} = G_{\nu\mu}^B t^B$, $A_\mu = A_\mu^B t^B$, and $D_\mu \equiv \partial_\mu - i g_s A_\mu$.
Another feature of the fixed point gauge is that it offers a gauge invariant Taylor expansion of quark fields, which will be useful in the derivation of the background field propagator. We start with an ordinary expansion of an arbitrary quark field $q(x)$

$$q(x) = q(0) + x^\mu (\partial_\mu q)_{x=0} + \frac{1}{2} x^\mu x^\nu (\partial_\mu \partial_\nu q)_{x=0} + \dots$$

Replacing $x^\mu \partial_\mu$ by $x^\mu D_\mu = x^\mu(\partial_\mu - i g_s A_\mu)$ (with $A_\mu = \lambda^A/2 A_\mu^A$) we can then write

$$q(x) = q(0) + x^\mu (D_\mu q)_{x=0} + \frac{1}{2} x^\mu x^\nu (D_\mu D_\nu q)_{x=0} + \dots \tag{3.11}$$

which is gauge-invariant. The quark fields satisfy the Dirac equation with the background gluon field in the covariant derivative $D_\mu = \partial_\mu - i g_s A_\mu$, $\overleftarrow{D}_\mu = \overleftarrow{\partial}_\mu + i g_s A_\mu$:

$$(i\not{D} - m_q) q(x) = 0 \qquad \bar{q}(x)(i\overleftarrow{\not{D}} + m_q) = 0$$

The following relations allow an easy determination of the covariant derivatives:

$$\begin{aligned} \not{D} q &= -i m_q q \\ [D^\mu, D^\nu] &= -i g_s G^{\mu\nu} \\ D^2 q &= \frac{1}{2} g_s \sigma_{\mu\nu} G^{\mu\nu} q + m_q^2 q \equiv \frac{1}{2} g_s \sigma \cdot G q + m_q^2 q \end{aligned} \tag{3.12}$$

where we have used the Dirac equation, eq. (2.2), and $i\sigma_{\mu\nu} = g_{\mu\nu} - \gamma_\mu \gamma_\nu$.

3.4 Operator Product Expansion

The high energy interpretation of the correlator (3.1) is found by applying an Operator Product Expansion (OPE). The OPE is an expansion of a time ordered product of two local operators (one at x and one at 0) in a set of local operators (ordered by their dimension). The OPE in pure perturbation theory was developped in [12]. The generic form of an OPE is:

$$T\{A(x)B(0)\} = \sum_n C_n^{AB}(x)\hat{O}_n(0) \quad (\text{ for } x \to 0), \tag{3.13}$$

where the C_n^{AB} are functions called Wilson Coefficients and the O_n are (composite) field operators. The strategy of the OPE is that the singularities in a time ordered product for $x \to 0$ are factored out to the Wilson coefficients (in the form of inverse powers of x^2) and the operators are well defined. In QCD the purely perturbative expansion is a priori no longer valid due to nonperturbative effects. It was shown in [13, 14] that to apply OPE beyond perturbation theory the operators and Wilson coefficients have to be defined at a normalization point μ:

$$T\{A(x)B(0)\} = \sum_n C_n^{AB}(x,\mu)\hat{O}_n(0,\mu) \quad (\text{ for } x \to 0).$$

Here, physics of momenta above μ is absorbed in the C_n^{AB}, and physics below μ in $\hat{O}_n$. In QCD sum rule calculations a simplified version is usually applied: perturbation theory is used for the coefficients whereas all nonperturbative effects are put in the vacuum expectation values of operators. This simplification is justified by the success of QCD sum rules. A reason is that there seems to be a range in which μ is sufficiently large that non-perturbative corrections to the coefficients can be neglected and at the same time μ is small enough so that the expectation values of operators (=condensates) are insensitive to μ.
All in all, after Fourier transform the OPE correlator takes the form

$$\Pi^{\mathrm{OPE}}(q^2) = \sum_n C_n(q^2)\langle\hat{O}_n\rangle \qquad \text{where } \langle\hat{O}_n\rangle \equiv \langle 0|\hat{O}_n|0\rangle$$

With increasing dimension of the operators $\hat{O}_n$ the dimension of the coefficient functions $C_n(q^2)$ will decrease, which is manifested in higher inverse powers of q^2. In the high energy limit $-q^2 \to \infty$ this assures OPE convergence. The OPE for the correlator (3.1) (i.e. operators and coefficients) will arise quite naturally in the method described in the following, which massively uses the background field method described in section 3.3.
As pointed out in section 3.3, the condensates present in QCD are parameterized by background fields (BF). The field η in (3.1) is made up of quark fields (u_a, d_b etc.). In the philosophy of the BF method the vacuum technically reduces to a perturbative one: the time ordered product in the correlator can be evaluated by applying Wick's theorem for the quark fields retaining only fully contracted terms, since the normal-ordered parts vanish in the trivial BF vacuum. As an example, consider the Wick contracted version of the correlator with the Ioffe-current (3.2):

$$\Pi(q) = -2i\varepsilon_{abc}\varepsilon_{a'b'c'} \int d^4x\ e^{iq\cdot x}\mathrm{Tr}[S^{uT}_{aa'}(x,0)C\gamma_\mu S^u_{bb'}(x,0)\gamma_\nu C]\ \gamma_5\gamma^\mu S^d_{cc'}(x,0)\gamma^\nu\gamma_5,$$

which is a product of quark propagators $S^q(x)$ and gamma matrices. All effects coming from the background fields are now explicitly included in the x-space propagator used for the contractions in Wick's theorem:

$$\begin{aligned} \underbrace{u^a_\alpha(x)\overline{u}^b_\beta}(0) &= [S^u_{ab}(x)]_{\alpha\beta}, \\ \underbrace{d^a_\alpha(x)\overline{d}^b_\beta}(0) &= [S^d_{ab}(x)]_{\alpha\beta}. \end{aligned}$$

These propagators include all information on the background fields and, consequently, the condensates. So, the propagator S^q_{ab} is the most essential ingredient in calculating the OPE.

$$\begin{aligned}[S^q_{ab}(x)]_{\alpha\beta} \equiv& \langle T[q_{a\alpha}(x)\bar{q}_{b\beta}(0)]\rangle \\ =& \frac{i\delta_{ab}}{2\pi^2}\,\frac{1}{(x^2)^2}\not{x}_{\alpha\beta} + \chi^q_{a\alpha}(x)\bar{\chi}^q_{b\beta}(0) - \frac{ig_s}{32\pi^2}\,t^B_{ab}F^B_{\mu\nu}\,\frac{1}{x^2}\,[\sigma^{\mu\nu}\not{x} + \not{x}\sigma^{\mu\nu}]_{\alpha\beta} + \dots \end{aligned} \tag{3.14}$$

Here, $q \in \{u, d\}$ denotes the quark flavour. The first term is simply the massless free propagator in x-space, the second term describes an interaction with the background quark field of the same flavour, and the third term an interaction with the gluon field where only the first term in the expansion (3.10) is included.
When this propagator is inserted into the Wick-contracted correlator the following identifications are made to replace the background fields by condensates:

$$\begin{aligned} \chi^q_{a\alpha}(x)\bar{\chi}^q_{b\beta}(0) &= \langle q^a_\alpha(x)\bar{q}^b_\beta(0)\rangle & F^A_{\kappa\lambda}F^B_{\mu\nu} &= \langle G^A_{\kappa\lambda}G^B_{\mu\nu}\rangle \\ \chi^q_a\bar{\chi}^q_b F^A_{\mu\nu} &= \langle q^a\bar{q}^b G^A_{\mu\nu}\rangle & \chi^q_{a\alpha}\bar{\chi}^q_{b\beta}\chi^q_{c\gamma}\bar{\chi}^q_{d\delta} &= \langle q^a_\alpha\bar{q}^b_\beta q^c_\gamma\bar{q}^d_\delta\rangle. \end{aligned} \tag{3.15}$$

Operators without an argument are evaluated at $x = 0$ (for the higher dimensional operators this means that only the first term in a Taylor series is included). One quark operator in the two-quark condensate in (3.15) is still non-local, so the covariant Taylor expansion (3.11) is applied, giving to leading order

$$\langle q^a_\alpha(x)\bar{q}^b_\beta(0)\rangle \approx -\frac{\delta_{ab}}{12}\langle\bar{q}q\rangle\delta_{\alpha\beta} \;+\; \dots$$

An extension of this equation will be motivated in section 4.2. The condensates in eq. (3.15) still carry color and Lorentz indices. These structures can be projected out leaving only scalar condensates. The following formulas are used.

$$\begin{aligned} \left\langle \frac{\alpha_s}{\pi} G^A_{\kappa\lambda}G^B_{\sigma\rho}\right\rangle &= \frac{1}{96}\delta^{AB}(g_{\kappa\sigma}g_{\lambda\rho} - g_{\kappa\rho}g_{\lambda\sigma})\left\langle\frac{\alpha_s}{\pi}G^2\right\rangle \\ \langle g_s q^a_\alpha\bar{q}^b_\beta G^A_{\mu\nu}\rangle &= -\frac{t^A_{ab}}{192}[\sigma_{\mu\nu}]_{\alpha\beta}\langle g_s\bar{q}\sigma\!\cdot\! Gq\rangle \end{aligned} \tag{3.16}$$

Here, we have defined $G^2 = G^A_{\mu\nu}G^{\mu\nu A}$ and $\sigma\!\cdot\! G = \sigma_{\mu\nu}G^{\mu\nu}$
Proof. (i) Lorentz invariance and asymmetry of $G_{\mu\nu}$ imply:

$$\left\langle \frac{\alpha_s}{\pi} G^A_{\kappa\lambda}G^B_{\sigma\rho}\right\rangle = C_1\delta^{AB}(g_{\kappa\sigma}g_{\lambda\rho} - g_{\kappa\rho}g_{\lambda\sigma})$$

where C_1 is a constant to be determined. Contracting yields:

$$\begin{aligned} \delta^{AB}g^{\kappa\sigma}g^{\lambda\rho}\left\langle \frac{\alpha_s}{\pi} G^A_{\kappa\lambda}G^B_{\sigma\rho}\right\rangle &= \left\langle \frac{\alpha_s}{\pi} G^A_{\kappa\lambda}G^{A\kappa\lambda}\right\rangle = \left\langle\frac{\alpha_s}{\pi}G^2\right\rangle \qquad \text{and} \\ \delta^{AB}g^{\kappa\sigma}g^{\lambda\rho}\;C_1\delta^{AB}(g_{\kappa\sigma}g_{\lambda\rho} - g_{\kappa\rho}g_{\lambda\sigma}) &= C_1\!\cdot\! 8(16-4) = 96C_1 \\ \Rightarrow \qquad C_1 &= \frac{1}{96}\left\langle\frac{\alpha_s}{\pi}G^2\right\rangle \end{aligned}$$

(ii) Obiously $\langle g_s q_{a\alpha}\bar{q}_{b\beta}G^A_{\mu\nu}\rangle = C_2 t^A_{ab}[\sigma_{\mu\nu}]_{\alpha\beta}$, C_2 being a constant again. Then

$$\begin{aligned} t^A_{ba}[\sigma^{\mu\nu}]_{\beta\alpha}\langle g_s q^a_\alpha\bar{q}^b_\beta G^A_{\mu\nu}\rangle &= -\langle g_s\bar{q}\sigma\!\cdot\! Gq\rangle \qquad \text{resp.} \\ t^A_{ba}[\sigma^{\mu\nu}]_{\beta\alpha}\;C_2 t^A_{ab}[\sigma_{\mu\nu}]_{\alpha\beta} &= C_2\;\mathrm{Tr}(t^A t^A)\mathrm{Tr}(\sigma_{\mu\nu}\sigma^{\mu\nu}) = C_2\cdot 4\cdot 48 \\ \Rightarrow \qquad C_2 &= -\frac{1}{192}\langle g_s\bar{q}\sigma\!\cdot\! Gq\rangle \end{aligned}$$

□

In the calculation of terms involving gluons there occur color structures which get paired with the ε-tensors from the interpolating fields. The results of the contractions are

$$\begin{aligned}
\varepsilon_{abc}\varepsilon_{a'b'c'}\delta_{aa'}t^A_{bb'}t^B_{cc'}\delta^{AB} &= \varepsilon_{abc}\varepsilon_{ab'c'}\delta_{aa'}t^A_{bb'}t^A_{cc'} \\
&= (\delta_{bb'}\delta_{cc'} - \delta_{bc'}\delta_{b'c})t^A_{bb'}t^A_{cc'} \\
&= (t^A_{bb}t^A_{cc} - t^A_{bc}t^A_{cb}) \\
&= \mathrm{Tr}(t^A)\mathrm{Tr}(t^A) - \mathrm{Tr}(t^At^A) = -4
\end{aligned}$$

$$\begin{aligned}
\varepsilon_{abc}\varepsilon_{a'b'c'}\delta_{aa'}\delta_{bb'}t^A_{cd}t^B_{dc'}\delta^{AB} &= \varepsilon_{abc}\varepsilon_{a'b'c'}\delta_{aa'}\delta_{bb'}t^A_{cd}t^A_{dc'} \\
&= \varepsilon_{abc}\varepsilon_{abc'}t^A_{cd}t^A_{dc'} \\
&= 2\delta_{cc'}t^A_{cd}t^A_{dc'} = 2t^A_{cd}t^A_{dc} = 2\mathrm{Tr}(t^At^A) = 8
\end{aligned}$$

Here we have used $\varepsilon_{abc}\varepsilon_{abc'} = 2\delta_{cc'}$. Together with eq. (3.16) these formulas are the major ingredients for calculation of gluonic terms. All that remains to be done now is the calculation of the Fourier transform. The following formulae [10, 11] are of great help:

$$\begin{aligned}
\int d^4x \; e^{iq\cdot x}\frac{1}{x^2} &= -\frac{4\pi^2 i}{q^2} \\
\int d^4x \; e^{iq\cdot x}\frac{1}{(x^2)^n} &= \frac{i(-1)^n 2^{4-2n}\pi^2}{\Gamma(n-1)\Gamma(n)}(q^2)^{n-2}\log(-q^2) + P_{n-2}(q^2) \qquad (n \geq 2)
\end{aligned} \tag{3.17}$$

where the $P_k(q^2)$ are polynomials of degree k with divergent coefficients. Integrals containing an $\not{x}$ can be computed using the fundamental property of the Fourier transform

$$\int d^4x \; e^{iq\cdot x}x_\mu f(x) = -i\partial^{(q)}_\mu \int d^4x \; e^{iq\cdot x}f(x) = -i\partial_\mu \hat{f}(q).$$

After the Fourier transform we have to identify the two invariant functions in $\Pi^{\mathrm{OPE}}(q)$. This can easily be accomplished by noting that

$$\begin{aligned}
\Pi^{\mathrm{OPE}}_s(q^2) &= \frac{1}{4}\mathrm{Tr}\left[\Pi^{\mathrm{OPE}}(q)\right], \\
\Pi^{\mathrm{OPE}}_q(q^2) &= \frac{1}{4}\mathrm{Tr}\left[\not{q}\Pi^{\mathrm{OPE}}(q)\right].
\end{aligned}$$

In order to account for higher energy excitations in the dispersion relation a model for this continuum must be set up. When approaching higher energies the OPE is supposed to gain reliability, so the continuum model is made up from terms in the OPE dominating in the limit $-q^2 \to \infty$ starting from a threshold s_0. These terms are equal to $(-q^2)^k \log(-q^2), k = 0, 1, 2$. This leads to an ansatz for the spectral function of the continuum model:

$$\rho^{\mathrm{cont}}_i(s) = \theta(s - s_0)\rho^{\mathrm{OPE}}_i(s). \tag{3.18}$$

The $\rho^{\mathrm{OPE}}_i(s)$ equals s^k up to a factor. It is crucial for the justification of the continuum model that the threshold s_0 satisfies at least $M_{\mathrm{N}} < s_0$.

We finish this section by giving numerical values for condensates which will be of importance later in this thesis. As already pointed out in section 2.3, the quark condensate takes a value around $(-240\,\mathrm{MeV})^3$. However, the values used for the quark condensate vary strongly throughout the literature. For a recent review see [15]. In the later sections we will use condensate values between $(-\langle\bar{q}q\rangle)^{1/3} = 225\,\mathrm{MeV}$ and $(-\langle\bar{q}q\rangle)^{1/3} = 245\,\mathrm{MeV}$ with an error of $\pm 20\,\mathrm{MeV}$. The gluon condensate $\left\langle \frac{\alpha_s}{\pi} G^2 \right\rangle = \langle \alpha_s/\pi G^A_{\mu\nu} G^{\mu\nu A}\rangle$ is usually set to

$$\left\langle \frac{\alpha_s}{\pi} G^2 \right\rangle = (330\,\mathrm{MeV})^4$$

in QCD sum rule calculations. We adopt this value with an error of $\pm 20\,\mathrm{MeV}$. The mixed quark-gluon condensate $\langle g_s \bar{q}\sigma{\cdot}Gq\rangle$ is parametrized in terms of the quark condensate $\langle\bar{q}q\rangle$ (see [5])

$$\langle g_s \bar{q}\sigma{\cdot}Gq\rangle = 2\lambda_q^2 \langle\bar{q}q\rangle \qquad \text{where } \lambda_q^2 \approx 0.36\mathrm{GeV}^2 \tag{3.19}$$

It has the same sign as the quark condensate using the field conventions of chapter 2. A condensate of special interest is the four-quark condensate, emerging from

$$\chi^q_{a\alpha}\bar{\chi}^q_{b\beta}\chi^q_{c\gamma}\bar{\chi}^q_{d\delta} = \langle q^a_\alpha \bar{q}^b_\beta q^c_\gamma \bar{q}^d_\delta \rangle$$

in eq. (3.15). The reason for its importance is, that these factors amount to diagrams not containing any loop integrations, and thus lacking numerical suppression factors associated with loop integrations. In the BF method these factors are present in the prefactors of the free part in the propagator (3.14). The problem with these terms is that the condensate $\langle\bar{q}q\bar{q}q\rangle$ is not very well known. The usual way out is to approximate the four quark condensate by the factorized value $\langle\bar{q}q\rangle^2$, which is equivalent to inserting a complete system of intermediate states and retaining only the contribution of the ground state $|0\rangle$

$$\langle 0|\bar{q}q\bar{q}q|0\rangle = \langle 0|\bar{q}q \left(\sum_n |n\rangle\langle n|\right) \bar{q}q|0\rangle \approx \langle 0|\bar{q}q|0\rangle^2$$

It is clear that $\langle\bar{q}q\bar{q}q\rangle \geq \langle\bar{q}q\rangle^2$. Considering the magnitude of possible pionic intermediate states the factorization hypothesis seems however very vague and we shall address it in a later section.

3.5 Derivation of QCD Sum Rules

We have now gathered all tools to build up QCD sum rules. The basic strategy is the following. First an appropriate interpolating field has to be identified (i.e. one which has the desired quantum numbers). The goals of the choice of η are: maximize the coupling to the intermediate nucleon state and minimize contributions of higher order corrections in the OPE. Then the Identification of the tensor structure of the correlator has to be made (see eq. (3.5)). Finally the two representations for each invariant function are calculated (i.e. the dispersion relation with phenomenological spectral densities and OPE for large spacelike q) and equated:

$$\Pi_i^{\mathrm{phen}}(q^2) = \Pi_i^{\mathrm{OPE}}(q^2) \qquad i \in \{s, q\}. \tag{3.20}$$

However, there remain some problems. There are polynomials (subtractions) and contributions from the higher energy part of the dispersion integral (3.6). A solution is provided by the use of the so-called Borel Transform (see also App. B).

$$\mathcal{B}\big[f(Q^2)\big] = \lim_{\substack{Q^2,n\to\infty \\ Q^2/n=M^2}} \frac{(Q^2)^{n+1}}{n!}\left(\frac{-d}{dQ^2}\right)^n f(Q^2). \tag{3.21}$$

The most important Borel transforms are

$$\begin{aligned} \mathcal{B}\Big[(Q^2)^k\Big] &= 0 & \mathcal{B}\left[\frac{1}{(Q^2)^k}\right] &= \frac{1}{(k-1)!}\left(\frac{1}{M^2}\right)^{k-1} \\ \mathcal{B}\Big[(Q^2)^k\ln(Q^2/\Lambda^2)\Big] &= k!(-M^2)^{k+1} & \mathcal{B}\left[\frac{1}{s+Q^2}\right] &= e^{-s/M^2}. \end{aligned} \tag{3.22}$$

The effect of the Borel transform is twofold. On the one hand polynomials are mapped to zero, so the subtractions are annihilated, and on the other hand the weighting factor $(s-q^2)^{-1}$ is replaced by an exponentially decreasing weighting factor e^{-s/M^2} which suppresses the continuum contribution. So one simply performs the Borel transform on both sides of (3.20) and the final form of the sum rules is:

$$\mathcal{B}\left[\Pi_i^{\text{phen}}(q^2)\right] = \int_0^\infty ds\ e^{-s/M^2}\rho_i(s) = \mathcal{B}\left[\Pi_i^{\text{OPE}}(q^2)\right] \qquad i\in\{s,q\}. \tag{3.23}$$

In this treatment the continuum model described in section 3.4 amounts to the following corrections for powers of M:

$$\begin{aligned} M^2 &\mapsto M^2\cdot E_0 \equiv M^2\left(1-e^{-s_0/M^2}\right) \\ M^4 &\mapsto M^4\cdot E_1 \equiv M^4\left(1-e^{-s_0/M^2}(s_0/M^2+1)\right) \\ M^6 &\mapsto M^6\cdot E_2 \equiv M^6\left(1-e^{-s_0/M^2}(s_0^2/2M^4+s_0/M^2+1)\right). \end{aligned}$$

The Borel scale M is ideally only an auxiliary parameter. Both sides of the sum rules (3.23) should actually coincide independently of M. However there were several approximations made: the truncation of the OPE, the phenomenological model of the continuum etc. So it remains to explore whether there is at least a window in M^2 where the equations (3.23) are valid.

We consider the simplest $m_q\equiv 0$ sum rules for the nucleon as an example. These sum rules will be extended in chapter 5. The OPE for the current 3.2 is given by:

$$\begin{aligned} \Pi_s^{\text{OPE}}(q^2) &= \frac{q^2}{4\pi^2}\log(-q^2) \\ \Pi_q^{\text{OPE}}(q^2) &= -\frac{(q^2)^2}{64\pi^4}\log(-q^2) - \frac{1}{32\pi^2}\log(-q^2)\left\langle\frac{\alpha_s}{\pi}G^2\right\rangle - \frac{2}{3q^2}\langle\bar{q}q\rangle^2 \end{aligned}$$

After inserting this equations as well as (3.9) into (3.23) we arrive at:

$$\begin{aligned} \lambda^{*2}M_{\text{N}}e^{-M_{\text{N}}^2/M^2} &= -\frac{1}{4\pi^2}\langle\bar{q}q\rangle M^4E_1 - \frac{1}{8\pi^2}\langle g_s\bar{q}\sigma\cdot Gq\rangle M^2E_0, \\ \lambda^{*2}e^{-M_{\text{N}}^2/M^2} &= \frac{1}{32\pi^4}M^6E_2 + \frac{2}{3}\langle\bar{q}q\rangle^2 + \frac{1}{32\pi^2}\left\langle\frac{\alpha_s}{\pi}G^2\right\rangle M^2E_0. \end{aligned}$$

The simplest sum rule, known as Ioffe's Formula (1.1), is obtained by keeping only the perturbative and the $\langle\bar{q}q\rangle$-contribution without continuum and dividing the two sum rules:

$$M_{\mathrm{N}} = -\frac{8\pi^2}{M^2}\langle\bar{q}q\rangle + \ldots \overset{\mathrm{M=1GeV}}{\approx} 1\mathrm{GeV}$$

This nice result is, however, accidental. It has to be noted that neglecting all other terms is extremely crude. Especially the four-quark condensate term in the sum rule at $\not{q}$ is quite decisive.

Chapter 4

Mass Expansion of the Background Field Propagator

The goal of this thesis is to extend the known nucleon sum rules to finite quark masses. We will follow the established works and incorporate condensates up to dimension 8. In order to compare the nucleon mass predictions to recent Lattice QCD calculations [2, 16], we have to cover the range from the physical point ($m_q \sim 5\,\mathrm{MeV}$) up to $m_q \sim 150 - 200\,\mathrm{MeV}$. To estimate the required m_q-order we notice that in the final sum rules any power of m_q lowers the accompanying power of the Borel parameter M because of dimensional reasons. From this we conclude that the natural expansion parameter is given by m_q/M. Anticipating the relevant M-regime to be around $1\,\mathrm{GeV}$ we can conclude that an expansion up to order 3 in the quark mass should be sufficient. Of course, the convergence in powers of m_q has to be strictly monitored. In the present chapter we derive expansions of the terms involving kinematics and quote the covariant Taylor expansion of the background quark field part $\chi_a^q(x)\chi_b^q(0)$ in the propagator. The full background field propagator consists of three parts

$$S^q(x) = S^{\mathrm{f}}(x) + S^{q,\mathrm{cond}}(x) + S^{\mathrm{gluon}}(x) \tag{4.1}$$

where $S^{\mathrm{f}}(x)$ is the flavour invariant free propagator, $S^{\mathrm{q,cond}}(x)$ describes interactions with the background quark field with the same flavour q, and $S^{\mathrm{gluon}}(x)$ is the part accounting for interactions with the classical gluon fields.

4.1 The Feynman Propagator

When going from negligible quark masses to finite masses the form of the free propagator gets more complicated. The calculation of the OPE in the background field method requires an x-space expression. Since the general form is not known we expand in m up to the desired order 3. Consider for demonstration the scalar propagator in euclidean momentum space given by $\Delta_E(\bar{k}) = \frac{1}{\bar{k}^2+m^2}$. The corresponding expression in configuration space is obtained by an inverse Fourier transform. Using the $SO(4)$ rotational symmetry we can set $\bar{x} = (0, 0, 0, -|\bar{x}|)$. We also define

$\bar{k} = (\mathbf{r}, k_4)$.

$$\begin{aligned}
\int d^4\bar{k}\; e^{-i\bar{k}\cdot\bar{x}} \frac{1}{\bar{k}^2 + m^2} &= \frac{1}{(2\pi)^4}\int d^3r \int_{-\infty}^{\infty} dk_4 e^{i|\bar{x}|k_4} \frac{1}{k_4^2 + (r^2+m^2)} \\
&= \frac{1}{4\pi^3}\int_0^\infty dr\, r^2\pi\; \frac{\exp(-|\bar{x}|\sqrt{r^2+m^2})}{\sqrt{r^2+m^2}} \\
&= \frac{1}{4\pi^2}\, m^2 \int_1^\infty dz \sqrt{z^2-1}\exp(-m|\bar{x}|z) \\
&= \frac{m}{4\pi^2|\bar{x}|} K_1(m|\bar{x}|).
\end{aligned}$$

Here the substitution $r = m\sqrt{z^2-1}$ was made. Inserting the expansion of the modified Bessel function $K_1(z)$

$$\begin{aligned}
K_1(z) =& \frac{1}{z} + \frac{z}{2}\left(\log\frac{z}{2} + \gamma_E - \frac{1}{2}\right) + \frac{z^3}{16}\left(\log\frac{z}{2} + \gamma_E - \frac{5}{4}\right) \\
&+ \frac{z^5}{384}\left(\log\frac{z}{2} + \gamma_E - \frac{5}{3}\right) + \frac{z^7}{18432}\left(\log\frac{z}{2} + \gamma_E - \frac{47}{24}\right) + \dots
\end{aligned}$$

we get for the mass expansion of the scalar propagator in Euclidean space:

$$\begin{aligned}
\Delta_E(x) =& \frac{1}{4\pi^2}\frac{1}{\bar{x}^2} + \frac{m^2}{8\pi^2}\left[\log\frac{m|\bar{x}|}{2} + \gamma_E - \frac{1}{2}\right] + \frac{m^4}{64\pi^2}\bar{x}^2\left[\log\frac{m|\bar{x}|}{2} + \gamma_E - \frac{5}{4}\right] \\
&+ \frac{m^6}{1536\pi^2}\bar{x}^4\left[\log\frac{m|\bar{x}|}{2} + \gamma_E - \frac{5}{3}\right] + \frac{m^8}{73728\pi^2}\bar{x}^6\left[\log\frac{m|\bar{x}|}{2} + \gamma_E - \frac{47}{24}\right].
\end{aligned}$$

The scalar propagator in Minkowski space is obtained by exchanging $\bar{x}^2$ for $-x^2$ and multiplying by $-i$. Applying $(i\not{\partial} + m)$ to it and multiplying by i we get the mass expansion of the free part of the modified propagator $S(x)$ used in the sum rule calculation:

$$\begin{aligned}
S^{\mathrm{f}}(x) =& \frac{i}{2\pi^2}\frac{\not{x}}{(x^2)^2} - \frac{m}{4\pi^2}\frac{1}{x^2} + \frac{im^2}{8\pi^2}\frac{\not{x}}{x^2} + \frac{m^3}{16\pi^2}\left[\log\frac{-m^2x^2}{4} + 2\gamma_E - 1\right] \\
&- \frac{im^4}{64\pi^2}\left[\log\frac{-m^2x^2}{4} + 2\gamma_E - \frac{3}{2}\right]\not{x} - \frac{m^5}{128\pi^2}x^2\left[\log\frac{-m^2x^2}{4} + 2\gamma_E - \frac{5}{2}\right] \\
&+ \frac{im^6}{768\pi^2}x^2\left[\log\frac{-m^2x^2}{4} + 2\gamma_E - \frac{17}{6}\right]\not{x} + \frac{m^7}{3072\pi^2}(x^2)^2\left[\log\frac{-m^2x^2}{4} + 2\gamma_E - \frac{47}{12}\right].
\end{aligned} \tag{4.2}$$

For comparison the mass expansion of the propagator in momentum space is given by:

$$\begin{aligned}
S^{\mathrm{f}}(p) &= \frac{i}{\not{p} - m} = i\frac{\not{p} + m}{p^2(1 - m^2/p^2)} = \frac{i(\not{p} + m)}{p^2}\left(1 + \frac{m^2}{p^2} + \frac{m^4}{(p^2)^2} + \frac{m^6}{(p^2)^3} + \dots\right) \\
&= i\left(\frac{\not{p}}{p^2} + \frac{m^2}{p^2} + \frac{m^2\not{p}}{(p^2)^2} + \frac{m^3}{(p^2)^2} + \frac{m^4\not{p}}{(p^2)^3} + \frac{m^5}{(p^2)^3} + \frac{m^6\not{p}}{(p^2)^4} + \frac{m^7}{(p^2)^4} + \dots\right).
\end{aligned} \tag{4.3}$$

4.2 The Quark Condensate Part

We consider a single background field quark line $\chi_a^q(x)\bar{\chi}_b^q(0)$ without interactions with other lines and review its systematic Taylor expansion. The covariant derivative in the Taylor expansion introduces higher order condensates including interactions with the background gluon field. As indicated above the Grassmann field part $\chi_a^q(x)\bar{\chi}_b^q(0)$ is identified with the quark condensate, such that (we add Dirac indices here for clarity)

$$\chi_{a\alpha}^q(x)\bar{\chi}_{b\beta}^q(0) = \langle q_\alpha^a(x)\bar{q}_\beta^b(0)\rangle.$$

Analyzing the Dirac and color structure we obtain

$$\langle q_\alpha^a(x)\bar{q}_\beta^b(0)\rangle = -\frac{\delta_{ab}}{12}\left[\langle\bar{q}(0)q(x)\rangle\delta_{\alpha\beta} + \langle\bar{q}(0)\gamma_\lambda q(x)\rangle\gamma_{\alpha\beta}^\lambda\right].$$

Inserting the Taylor expansion (3.11) for $q(x)$ yields:

$$\begin{aligned} S_{ab,\alpha\beta}^{q,\mathrm{cond}}(x) &= \chi_{a\alpha}^q(x)\bar{\chi}_{b\beta}^q(0) = \langle q_\alpha^a(x)\bar{q}_\beta^b(0)\rangle \\ &= -\frac{\delta_{ab}}{12}\left(\langle\bar{q}q\rangle + x^\mu\langle\bar{q}D_\mu q\rangle + \frac{1}{2}x^\mu x^\nu\langle\bar{q}D_\mu D_\nu q\rangle + \dots\right)\delta_{\alpha\beta} \\ &\quad -\frac{\delta_{ab}}{12}\left(\langle\bar{q}\gamma_\lambda q\rangle + x^\mu\langle\bar{q}\gamma_\lambda D_\mu q\rangle_{\rho_N} + \frac{1}{2}x^\mu x^\nu\langle\bar{q}\gamma_\lambda D_\mu D_\nu q\rangle + \dots\right)\gamma_{\alpha\beta}^\lambda. \end{aligned}$$

In order to get evaluable condensate structures we have to proceed further and address the Lorentz structure of the condensates. In vacuum $\langle\bar{q}D_\mu q\rangle$, $\langle\bar{q}\gamma_\lambda q\rangle$ as well as all other condensates with an odd number of Lorentz indices vanish due to Lorentz invariance (i.e. there is no four vector or $g_{\mu\nu}$ construction, which they could be proportional to). This situation is different for $\langle\bar{q}D_\mu D_\nu q\rangle$ and $\langle\bar{q}\gamma_\mu D_\nu q\rangle$. From Lorentz invariance it is clear that they have to be proportional to $g_{\mu\nu}$. Contracting with $x^\mu x^\nu$ resp. $\gamma^\mu x^\nu$ and using Dirac's equation we arrive at:

$$\begin{aligned} \frac{1}{2}x^\mu x^\nu\langle\bar{q}D_\mu D_\nu q\rangle &= \frac{x^2}{8}\langle\bar{q}D^2 q\rangle \\ x^\mu\gamma^\lambda\langle\bar{q}\gamma_\lambda D_\mu q\rangle &= \frac{m_q}{4i}\langle\bar{q}q\rangle\,\not{x}. \end{aligned}$$

Analogous considerations can be carried out for the higher derivatives. The final form of the quark part is then given by (see [19]):

$$\begin{aligned} S_{ab}^{q,\mathrm{cond}}(x) = -\frac{\delta_{ab}}{12}&\left[\left(\langle\bar{q}q\rangle + \frac{x^2}{8}\langle\bar{q}D^2q\rangle + \frac{(x^2)^2}{2^8 3^2}\langle\bar{q}q\rangle\left\langle\frac{\alpha_s}{\pi}G^2\right\rangle + \dots\right)\mathbb{1}\right. \\ &\left. + \left(\frac{m_q}{4i}\langle\bar{q}q\rangle - \frac{ix^2}{2^4 3}\,m_q\langle\bar{q}D^2q\rangle + \dots\right)\not{x}\right]. \end{aligned} \tag{4.4}$$

Already at this level condensates involving quarks are factorized, since when two lines are constituted by a background quark the resulting diagram bears a factor of $\langle\bar{q}q\rangle^2$ (or products of higher order condensates).

Recall that (4.4) is used only for diagrams without interactions between two lines. When treating diagrams containing an interaction with the mixed quark-gluon condensate the procedure of

projecting out Dirac and color structure is not possible. It should be noted here that the Taylor expansion of the field $q(x)$ is indeed the fundamental step in setting up an Operator Product expansion, the operators are thereby made local, whereas the x-dependence is moved to the coefficient.
For a physical interpretation of the various terms in eq. (4.4) we split up the second derivative $2\langle\bar{q}D^2q\rangle = \langle g_s\bar{q}\sigma\cdot Gq\rangle + 2m_q^2\langle\bar{q}q\rangle$, then the terms carrying a $\langle g_s\bar{q}\sigma\cdot Gq\rangle$ can in parts be interpreted as processes of the form [17, 18]

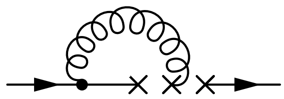

$$\propto \langle g_s\bar{q}\sigma\cdot Gq\rangle$$

and the term with $\langle\bar{q}q\rangle\left\langle\frac{\alpha_s}{\pi}G^2\right\rangle$ describes a coupling to both the quark and the gluon field separately

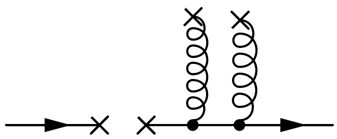

$$\propto \langle\bar{q}q\rangle\left\langle\frac{\alpha_s}{\pi}G^2\right\rangle$$

4.3 The Gluonic Part

Gluonic contributions to sum rules emerge in parts from the covariant Taylor expansion of the background fields and on the other hand from perturbative quarks emitting gluons. In the second case there is kinematics involved which depends of course on the quark mass. We therefore have to extend the well known configuration space expressions in the chiral limit to finite quark masses. To this end we expand the kinematics in momentum space and translate the result to x-space. The expansion of the free propagator provides useful guidance at this point. The gluonic contribution is divided into parts involving one resp. two gluons:

$$S^{\text{gluon}}(x) = S^{\text{G}}(x) + S^{\text{GG}}(x)$$

4.3.1 The One-Gluon Line

The part of the quark propagator with a single gluon interaction is given by [10]:

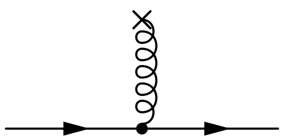

$$= -\frac{ig}{4}\, t^A_{ab}F^A_{\mu\nu}\,\frac{1}{(q^2-m^2)^2}(\sigma^{\mu\nu}(\not{q}+m) + (\not{q}+m)\sigma^{\mu\nu})$$

The translation to x-space is carried out as follows. We first expand the expression as it stands to third order in m using

$$\frac{\not{q}+m}{(q^2-m^2)^2} \approx \frac{\not{q}+m}{(q^2)^2-2m^2q^2} = \frac{\not{q}+m}{(q^2)^2(1-2m^2/q^2)} = (\not{q}+m)\left(1+\frac{2m^2}{q^2}+\dots\right) \qquad (4.5)$$

The arising q-structures are the same ones as in (4.3). Next, we identify the appropriate inverse Fourier transforms by comparing coefficients of different orders in m according to equations (4.2) and (4.3). For example, the first term in (4.5) $\not{q}/(q^2)^2$ appears in (4.3) at order m^2, in (4.2) there is $i\not{x}/(8\pi^2 x^2)$ at order m^2. So the inverse Fourier transform of $\not{q}/(q^2)^2$ is easily found. The analogous procedure for all terms in eq. (4.5) finally gives

$$\begin{aligned} S^{\mathrm{G}}_{ab}(x) = -\frac{ig_s F^A_{\kappa\lambda}(0) t^A_{ab}}{4} \Bigg\{ & \frac{1}{8\pi^2 x^2}(\sigma^{\kappa\lambda}\not{x} + \not{x}\sigma^{\kappa\lambda}) \\ & + \frac{m}{8\pi^2 i}\sigma^{\kappa\lambda}\left[\log\left(-\frac{m^2x^2}{4}\right) + 2\gamma_E - 1\right] \\ & - \frac{m^2}{32\pi^2}(\sigma^{\kappa\lambda}\not{x} + \not{x}\sigma^{\kappa\lambda})\left[\log\left(-\frac{m^2x^2}{4}\right) + 2\gamma_E - \frac{3}{2}\right] \\ & + \frac{im^3}{32\pi^2}\sigma^{\kappa\lambda}x^2\left[\log\left(-\frac{m^2x^2}{4}\right) + 2\gamma_E - \frac{5}{2}\right]\Bigg\} \end{aligned} \tag{4.6}$$

for the part of the interaction with the background gluon field.

4.3.2 The Two-Gluon Line.

A quark line with two gluon insertions in momentum space is given by ([10]):

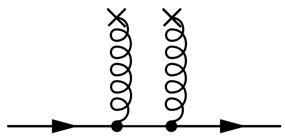

$$= -\frac{i}{4} g_s^2 t^A t^B F^A_{\alpha\beta} F^B_{\kappa\lambda} \frac{\not{q} + m}{(q^2 - m^2)^5} [f^{\alpha\beta\kappa\lambda} + f^{\alpha\kappa\beta\lambda} + f^{\alpha\kappa\lambda\beta}](\not{q} + m)$$

where $f^{\alpha\beta\kappa\lambda} = \gamma^\alpha(\not{q} + m)\gamma^\beta(\not{q} + m)\gamma^\kappa(\not{q} + m)\gamma^\lambda$. In essentially all cases diagrams involving this part of the propagator give a contribution proportional to $\left\langle \frac{\alpha_s}{\pi} G^2 \right\rangle$, so that the two gluon fields in this expression can directly be translated to the gluon condensate. Now inserting the tensor part of the formula

$$\left\langle \frac{\alpha_s}{\pi} G^A_{\alpha\beta} G^B_{\kappa\lambda} \right\rangle = \frac{1}{96} \delta^{AB} (g_{\alpha\kappa} g_{\beta\lambda} - g_{\alpha\lambda} g_{\beta\kappa}) \left\langle \frac{\alpha_s}{\pi} G^2 \right\rangle$$

we see that the complicated Dirac structure of the two-gluon line massively simplifies:

$$\begin{aligned} (g_{\alpha\kappa} g_{\beta\lambda} - g_{\alpha\lambda} g_{\beta\kappa})(\not{q} + m)[f^{\alpha\beta\kappa\lambda} + f^{\alpha\kappa\beta\lambda} + f^{\alpha\kappa\lambda\beta}](\not{q} + m) = \\ 24(-m(q^2)^2 - m^2 q^2 \not{q} + m^3 q^2 + m^4 \not{q}). \end{aligned}$$

Obviously, this contribution vanishes in the massless case, which is the reason for its being discarded in previous nucleon sum rule calculations. For $m \neq 0$ contributions of this line can by no means be neglected. In translating this part to configuration space we follow in principle the same idea as above, the denominator is first approximated by $(q^2 - m^2)^5 \simeq (q^2)^5 - 5(q^2)^4 m^2 = (q^2)^5(1 - 5m^2/q^2)$ and then the geometric series is applied $(1 - 5m^2/q^2)^{-1} = 1 + 5m^2/q^2 + 25m^4/(q^2)^2$. For the inverse Fourier transform we again identify the q-structures, compare them with the ones in the low mass expansion of the free Feynman propagator (4.3). These are then compared order by order with the x-structures in the configuration space m-expansion (4.2). The result is given by:

$$
\begin{aligned}
S_{ab}^{\mathrm{GG}}(x) = \frac{i\pi^2}{4}(t^A t^A)_{ab}\left\langle \frac{\alpha_s}{\pi}G^2\right\rangle \Bigg\{ & \frac{im}{64\pi^2}x^2\left[\frac{1}{2}\log\left(-\frac{m^2x^2}{4}\right)+\gamma_E-\frac{5}{4}\right] \\
& + \frac{m^2}{384\pi^2}x^2\left[\frac{1}{2}\log\left(-\frac{m^2x^2}{4}\right)+\gamma_E-\frac{17}{12}\right] \not{x} \\
& - \frac{im^3}{384\pi^2}(x^2)^2\left[\frac{1}{2}\log\left(-\frac{m^2x^2}{4}\right)+\gamma_E-\frac{47}{24}\right]\Bigg\}.
\end{aligned}
$$

4.4 The Quark-Gluonic Interaction Part.

We now have to deal with the gluon exchange between a perturbative quark and a background field quark giving rise to contributions from the mixed quark-gluonic condensate $\langle g_s\bar{q}\sigma\cdot Gq\rangle$. One of the quark lines involved is the background field part $\chi_a^q(x)\bar{\chi}_b^q(0)$, the other one constitutes a perturbative quark emitting a gluon $F^{\mu\nu}$ (see eq. (4.6)). The product of the three fields is the identified with the mixed condensate:

$$
g_s\chi_a^q(x)\bar{\chi}_b^q(0)F_{\mu\nu}^A = \langle g_s q^a(x)\bar{q}^b G_{\mu\nu}^A\rangle
$$

In this case a Taylor expansion and identification of Lorentz and color structure yield (see [19]):

$$
\begin{aligned}
\langle\Omega|T\{q^a(x)g_sG_{\mu\nu}^A\bar{q}^b(0)\}|\Omega\rangle = & -\frac{1}{2^6 3}\langle g_s\bar{q}\sigma\cdot Gq\rangle\sigma_{\mu\nu}t_{ab}^A + \frac{im}{2^8 3}\langle g_s\bar{q}\sigma\cdot Gq\rangle\left(\not{x}\sigma_{\mu\nu}+\sigma_{\mu\nu}\not{x}\right)t_{ab}^A \\
& - \frac{\pi^2x^2}{2^8 3^2}\langle\bar{q}q\rangle\left\langle\frac{\alpha_s}{\pi}G^2\right\rangle\sigma_{\mu\nu}t_{ab}^A
\end{aligned}
\tag{4.7}
$$

4.5 List of Contributing Feynman Diagrams.

In this section we list all diagrams contributing to the OPE of the sum rules. The different types of diagrams emerge from the physical interpretation of the individual terms in the propagator described in the previous sections. In all cases permutations of the three lines are omitted.
For the operators $\mathbb{1}$, $\langle \bar{q}q \rangle$, and $\langle \bar{q}q\bar{q}q \rangle$ there is only one type of diagram each:

$\langle 1 \rangle$:

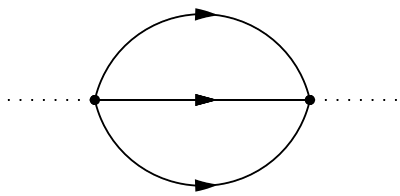

$\langle \bar{q}q \rangle$:

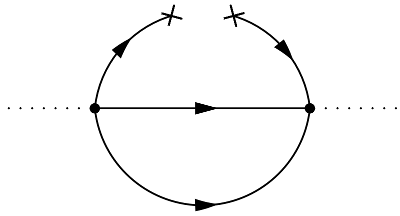

$\langle \bar{q}q\bar{q}q \rangle$:

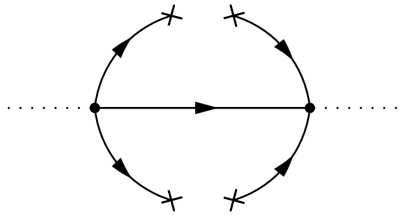

Contributions to the operator $\left\langle \frac{\alpha_s}{\pi} G^2 \right\rangle$ arise from the one- and two-gluon lines given in section 4.3.

$\left\langle \dfrac{\alpha_s}{\pi} G^2 \right\rangle$:

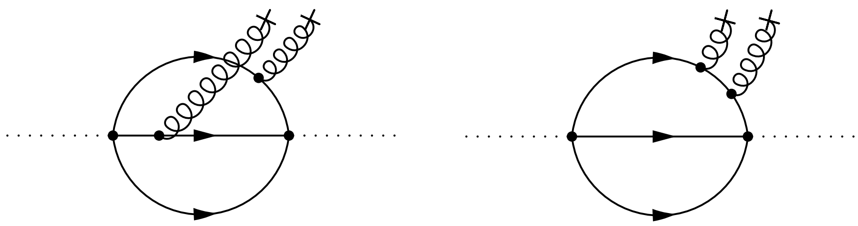

The $\langle g_s \bar{q}\sigma G q \rangle$-terms are generated in parts by interactions between two lines on the one hand, and terms emerging from the covariant Taylor expansion of the quark fields $\chi_a^q(x)$ in the background field propagator on the other hand.

$\langle g_s \bar{q}\sigma \cdot G q \rangle$:

The dimension 7 operator terms involve terms from the one and two gluon lines, as well as a process from the Taylor expansion of the fields $\chi_a^q(x)$.

$\langle \bar{q}q \rangle \left\langle \frac{\alpha_s}{\pi} G^2 \right\rangle$:

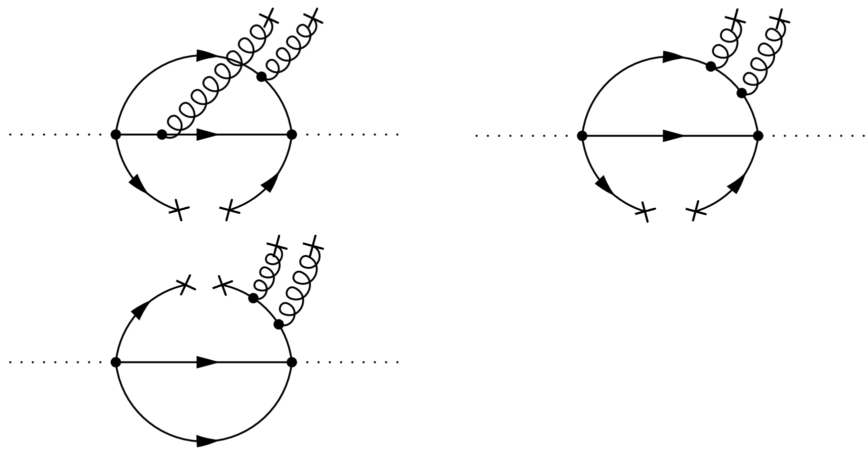

Last, the dimension 8 operator is constructed from two lines interacting with the background quark field.

$\langle \bar{q}q \rangle \langle g_s \bar{q} \sigma \cdot G q \rangle$:

Chapter 5

Spin-1/2 Interpolating Field

In this chapter we calculate nucleon sum rules using the general spin 1/2 interpolating field and the propagator described in the previous chapter. Our extended and improved method applied in the sum rule analysis is described in detail. It reliably accounts for uncertainties in the condensate values and provides a consistent error analysis for the extracted nucleon masses. Then the numerical results are discussed. It will be seen that the assumption of factorization together with the neglect of perturbative α_s-corrections does not provide results in agreement with the physical point and the Lattice data. Following this discussion, factorization is abandoned through the introduction of a phenomenological factorization parameter and known perturbative corrections for the leading terms are included.

5.1 Preliminaries

In order to maximize the flexibility of the sum rules, we start with a general nucleon interpolating field. The two linearly independent interpolating fields for the nucleon are given by [21]

$$\eta_1(x) = \varepsilon_{abc}\left[u_a^T(x) C\gamma_5 d_b(x)\right] u_c(x)$$
$$\eta_2(x) = \varepsilon_{abc}\left[u_a^T(x) C d_b(x)\right] \gamma_5 u_c(x)$$

Any interpolating field for the spin-1/2 nucleon can be written as

$$\eta(x) = \alpha\eta_1(x) + \beta\eta_2(x).$$

$\eta_1(x)$ is known to be indispensable for a nucleon interpolating field since its overlap with the nucleon wave function is large [22], whereas $\eta_2(x)$ excites pure continuum. However, it is argued in [19] that inclusion of η_2 components can serve in reducing the continuum contamination of the η_1 part. We follow this statement and fix the η_1-part leaving the η_2-part variable for the purpose of optimizing:

$$\eta_\beta(x) = 2\left[\eta_1(x) + \beta\eta_2(x)\right]. \tag{5.1}$$

The choice of the parameter β will be of great importance for the reliability of the sum rules. By varying β one can get anything reaching from fine pole dominance to pure continuum excitation. However, the results should not be too sensitive to the precise choice of β, i.e. a variation of β

within 5% should not change the results significantly. $\beta = -1$ corresponds to the current (3.2) proposed by Ioffe [5]. Applying Wick's Theorem to the correlator with the current $\eta_\beta(x)$ yields:

$$\begin{aligned}\Pi(q) = -4i\varepsilon_{abc}\varepsilon_{a'b'c'}\int d^4x\ e^{iq\cdot x}\Big\{&\mathrm{Tr}\left[S^{uT}_{aa'}(x)C\gamma_5 S^d_{bb'}(x)\gamma_5 C\right] S^u_{cc'}(x)\\ &+ S^u_{aa'}(x)\gamma_5 C S^{dT}_{bb'}(x)C\gamma_5 S^u_{cc'}(x)\\ &+ \beta\ \mathrm{Tr}[S^{uT}_{aa'}(x)CS^d_{bb'}(x)\gamma_5 C]\gamma_5 S^u_{cc'}(x)\\ &+ \beta\gamma_5 S^u_{aa'}(x)\gamma_5 C S^{dT}_{bb'}(x)CS^u_{cc'}(x))\\ &+ \beta\ \mathrm{Tr}[S^{uT}_{aa'}(x)C\gamma_5 S^d_{bb'}C]S^u_{cc'}(x)\gamma_5\\ &+ \beta S^u_{aa'}(x)CS^{dT}_{bb'}(x)C\gamma_5 S^u_{cc'}(x)\gamma_5\\ &+ \beta^2\mathrm{Tr}[S^{uT}_{aa'}(x)CS^d_{bb'}(x)C]\gamma_5 S^u_{cc'}(x)\gamma_5\\ &+ \beta^2\gamma_5 S^u_{aa'}(x)CS^{dT}_{bb'}(x)CS^u_{cc'}(x)\gamma_5\Big\}\end{aligned} \tag{5.2}$$

When considering the propagator specified in chapter 4 we deserve that the expansion in m_q introduces many logarithms. Regarding the Fourier transform in the correlator this implies that we have to cope with functions of the type

$$\frac{\log^k(-m_q^2x^2/4)}{(x^2)^n}, \quad k = 0, 1, 2; n = 0, ..., 4$$

The formulae given in eq. (3.17) are not sufficient. The same is true for the Borel transform. In Appendix A and B we therefore derive an efficient algorithm for the treatment of these functions. The method can in principle be used for arbitrary k and n. Appendix C lists all required formulas for the evaluation of eq. (5.2).

Perturbative corrections proportional to α_s^n for the leading terms (not including m_q) are taken into account as usual in sum rules in the leading logarithmic approximation through anomalous-dimension factors [4]. After the Borel transform, the effect of these corrections is to multiply each term on the OPE side by the factor [4, 10]

$$L^{-2\Gamma_\eta+\Gamma_{O_n}} \equiv \left[\frac{\log(M/\Lambda_{\mathrm{QCD}})}{\log(\mu/\Lambda_{\mathrm{QCD}})}\right]^{-2\Gamma_\eta+\Gamma_{O_n}} \tag{5.3}$$

where Γ_η is the anomalous dimension factor of the interpolating field η, Γ_{O_n} is the anomalous dimension of the corresponding local operator, μ is the normalization point of the OPE, and Λ_{QCD} is the QCD scale parameter. For higher dimensional condensates or terms including powers of m_q we do not include these factors because the uncertainties in the condensates are dominant. We use $\Lambda_{\mathrm{QCD}} = 100\,\mathrm{MeV}$ which is at the lower end of the range used in QCD sum rules: $100\,\mathrm{MeV} < \Lambda_{\mathrm{QCD}} < 200\,\mathrm{MeV}$ (see for example [6, 19]). The predictions will be rather insensitive to this value. $\mu = 500\,\mathrm{MeV}$ is used for the low mass limit (in accordance with the sum rule literature). As we shall see, the Borel regime will move upward when increasing m_q. In order to retain reasonable correction factors (5.3) we increase μ with m_q by linearly interpolating between $500\,\mathrm{MeV}$ at $m_q = 0$ and $1000\,\mathrm{MeV}$ at $m_q = 200\,\mathrm{MeV}$. This choice seems quite arbitrary. However, since the dependence is logarithmic the predictions are not too sensitive to the precise value of μ.

The resulting sum rule related to the structure $\mathbb{1}$ with interpolating field (5.1) is given by

$$
\begin{aligned}
\lambda_{\mathrm{N}}^2 M_{\mathrm{N}} e^{-M_{\mathrm{N}}^2/M^2} = \Pi_s'(M^2) \equiv & \\
& -\frac{7-2\beta-5\beta^2}{16\pi^2}\langle\bar{q}q\rangle M^4 E_1 + \frac{7-2\beta-5\beta^2}{16\pi^2}\langle\bar{q}D^2q\rangle M^2 E_0 L^{-14/27} \\
& -\frac{1-2\beta+\beta^2}{32\pi^2}\langle g_s\bar{q}\sigma\!\cdot\! Gq\rangle M^2 E_0 L^{-14/27} - \frac{19+10\beta-29\beta^2}{288}\langle\bar{q}q\rangle\left\langle\frac{\alpha_s}{\pi}G^2\right\rangle \\
& +\frac{7-2\beta-5\beta^2}{64\pi^4} m_q M^6 E_2 L^{-8/9} + \frac{2(2+2\beta+5\beta^2)}{3} m_q\langle\bar{q}q\rangle^2 \\
& +\frac{5+2\beta-7\beta^2}{128\pi^2} m_q\left\langle\frac{\alpha_s}{\pi}G^2\right\rangle M^2 E_0 + \frac{5+2\beta+5\beta^2}{12} m_q\langle\bar{q}q\rangle\langle g_s\bar{q}\sigma\!\cdot\! Gq\rangle\frac{1}{M^2} \\
& +\frac{1}{128\pi^2} m_q\left\langle\frac{\alpha_s}{\pi}G^2\right\rangle M^2\left[H(M^2)(12\beta^2-12)-21+6\beta+15\beta^2\right] \\
& +\frac{3(1-2\beta-5\beta^2)}{4\pi^2} m_q^2\langle\bar{q}q\rangle M^2 E_0 - \frac{13-36\beta-85\beta^2}{48\pi^2} m_q^2\langle\bar{q}D^2q\rangle \\
& +\frac{3-3\beta^2}{16\pi^2} m_q^2\langle g_s\bar{q}\sigma\!\cdot\! Gq\rangle + \frac{85+35\beta+109\beta^2}{144} m_q^2\langle\bar{q}q\rangle\left\langle\frac{\alpha_s}{\pi}G^2\right\rangle\frac{1}{M^2} \\
& -\frac{m_q^2}{64\pi^2}\langle g_s\bar{q}\sigma\!\cdot\! Gq\rangle\left[16\left(H(M^2)\right)(1+\beta+\beta^2)-(19+10\beta+19\beta^2)\right] \\
& -\frac{5+2\beta+5\beta^2}{24} m_q^2\langle\bar{q}q\rangle\left\langle\frac{\alpha_s}{\pi}G^2\right\rangle\frac{1}{M^2}\left[H(M^2)+1\right] \\
& -\frac{5+2\beta+5\beta^2}{2} m_q^3\langle\bar{q}q\rangle^2\frac{1}{M^2} - \frac{9(3-2\beta-5\beta^2)}{64\pi^4} m_q^3 M^4 E_1 \\
& +\frac{3(-7+2\beta+5\beta^2)}{64\pi^4} m_q^3 M^4\left[H(M^2)-\frac{1}{2}\right] \\
& -\frac{m_q^3}{1152\pi^2}\left\langle\frac{\alpha_s}{\pi}G^2\right\rangle\left[H(M^2)(153+234\beta+261\beta^2)+289+550\beta+781\beta^2\right] \\
& +\frac{m_q^3}{64\pi^2}\left\langle\frac{\alpha_s}{\pi}G^2\right\rangle(5+2\beta+5\beta^2)\left[\left(H(M^2)+1\right)^2-\frac{\pi^2}{6}\right] \\
& -\frac{m_q^3}{64\pi^2}\left\langle\frac{\alpha_s}{\pi}G^2\right\rangle(1-2\beta+\beta^2)\left[\left(H(M^2)+1\right)\left(H(M^2)+\frac{3}{2}\right)-\frac{\pi^2}{6}\right] \qquad (5.4)
\end{aligned}
$$

where we have defined

$$H(M^2) = \log\frac{M^2}{m_q^2} + \gamma_E.$$

As expected, there is a perturbative term involving the quark mass in leading order $\sim m_q M^6$. A first glance shows that $\beta \approx -1$ makes the contribution of this term positive. Thus it goes into the right direction. The same holds for the $m_q\langle\bar{q}q\rangle^2$ term. The sum rule connected with the structure

$\not q$ and with interpolating field (5.1) is given by.

$$
\begin{aligned}
\lambda_{\rm N}^2 e^{-M_{\rm N}^2/M^2} = {} & \Pi_q'(M^2) \equiv \\
& \frac{5+2\beta+5\beta^2}{256\pi^4} M^6 E_2 L^{-4/9} + \frac{7-2\beta-5\beta^2}{6} \langle\bar q q\rangle^2 L^{4/9} \\
& + \frac{5+2\beta+5\beta^2}{256\pi^2} \left\langle \frac{\alpha_s}{\pi} G^2 \right\rangle M^2 E_0 L^{-4/9} + \frac{1-2\beta+\beta^2}{24} \langle\bar q q\rangle \langle g_s \bar q \sigma\cdot G q\rangle \frac{1}{M^2} \\
& - \frac{7-2\beta-5\beta^2}{6} \langle\bar q q\rangle \langle\bar q D^2 q\rangle \frac{1}{M^2} + \frac{-13+14\beta+35\beta^2}{32\pi^2} m_q \langle\bar q q\rangle M^2 E_0 \\
& + \frac{19-2\beta-5\beta^2}{16\pi^2} m_q \langle\bar q D^2 q\rangle + \frac{1+\beta+\beta^2}{8\pi^2} m_q \langle g_s \bar q \sigma\cdot G q\rangle \\
& + \frac{m_q}{48} \langle\bar q q\rangle \left\langle \frac{\alpha_s}{\pi} G^2 \right\rangle \frac{1}{M^2} \left[\left(H(M^2)+4\right)(7-2\beta-5\beta^2) \right] \\
& + \frac{3(\beta^2-1)}{8\pi^2} m_q \langle g_s \bar q \sigma\cdot G q\rangle H(M^2) + \frac{19+2\beta+41\beta^2}{576} m_q \langle\bar q q\rangle \left\langle \frac{\alpha_s}{\pi} G^2 \right\rangle \frac{1}{M^2} \\
& - \frac{2+2\beta+5\beta^2}{16\pi^4} m_q^2 M^4 E_1 + \frac{-41+22\beta+55\beta^2}{24} m_q^2 \langle\bar q q\rangle^2 \frac{1}{M^2} \\
& - \frac{5+2\beta+5\beta^2}{128\pi^2} m_q^2 \left\langle \frac{\alpha_s}{\pi} G^2 \right\rangle - \frac{4-2\beta-3\beta^2}{12} m_q^2 \langle\bar q q\rangle \langle g_s \bar q \sigma\cdot G q\rangle \frac{1}{M^4} \\
& - \frac{m_q^2}{768\pi^2} \left\langle \frac{\alpha_s}{\pi} G^2 \right\rangle \left[H(M^2)(656-424\beta-1072\beta^2) + 857 - 694\beta - 1735\beta^2) \right] \\
& + \frac{3(\beta^2-1)}{32\pi^2} m_q^2 \left\langle \frac{\alpha_s}{\pi} G^2 \right\rangle \left[2\left(H(M^2)+1\right) - \left(H(M^2)+1\right)^2 + \frac{\pi^2}{6} - 2 \right] \\
& - \frac{-5+22\beta+55\beta^2}{16\pi^2} m_q^3 \langle\bar q q\rangle + \frac{7-2\beta-5\beta^2}{4\pi^2} m_q^3 \langle\bar q q\rangle H(M^2) \\
& - \frac{19-26\beta-65\beta^2}{48\pi^2} m_q^3 \langle\bar q D^2 q\rangle \frac{1}{M^2} - \frac{7-2\beta-5\beta^2}{8\pi^2} m_q^3 \langle\bar q D^2 q\rangle \frac{1}{M^2} \left[H(M^2)+1 \right] \\
& + \frac{m_q^3}{64\pi^2} \langle g_s \bar q \sigma\cdot G q\rangle \frac{1}{M^2} \left[H(M^2)(12+12\beta^2) - (28+4\beta-44\beta^2) \right] \\
& + \frac{m_q^3}{96} \langle\bar q q\rangle \left\langle \frac{\alpha_s}{\pi} G^2 \right\rangle \frac{1}{M^4} \left[H(M^2)(8+8\beta-16\beta^2) + (7+10\beta-17\beta^2) \right] \\
& - \frac{67-50\beta-53\beta^2}{288} m_q^3 \langle\bar q q\rangle \left\langle \frac{\alpha_s}{\pi} G^2 \right\rangle \frac{1}{M^4}
\end{aligned}
\tag{5.5}
$$

The first m_q-correction in this sum rule is the one involving the quark condensate, as expected from dimensionality. Again, inserting $\beta = -1$ makes the prefactor positive, and thereby the whole term negative. So, this term also supports the rise of the nucleon mass with increasing m_q. These conclusions indicate that the sum rules are consistend with the expected qualitative behaviour.

5.2 Sum Rule Analysis

It is very important that the method of analysis applied to the sum rules properly incorporates important features (such as the pole plus continuum ansatz on the phenomenological side and

OPE convergence) and takes care of the uncertainties in the condensates as input parameters on the QCD side. For the analysis of the sum rules we thus follow the approach proposed in [19]. The two sum rules are considered over a Borel window which dependends on m_q. The main goal in choosing the Borel window is to keep the continuum contributions at a reasonable size. The spectral model for the phenomenological side strongly relies upon the validity of the pole plus approximate continuum model. To quantify pole dominance we require that the continuum contribution to the modified OPE part in each Π_i' does not exceed fifty percent. Another issue is the contribution from higher order condensates. For convergence of the OPE it is imperative that they are not too big. This question was studied in detail in [19]. The most important of these terms are the ones without a power of m_q. With increasing m_q lower dimensional condensate terms with a power of m_q become more important and the significance of the high dimensional condensates is reduced. Furthermore the Borel parameters M^2 involved will rise with m_q which leads to a suppression of these terms since they carry either no or an inverse power of M^2. In the following outline of the method of analysis we will assume that we have already found a valid Borel window $[M_a, M_b]$.

The condensate values are not known accurately. It is therefore important to investigate how their uncertainties propagate into predicted observables. A reliable way of qualifying the sensitivity of the observables to the input parameters has to be found. The main idea behind the method of [19] is to address the uncertainties in the condensates by a Monte Carlo based error analysis: many different sets of condensates, i.e. $(\langle \bar{q}q \rangle, \left\langle \frac{\alpha_s}{\pi} G^2 \right\rangle, \lambda_q^2)$, are generated by assuming Gaussian distributions for each condensate and taking randomly chosen values for each one. Each parameter set gives values for M_{N}, s, and λ_{N}^2. Averaging the results for each parameter set and calculating standard deviations provides an overall prediction as well as an error estimate for each of the three phenomenological parameters M_{N}, s, and λ_{N}^2. In this manner the full predictive power of sum rules can be determined.

First of all, a measure for the agreement of the phenomenological and the OPE sides of the two sum rules has to be found. For clarity, we restrict the explanation to one sum rule for the moment. A natural choice would be some sort of an $L^2([M_a, M_b])$ norm. Consider a given Borel window $[M_a, M_b]$ and evenly spaced points $M_j, j = 1, ..., N_B$ therein. Then an appropriate norm is given by

$$||f||_B^2 = \sum_{j=1}^{N_B} f(M_j)^2.$$

This norm obviously treats all points in the Borel window equally. However, the uncertainties in the OPE are larger at the lower end due to relatively higher contributions from higher order condensates and their large uncertainties. One can quantify this M-dependent OPE-uncertainty by inserting many condensate sets for fixed M_j and considering the sensitivity of the OPE at that point to condensate values through the variance of the results. We generate N_p normally distributed condensate sets $(\langle \bar{q}q \rangle_k, \left\langle \frac{\alpha_s}{\pi} G^2 \right\rangle_k, (\lambda_q^2)_k), k = 1, \ldots, N_p$ and compute

$$\sigma_{\mathrm{OPE}}^2(M_j) = \frac{1}{N_p - 1} \sum_{k=1}^{N_p} \left[\Pi^{\mathrm{OPE}}(M_j; k) - \overline{\Pi^{\mathrm{OPE}}}(M_j) \right]^2 \qquad \text{where}$$

$$\overline{\Pi^{\mathrm{OPE}}}(M_j) = \frac{1}{N_p} \sum_{k=1}^{N_p} \Pi^{\mathrm{OPE}}(M_j; k).$$

Here $\Pi^{\mathrm{OPE}}(M_j;k)$ denotes the pure OPE (without the s-dependent corrections to M^2, M^4, M^6) with the k-th condensate set $(\langle\bar{q}q\rangle_k, \left\langle\frac{\alpha_s}{\pi}G^2\right\rangle_k, (\lambda_q^2)_k)$. Now the χ^2-measure for the k-th condensate set is defined by:

$$\chi_k^2 = \sum_{j=1}^{N_B} \frac{\left[\Pi^{\mathrm{OPE}}(M_j;k) - \Pi^{\mathrm{phen}}(M_j;M_{\mathrm{N}},s_0,\lambda_{\mathrm{N}})\right]^2}{\sigma_{\mathrm{OPE}}^2(M_j)}$$

where $\Pi_i^{\mathrm{phen}}(\cdot;M_{\mathrm{N}},s,\lambda_{\mathrm{N}}^2)$ is the l.h.s. of the sum rules plus all s_0-dependent terms of the right hand side. $\sigma_{\mathrm{OPE}}^2(M_j)$ will, of course, decrease as M_j increases, placing emphasis on the upper end of the Borel window where the the OPE is supposed to be more reliable.
All preceding considerations apply to both sum rules, the one for Π_s and the one for Π_q. In order to get an optimal phenomenological parameter set for both sum rules we have to combine the two χ_k^2:

$$\tilde{\chi}_k^2 = \chi_{k,(s)}^2 + \chi_{k,(q)}^2.$$

The measure $\tilde{\chi}_k^2$ is now minimized numerically yielding results $M_{\mathrm{N}}^{(k)}$, $s_0^{(k)}$, and $(\lambda_{\mathrm{N}}^2)^{(k)}, k = 1,\ldots,N_p$. Eventually the prediction and an error estimate for M_{N} are given by

$$\overline{M}_{\mathrm{N}} = \frac{1}{N_p}\sum_{k=1}^{N_p} M_{\mathrm{N}}^{(k)} \qquad \text{resp.} \qquad \sigma_{M_{\mathrm{N}}}^2 = \frac{1}{N_p-1}\sum_{k=1}^{N_p}(M_{\mathrm{N}}^{(k)} - \overline{M}_{\mathrm{N}})^2. \tag{5.6}$$

$\bar{s}_0$ and $\sigma_{s_0}^2$ resp. $\bar{\lambda}_{\mathrm{N}}^2$ and $\sigma_{\lambda_{\mathrm{N}}^2}^2$ are defined analogously. The procedure of finding the Borel window and an adequate β is now found self-consistently in the following way. We start by guessing a Borel window and a value for β and optimize the measure χ^2 for the central condensate values. If the continuum turns out to be too large in one of the two sum rules, either the Borel window is altered or β is readjusted. This process is iterated until satisfactory $[M_a, M_b]$ and β are found. We decide to apply another criterion concerning the agreement of the two sides of each sum rule, namely we try to avoid errors exceeding 15% on either end of the window. As already pointed out earlier it is necessary for a reliable analysis that when having found the window and β a slight variation of both elements does not result in a significant change of the output.

5.3 Results

First, we analyze the sum rules using the factorization hypothesis $\langle\bar{q}q\bar{q}q\rangle = \langle\bar{q}q\rangle^2$. The two condensates involving gluons are fixed:

$$\begin{aligned} \left\langle\frac{\alpha_s}{\pi}G^2\right\rangle^{1/4} &= 330\,\mathrm{MeV} & \sigma_{\left\langle\frac{\alpha_s}{\pi}G^2\right\rangle^{1/4}} &= 20\,\mathrm{MeV} \\ \lambda_q^2 &= 0.36\,\mathrm{GeV}^2 & \sigma_{\lambda_q^2} &= 1.0\,\mathrm{GeV}^2, \end{aligned} \tag{5.7}$$

where $\langle g_s\bar{q}\sigma\cdot Gq\rangle = 2\lambda_q^2\langle\bar{q}q\rangle$. For $\langle\bar{q}q\rangle$ different central values are used. It was pointed out in [19] that under the conditions stated in the previous section no Borel window for the sum rules at $m_q = 0$ is found. The M^6-term in the sum rule for Π_q (5.5) carries a potentially very large continuum factor E_2 which prevents the formation of a valid Borel regime. Still, the inset of the m_q-terms leads to an attenuation of the dominance of this term and a valid and sufficiently large Borel regime is found for $40\,\mathrm{MeV} \lesssim m_q$, see fig. 5.1. An appropriate value for β is found

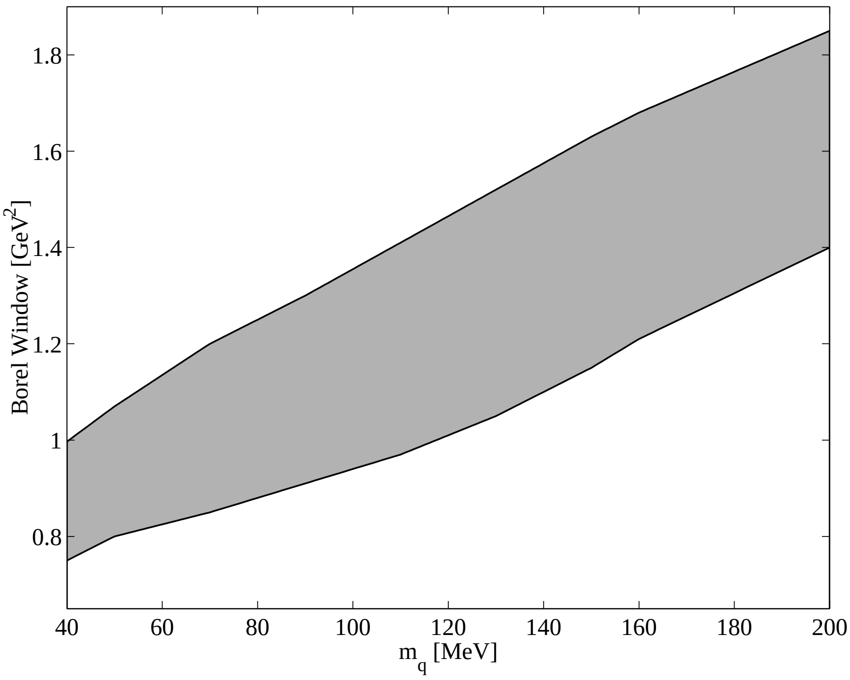

Figure 5.1: The valid Borel window as a function of m_q

to be -1.2 up to quark mass 70 MeV, which is the value identified as the optimal one for this sum rule in the chiral limit in [19]. For $m_q \geq 80\,\mathrm{MeV}$ $\beta = -1.1$ is used. In order to compare the results to lattice data, the quark mass is converted to the squared pion mass via the Gell-Mann–Oakes–Renner relation (2.4) which is known to hold in a large range of m_q [20]. The results of calculations using $N_p = 500$ parameter sets performed for $\langle \bar{q}q \rangle$ ranging between $(-235 \pm 20\,\mathrm{MeV})^3$ and $(-245 \pm \,\mathrm{MeV})^3$ in the quark mass range $m_q = 50, \ldots, 200\,\mathrm{MeV}$ are displayed in the figures 5.2 and 5.3. The error bands are constructed from the mean values and the standard deviations that come from the Monte Carlo uncertainty analysis. Figs.5.2 and 5.3 show that the sum rule predictions are not completely off the lattice data in either case, which is a nontrivial fact. The errors stay at the 10% level throughout the whole quark mass range. When increasing the quark condensate, the mass rises for fixed m_q, just as expected. This effect is partially corrected by the translation of quark to squared pion mass using the GOR-relation so that the difference between the two figures is minor. This indicates that the sum rules together with the GOR-relation are quite stable concerning the input parameter $\langle \bar{q}q \rangle$. However, in both cases the sum rules provide higher masses than the Lattice simulations. When extrapolating the bands linearly to the low quark mass range the mean values tend to $\approx 1000\,\mathrm{MeV}$ such that the physical point is at most at the boundary of the error bands thanks to a slightly higher slope than the one indicated by the Lattice data. What we can conclude is that the analysis of the sum rules using factorization and disregarding α_s-corrections already gives a qualitatively reasonable prediction of $M_{\mathrm{N}}(m_\pi^2)$. Compared to the case $m_q = 0$ a stabilization of the sum rules driven by m_q-terms takes place which is manifest in the existence of relatively broad Borel regimes.

The results for s_0 and λ_{N}^2 are physically reasonable, especially in the case of s_0. Nevertheless, the errors associated with these two parameters come out extremely large, typically at the 100%

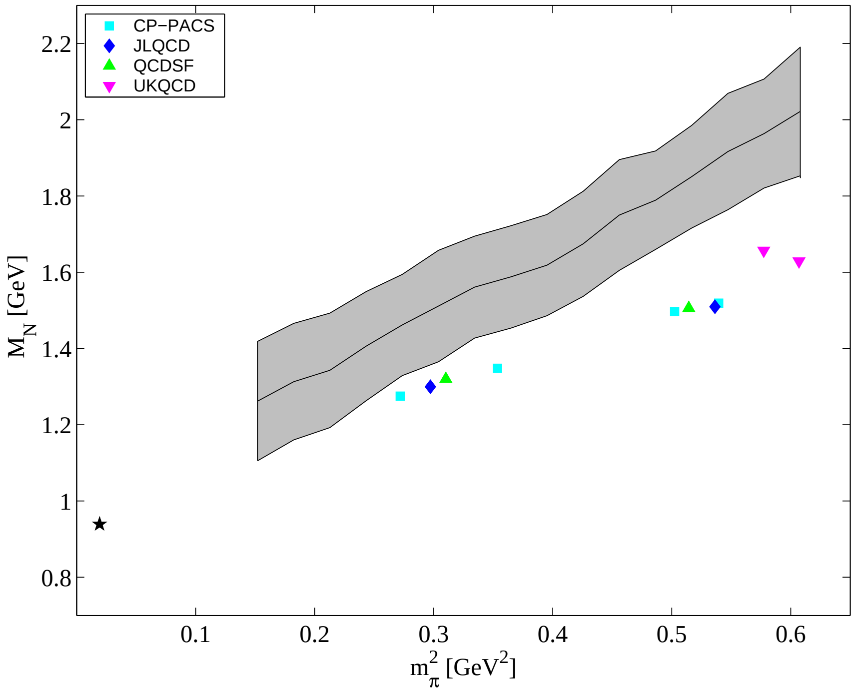

Figure 5.2: Sum rule predictions of $M_{\rm N}(m_\pi^2)$ using $\langle\bar{q}q\rangle = (-235\,{\rm MeV})^3$

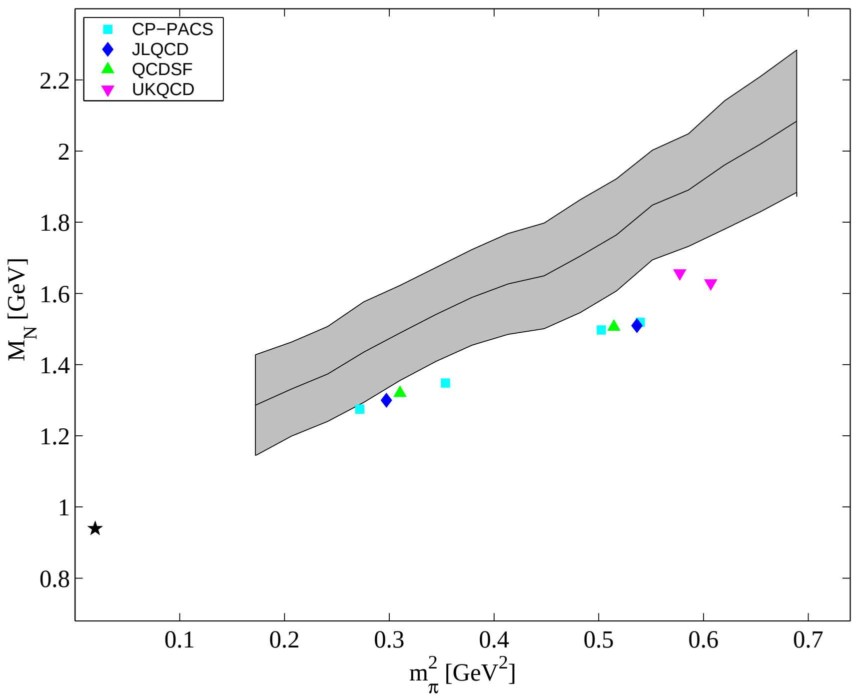

Figure 5.3: Sum rule predictions of $M_{\rm N}(m_\pi^2)$ using $\langle\bar{q}q\rangle = (-245\,{\rm MeV})^3$

level. The reason is that there occur extreme outliers which make the standard deviations big, whereas the mean values stay at a moderate and sensible magnitude. In any case, for almost all condensate sets, the condition $s_0 > M_{\mathrm{N}}$ holds. A more detailed interpretation of the mean values $\bar{s}_0(m_q)$ in terms of a real spectral parameter is not possible.
To estimate the significance of Ioffe's formula (1.1) it is interesting to resolve the different contributions to the sum rule (5.4) as a function of m_q. Fig. 5.4 distinguishes between pieces involving purely perturbative terms, condensates involving two quarks, and (factorized) condensates involving four quarks, i.e. $\langle \bar{q}q \rangle^2$, $\langle \bar{q}q \rangle \langle g_s \bar{q} \sigma \cdot G q \rangle$, and $\langle \bar{q}q \rangle \langle \bar{q} D^2 q \rangle$. Since the different contributions vary slightly within the Borel regime, the contributions are evaluated at the lower and upper ends of the Borel regime. The strong role played by the quark condensate terms involving $\langle \bar{q}q \rangle$

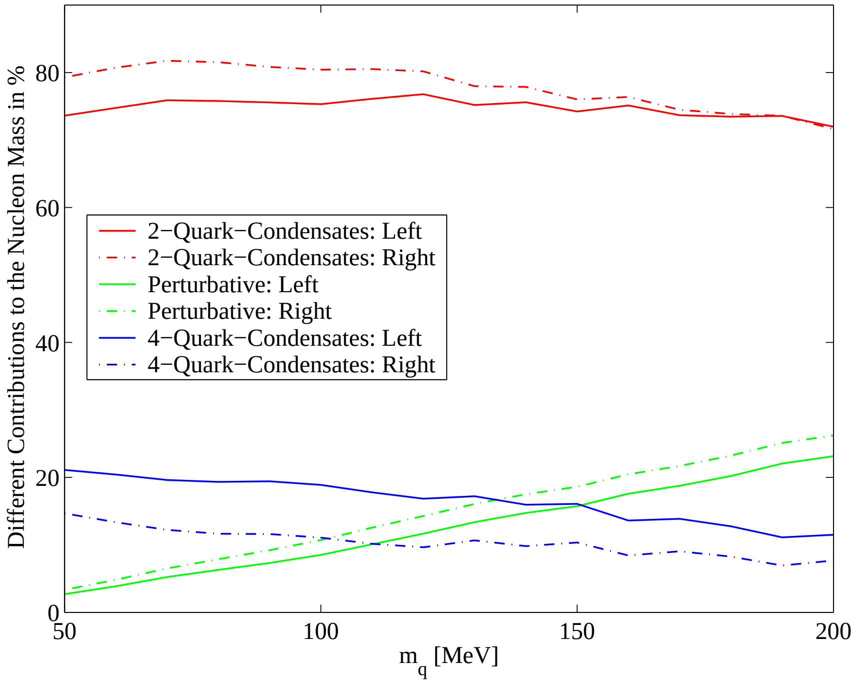

Figure 5.4: Individual contributions of purely perturbative terms as well as condensates involving two resp. four quarks to the sum rule (5.4) evaluated at the left and right end of the Borel regime as a function of the quark mass.

is almost independent of m_q. The contribution of purely perturbative terms $m_q M^6$ and $m_q^3 M^4$ increases with the quark mass because of higher M^2, for which the suppression of higher dimensional condensates improves. This becomes obvious in the behaviour of the 4-quark condensate terms.

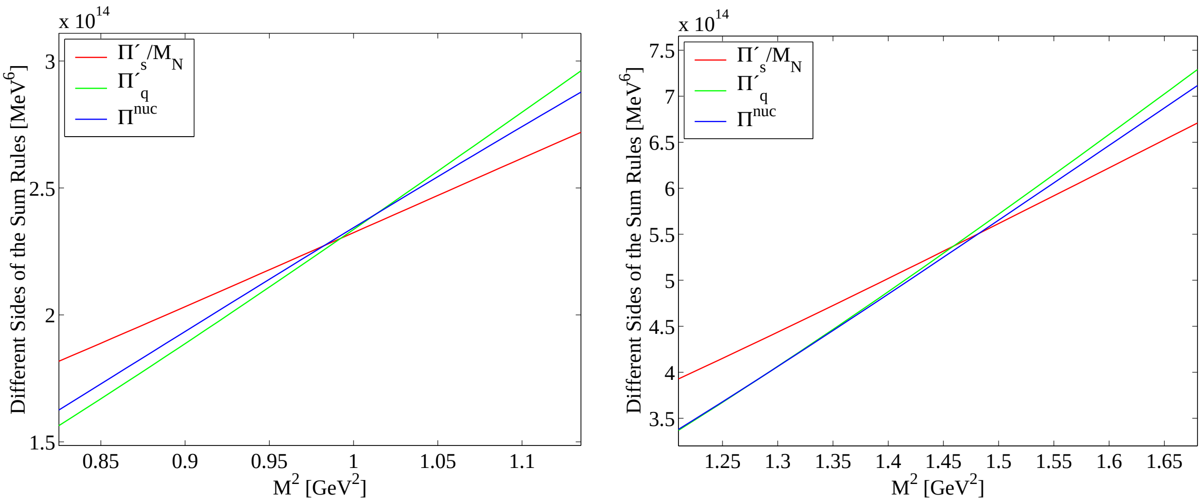

Figure 5.5: Comparison of different sum rule sides at $m_q = 60\,\mathrm{MeV}$ (left) and $m_q = 160\,\mathrm{MeV}$ (right) along the particular Borel regimes.

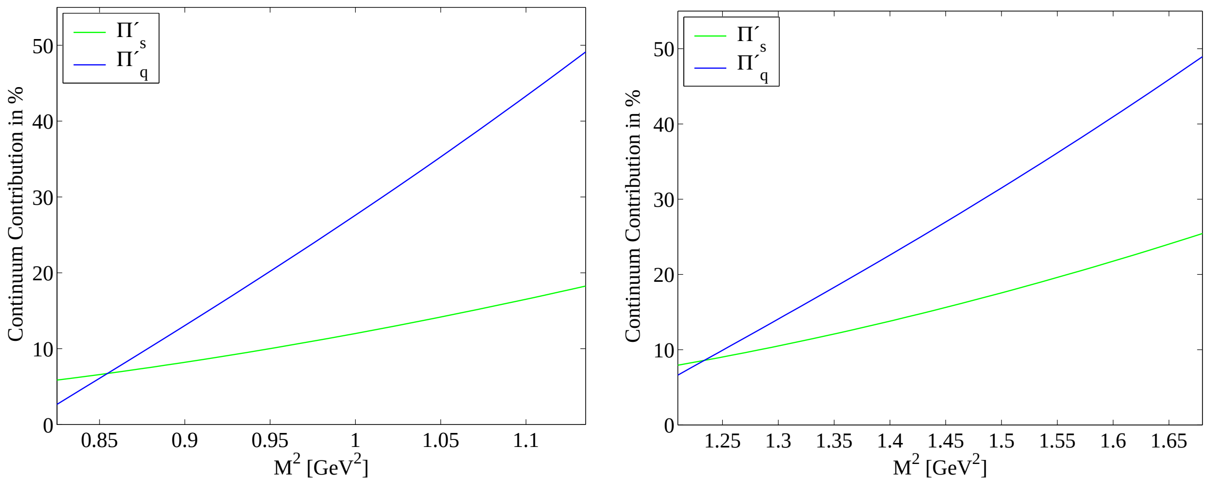

Figure 5.6: Continuum contributions to the OPE sides at $m_q = 60\,\mathrm{MeV}$ and $m_q = 160\,\mathrm{MeV}$

Important points of the sum rule analysis include the continuum contribution to the OPE parts, a resolution of the quark mass orders and the amount of consistency of the system of sum rules after the optimization of the phenomenological parameters. In general, these questions depend on the Borel parameter and have to be studied along the whole Borel regime. For example, rhe size of agreement of different sides of the sum rules for optimized parameters M_{N}, s_0, and λ_{N}^2 for the central condensate values can be seen in fig.5.5 where the two OPE sides Π'_s, Π'_q and the nucleon pole term Π^{nuc} are compared. Here, we have defined

$$\Pi^{\mathrm{nuc}} = \lambda_{\mathrm{N}}^2 e^{-M_{\mathrm{N}}^2/M^2}.$$

The deviations depend on the size of the Borel regime and have been limited to $\approx 15\%$ in the

determination of the Borel interval.
The form of the continuum contributions to the right hand side of the sum rules (5.4) and (5.5) can be obtained from fig. 5.6. As already pointed out, the continuum contribution to (5.5) including the continuum factor E_2 primarily restricts the upper end of the Borel window.

Another important point is the validity of the $\mathcal{O}(m_q^3)$-mass expansion. An estimate of its

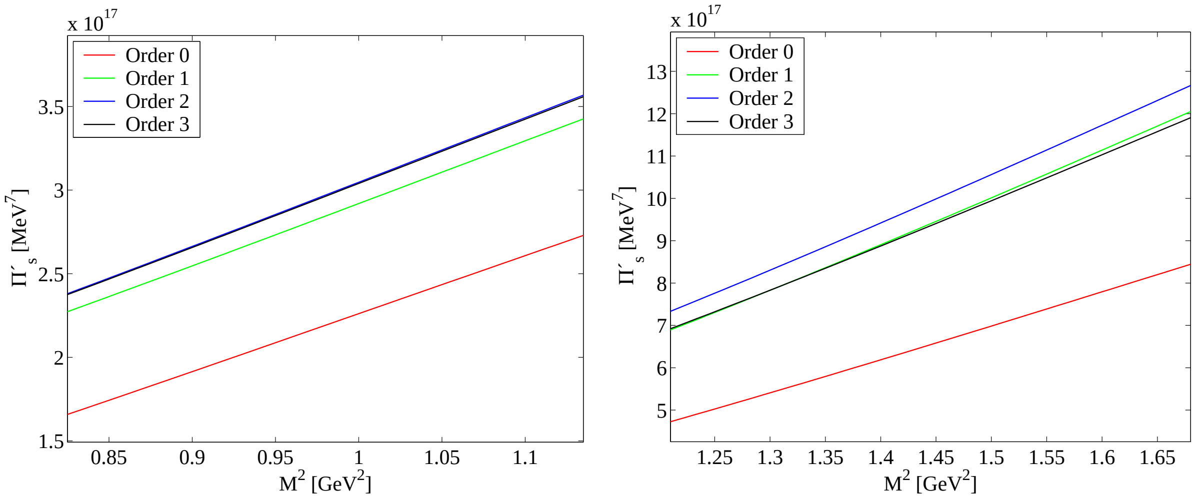

Figure 5.7: Different orders in the OPE of (5.4) at $m_q = 60\,\mathrm{MeV}$ and $m_q = 160\,\mathrm{MeV}$

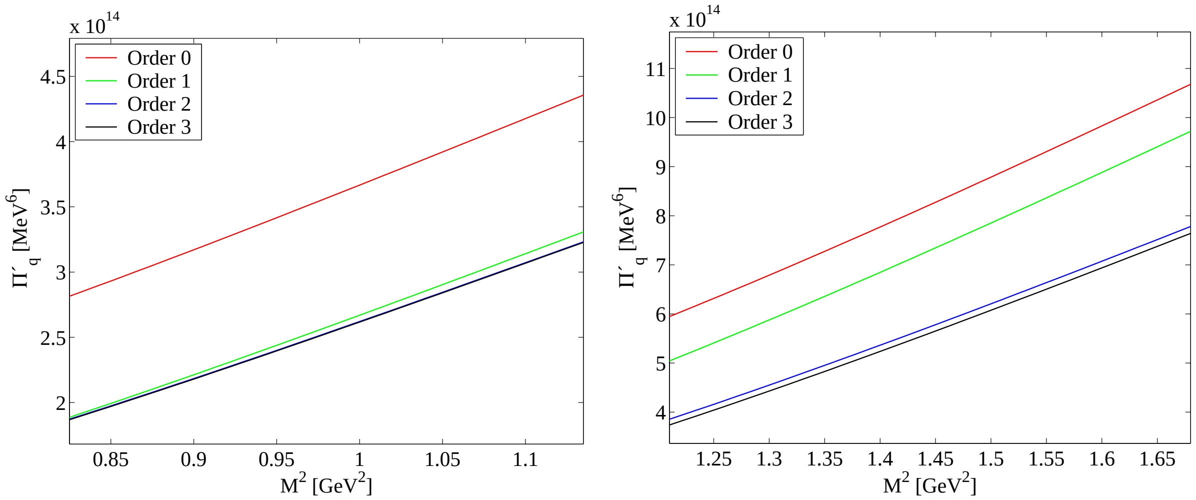

Figure 5.8: Different orders in the OPE of (5.5) at $m_q = 60\,\mathrm{MeV}$ and $m_q = 160\,\mathrm{MeV}$

reliability is provided by figs. 5.7 and 5.8 where the contributions of different orders of m_q to the OPEs of the two sum rules are displayed. In the case of the sum rule (5.4) the third order shows up at $m_q = 160\,\mathrm{MeV}$ due to the term m^3M^4. Here, it can be summarized that the expansion up to order three is definitely sufficient, considering the limited accuracy on the input condensate side.
In the sum rule (5.5) the third order does not have any significance, whereas the second order

is quite prominently present with a conbtribution around 20% along the Borel window, driven mainly by the terms $\sim m_q^2 M^4$ and $\sim m_q^2 \langle\bar{q}q\rangle^2/M^2$. Considering the involved condensates it is not surprising that the second order exceeds the first. It is to be expected that the fourth and third order behave similarly such that a calculation of the fourth order would be necessary to be on the save side. The uncertainty emerging from the missing fourth order is estimated to be at the percent level. Another remarkable fact becoming obvious in fig. 5.8 is the size of the first order in (5.5) already at $m_q = 60\,\mathrm{MeV}$. This is a major factor in the formation of the Borel regime for quark masses higher than $\sim 50\,\mathrm{MeV}$.

5.4 Violation of Factorization and Inclusion of α_s-Corrections

The probably most prominent difficulty concerning sum rules in general (and especially nucleon sum rules) lies in the value of the four quark condensate. Even though the factorization hypothesis, i.e. the neglect of any kind of pionic dynamics involved in the four quark operator, is extremely crude, it provides the one and only naïve estimation of this parameter. In the following we parametrize the four quark condensate in terms of $\langle\bar{q}q\rangle$

$$\langle\bar{q}q\bar{q}q\rangle = \kappa\langle\bar{q}q\rangle^2 \tag{5.8}$$

and try several values for $\kappa \geq 1$ that seem to be reasonable. For simplicity, the same parametrization factor κ is used for all terms proportional to $\langle\bar{q}q\rangle^2$. The four quark condensate with the biggest influence should of course be the first $\langle\bar{q}q\rangle^2$ term in (5.5). Regarding figs. 5.2 and 5.3 a higher value of the four quark condensate should lead to a shift towards smaller $M_\mathrm{N}(m_\pi^2)$. It turns out that $\kappa \geq 3$ makes the sum rules very sensitive to β since the four quark condensate term gains importance so that its prefactor, which is a polynomial in β, gets rather decisive. This phenomenon can also be read off from large errors in the uncertainty analysis. We therefore restrict ourselves to $\kappa \in [1.0, 2.0]$. Of course, the Borel windows have to be determined anew. The determined Borel windows for $\kappa = 2$ are given in fig. 5.9 and used also for $\kappa = 1.5$. β is set to -1.35 at $m_q = 50\,\mathrm{MeV}$ and then continuously decreased to -0.95 at $m_q = 200\,\mathrm{MeV}$. The calculations are performed for $m_q \leq 200\,\mathrm{MeV}$. The results of the Monte Carlo analysis for $\kappa = 1.5$ and 2.0 (both using $\langle\bar{q}q\rangle = (-235 \pm 20\,\mathrm{MeV})^3$) are displayed in figs. 5.10 and 5.11. Just as expected, the error bands are shifted downwards compared to the calculation with $\kappa = 1$. An extrapolation to $m_\pi^2 = 0$ is hard because the near linearity of figs. 5.2 and 5.3 is lost, see especially fig. 5.11. This curved form is even more pronounced for $\kappa = 2.5$. For higher m_π^2 fig. 5.10 shows a quite large deviation from the Lattice points.

The next step of refining the sum rules (5.4) and (5.5) is the inclusion of α_s-corrections. Throughout this section we use

$$\frac{\alpha_s(1\,\mathrm{GeV}^2)}{\pi} \simeq 0.117$$

We will restrict ourselves to corrections for the leading terms in both sum rules. The first order corrected form of the coefficient of $\langle\bar{q}q\rangle$ in 5.4 is [23]

$$7\left(1 + \frac{15}{14}\frac{\alpha_s}{\pi}\right) - 2\beta\left(1 + \frac{3}{2}\frac{\alpha_s}{\pi}\right) - 5\beta^2\left(1 + \frac{7}{10}\frac{\alpha_s}{\pi}\right) \tag{5.9}$$

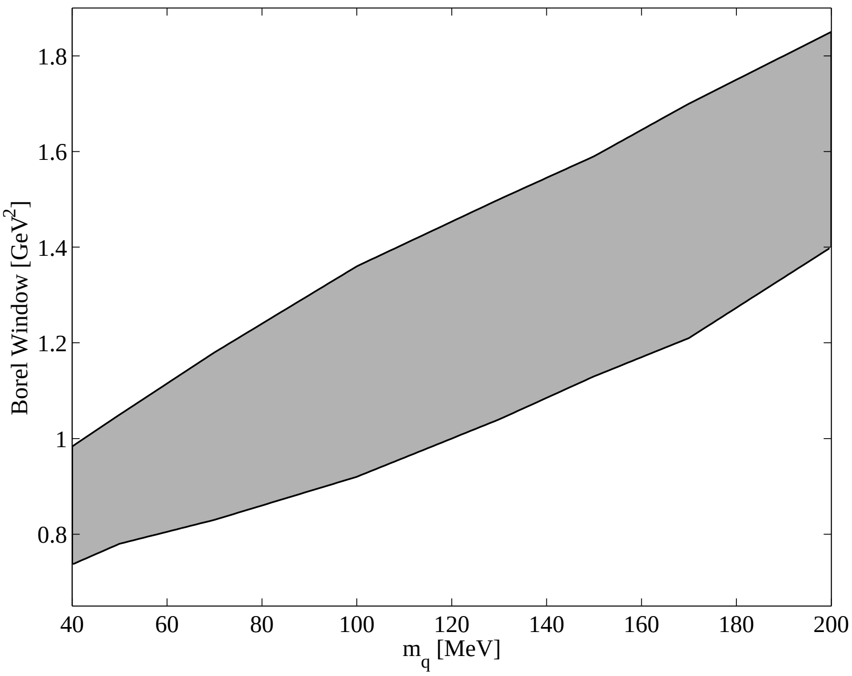

Figure 5.9: The valid Borel window for $\kappa = 2$ as a function of m_q

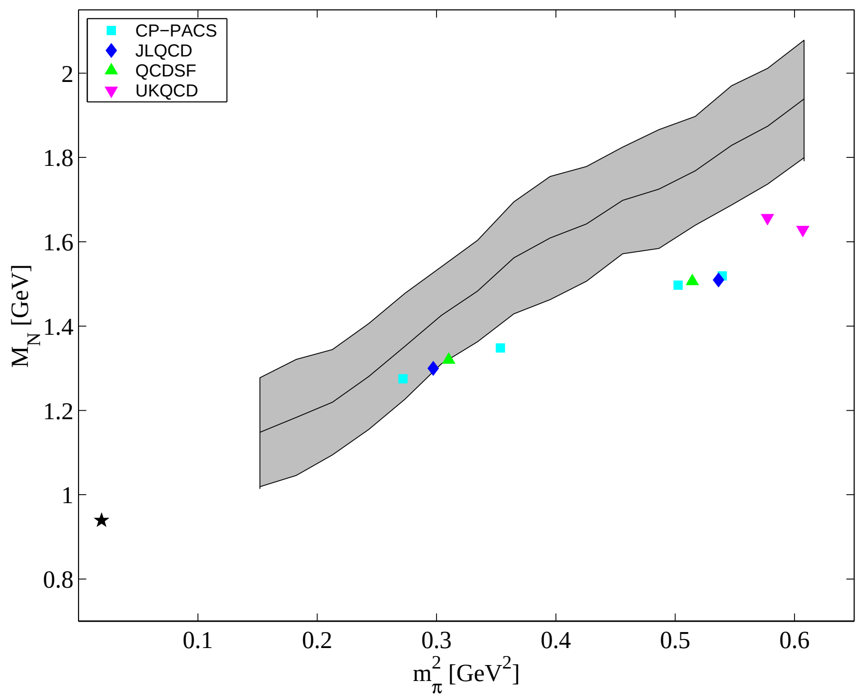

Figure 5.10: Sum rule predictions of $M_{\rm N}(m_\pi^2)$ using $\langle \bar{q}q \rangle = (-235\,\mathrm{MeV})^3$ and $\kappa = 1.5$

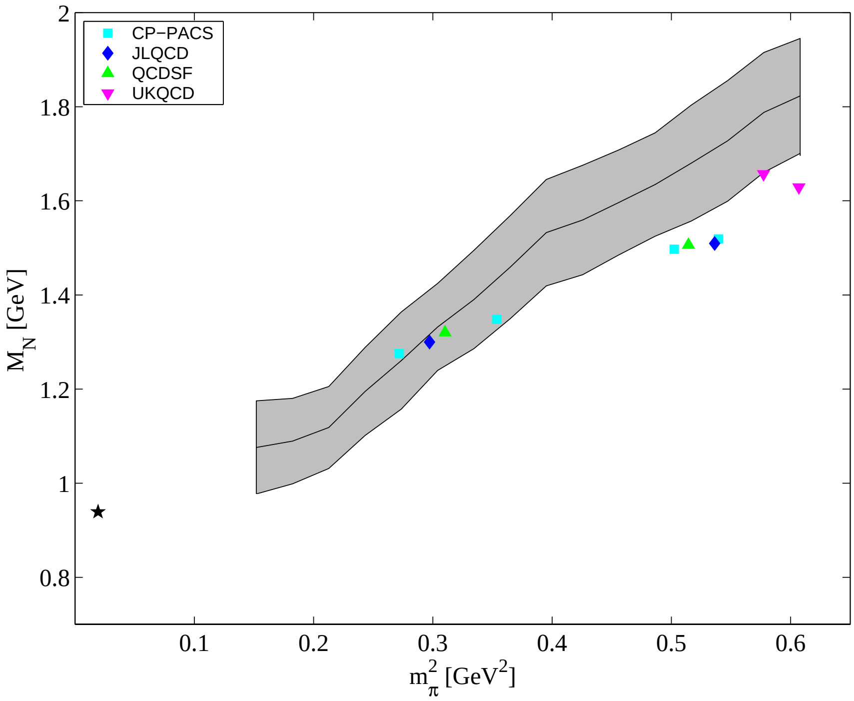

Figure 5.11: Sum rule predictions of $M_\mathrm{N}(m_\pi^2)$ using $\langle\bar{q}q\rangle = (-235\,\mathrm{MeV})^3$ and $\kappa = 2.0$

Here, the corrections are at the order of 10%. The M^6-term in 5.5 gets an α_s-correction factor given by [23]

$$1 + \frac{\alpha_s}{\pi}\left(\frac{53}{12} + \gamma_E\right) \tag{5.10}$$

where $\gamma_E = \psi(1) =\simeq 0.58$ is the Euler-Mascheroni constant. In this case the corrections are at the order of 50% which is extremely high. It was argued in [19] that in this case the convergence of the identity operator term in the OPE is not well established. We will nevertheless include the two correction factors (5.9) and (5.10) in eqs. (5.4) and (5.5) for an analysis.

Once again the Borel regimes have to be determined. The growth of the prefactor of M^6E_2 in 5.5 has no strong influence on the presence of valid Borel regimes. These are displayed in fig. 5.12. Results of the calculations using $\kappa = 1$ resp. $\kappa = 1.5$ are given in figs. 5.13 and 5.14. Figure 5.13 with $\kappa = 1$ shows a similar tendency as the calculation without α_s-corrections in fig. 5.2. The band lies slightly too high but the slope is somewhat smaller, yielding better agreement with the higher m_π^2 Lattice data. Even the extrapolation to the physical point looks better than in fig. 5.2. An increase of κ again brings the band down, in this case the agreement with the Lattice points is nice.

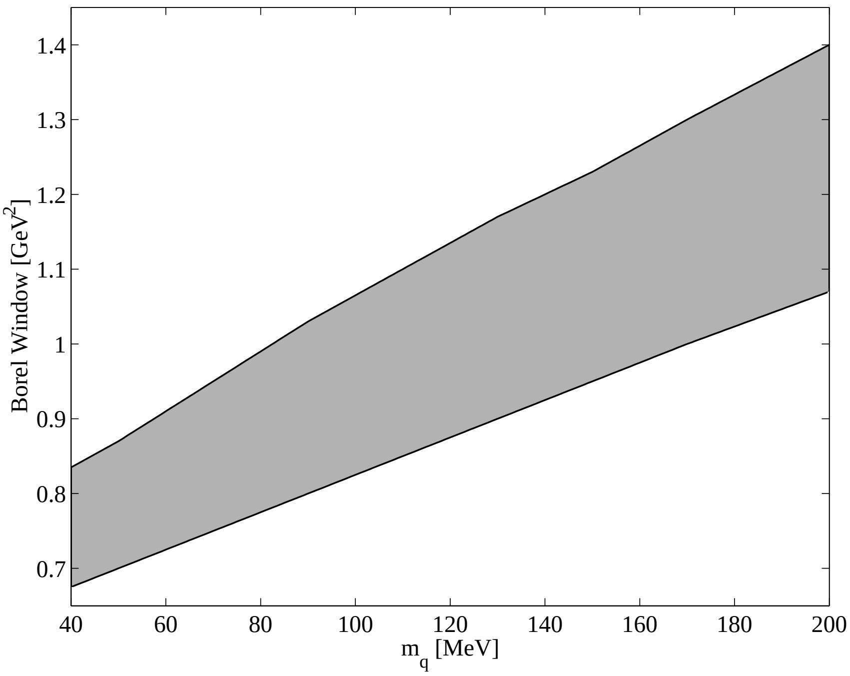

Figure 5.12: The valid Borel window for the α_s-corrected sum rules as a function of m_q

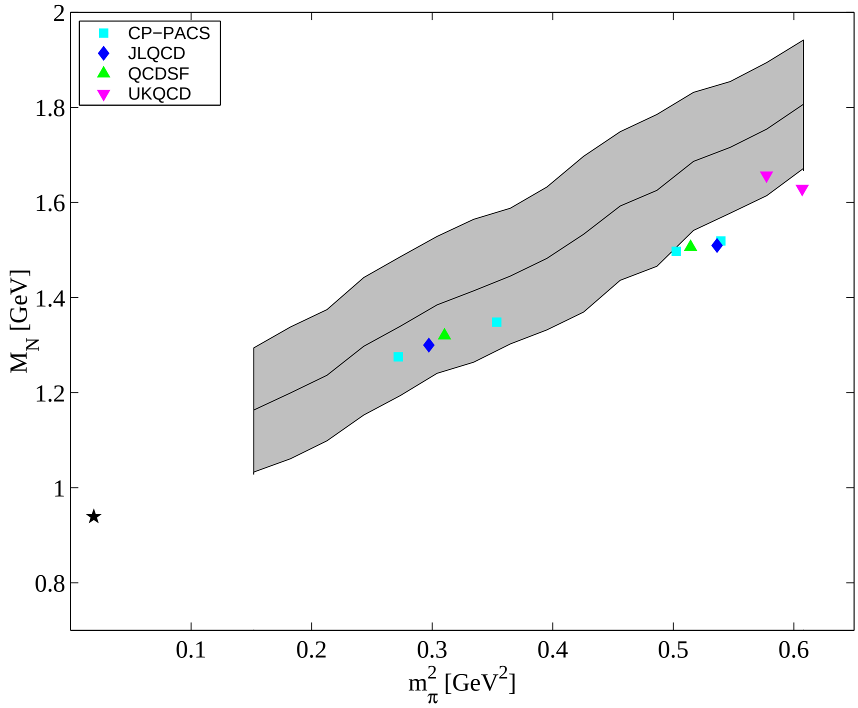

Figure 5.13: $M_{\mathrm{N}}(m_\pi^2)$ from the α_s-corrected sum rules using $\langle \bar{q}q \rangle = (-235\,\mathrm{MeV})^3$ and $\kappa = 1.0$

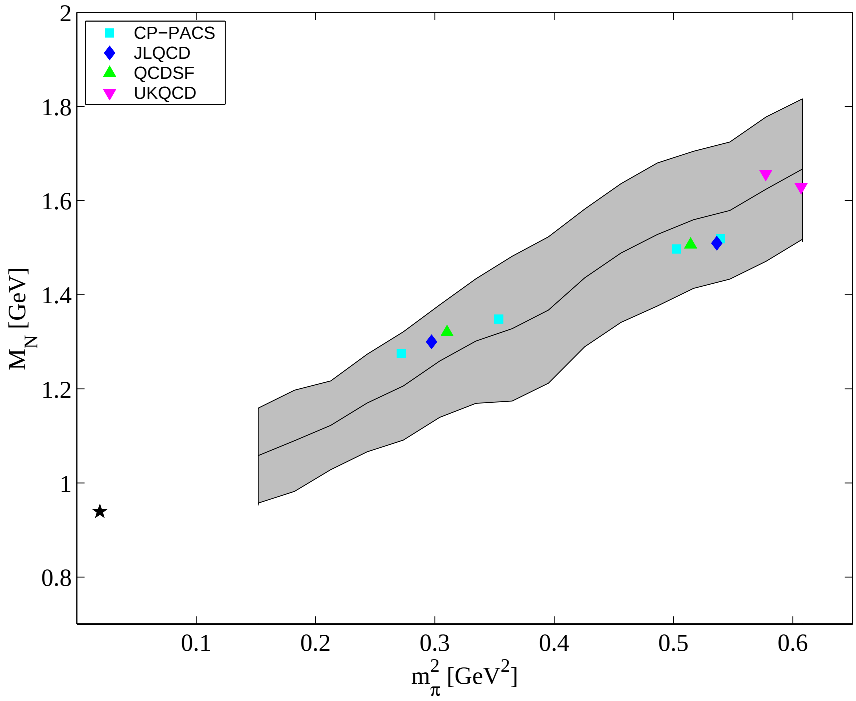

Figure 5.14: $M_{\mathrm{N}}(m_\pi^2)$ from the α_s-corrected sum rules using $\langle\bar{q}q\rangle = (-235\,\mathrm{MeV})^3$ and $\kappa = 1.5$

Summarizing this chapter, we can conclude that the extension of known sum rules for the general nucleon interpolating field gives a physically reasonable approximation of the quark mass dependence of the nucleon mass. A detailed Monte Carlo based analysis for the two sum rules relying on the factorization hypothesis yields an errorband above the Lattice results. A first refinement is a guess of the amount of violation of factorization within reasonable bounds. This procedure shifts the predictions of the sum rules down but the agreement with the Lattice results is still not convincing. A rather strong modification for lower quark masses is provided by the inclusion of α_s-corrections, since the leading term one of the sum rules is altered by 50%. Together with a parametrization of factorization the inclusion of α_s-corrections for the leading terms yields good agreement of the sum rule results with the Lattice data. To finally judge the agreement of spin-1/2 sum rules it is necessary to resolve the four quark condensate contributions in greater detail, see Chapter 7.

Chapter 6

Tensor Interpolating Field

As we have seen the sum rules for a nucleon spin-1/2 interpolating field suffer from difficulties in the small quark mass region because of uncertainties in the strongly contributing four quark condensate and large perturbative corrections. For the physical point no valid Borel regime could be found. An interesting alternative is provided by correlation functions of appropriate tensor fields for the nucleon, which are known to have fair overlap with the nucleon wave function [22]. In [19] sum rules for tensor fields for the nucleon at $m_q = 0$ have already been calculated and it has been observed that there are major advantages compared to the spin-1/2 case. We extend these sum rules to finite quark masses using the same techniques as in the previous chapter.

6.1 Preliminaries

The tensor interpolating field for the nucleon is [21, 24]

$$\eta_T^\mu(x) = \varepsilon^{abc}\left[\left(u^{aT}(x)C\sigma_{\kappa\lambda}d^b(x)\right)\sigma^{\kappa\lambda}\gamma_\mu u^c(x) - \left(u^{aT}(x)C\sigma_{\kappa\lambda}u^b(x)\right)\sigma^{\kappa\lambda}\gamma^\mu d^c(x)\right] \tag{6.1}$$

The nucleon to vacuum matrix element of η_T^μ is defined as

$$\langle 0|\eta_T^\mu|1/2^+, p\rangle = (\alpha p^\mu + \lambda_T\gamma^\mu)\gamma_5 u(p)$$

where $u(p)$ is the Dirac spinor of the nucleon. The γ_5 on the right-hand side matches the parity of η_T^μ. Using $\gamma_\mu\eta_T^\mu = 0$ which is obeyed by Rarita-Schwinger spinors, together with the Dirac equation $(\not{p} - M_\mathrm{N})u(p) = 0$ we get the relation

$$\alpha = \frac{4\lambda_T}{M_\mathrm{N}}$$

The spin-1/2 interpolating field $\eta_{1/2}(x) = 2(\eta_1(x) + \beta\eta_2(x))$ can easily be translated to a tensor field:

$$\eta_G^\mu(x) = \gamma^\mu\gamma_5\eta_{1/2}(x) \tag{6.2}$$

with the matrix element

$$\langle 0|\eta_G^\mu|1/2^+\rangle = \lambda_G\gamma^\mu\gamma_5 u(p)$$

The correlator of the tensor fields is now defined by :

$$\Pi^{\mu\nu}(q) = i \int d^4x \; e^{iq\cdot x} \langle 0|T\{\eta_G^\mu(x)\bar{\eta}_T^\nu(0)\}|0\rangle. \tag{6.3}$$

Overlap of the tensor field with the generalized spin-1/2 interpolator gives

$$\begin{aligned}
\langle 0|\eta_G^\mu|1/2^+\rangle\langle 1/2^+|\bar{\eta}_T^\nu|0\rangle &= \lambda_T\lambda_G \left[\gamma^\mu\gamma^5 u(q)u^\dagger(q)\gamma^{5\dagger}\left(\frac{4}{M_\mathrm{N}}q^\nu + \gamma^{\nu\dagger}\right)\gamma_0\right] \\
&= -\lambda_T\lambda_G \left[\gamma_\mu\gamma^5 u(q)\bar{u}(q)\gamma_5\frac{4}{M_\mathrm{N}}q^\nu + \gamma^\mu\gamma^5 u(q)\bar{u}(q)\gamma_5\gamma^\nu\right] \\
&= -\lambda_T\lambda_G \left[\gamma^\mu\gamma^5(\not{q} + M_\mathrm{N})\gamma_5\frac{4}{M_\mathrm{N}}q^\nu + \gamma^\mu\gamma^5(\not{q} + M_\mathrm{N})\gamma^5\gamma^\nu\right] \\
&= \lambda_T\lambda_G \left[\gamma^\mu\not{q}\frac{4}{M_\mathrm{N}}q^\nu - 4\gamma^\mu q^\nu + \gamma^\mu\not{q}\gamma^\nu - \gamma^\mu\gamma^\nu M_\mathrm{N}\right] \\
&= \lambda_T\lambda_G \left[\gamma^\mu q^\nu\not{q}\frac{4}{M_\mathrm{N}} - 2\gamma^\mu q^\nu - \gamma^\mu\gamma^\nu\not{q} - \gamma^\mu\gamma^\nu M_\mathrm{N}\right].
\end{aligned} \tag{6.4}$$

Since the product $\lambda_{3/2}\lambda_G$ is found to be negative in the forthcoming analysis, we define $\tilde{\lambda}^2 = -\lambda_T\lambda_G$ in order to reduce the number of minus signs. We obtain 4 Dirac structures (compared to 2 in the case of the spin-1/2 field) such that the OPE version of the correlator involves four invariant functions:

$$(\Pi^{\mathrm{OPE}})^{\mu\nu}(q) = \Pi_1(q^2)\gamma^\mu\gamma^\nu - \Pi_2(q^2)\gamma^\mu q^\nu\not{q} + \Pi_3(q^2)\gamma^\mu\gamma^\nu\not{q} + \Pi_4(q^2)\gamma^\mu q^\nu.$$

The four invariant functions can be extracted using the following identities

$$\begin{aligned}
\Pi_1(q^2) &= \frac{1}{12}\left\{\mathrm{Tr}\left[\gamma_\mu\gamma_\nu(\Pi^{\mathrm{OPE}})^{\mu\nu}(q)\right] - \frac{q_\mu q_\nu}{q^2}\mathrm{Tr}\left[(\Pi^{\mathrm{OPE}})^{\mu\nu}(q)\right]\right\} \\
\Pi_2(q^2) &= \frac{1}{12q^2}\left\{\mathrm{Tr}\left[\gamma_\mu\gamma_\nu(\Pi^{\mathrm{OPE}})^{\mu\nu}(q)\right] - 4\frac{q_\mu q_\nu}{q^2}\mathrm{Tr}(\Pi^{\mathrm{OPE}})^{\mu\nu}(q)\right\} \\
\Pi_3(q^2) &= \frac{1}{48q^2}\left\{q_\nu\mathrm{Tr}\left[\gamma_\mu(\Pi^{\mathrm{OPE}})^{\mu\nu}(q)\right] - 4q_\mu\mathrm{Tr}\left[\gamma_\nu(\Pi^{\mathrm{OPE}})^{\mu\nu}(q)\right]\right\} \\
\Pi_4(q^2) &= \frac{1}{24q^2}\left\{q_\nu\mathrm{Tr}\left[\gamma_\mu(\Pi^{\mathrm{OPE}})^{\mu\nu}(q)\right] + 2q_\mu\mathrm{Tr}\left[\gamma_\nu(\Pi^{\mathrm{OPE}})^{\mu\nu}(q)\right]\right\}
\end{aligned}$$

It turns out that the sum rules related to the structures $\gamma^\mu p^\nu$ and $\gamma^\mu\gamma^\nu\not{p}$ are identical. One principal advantage is that the leading four quark condensate term will appear only in one of the three remaining sum rules, so this sum rule can simply be disregarded, removing a source of uncertainty from the analysis. However, this fact provides an interesting chance to estimate the 4 quark condensate contributions to the neglected sum rule by simply inserting the optimized spectral parameters M_N, s_0, and $\tilde{\lambda}^2$ into this sum rule.
To derive sum rules for the spin-3/2 correlator the OPE for eq. (6.3) has to be calculated. Once

again using Wick's Theorem to evaluate the time ordered product we end up with:

$$
\begin{aligned}
\Pi^{\mu\nu}(q) = i\varepsilon_{abc}\varepsilon_{a'b'c'} \int d^4x\, e^{iq\cdot x} \Big\{ & \gamma^\mu\gamma^5 S^u_{aa'}(x)\gamma^\nu\sigma^{\kappa\lambda}\mathrm{Tr}[S^{uT}_{bb'}(x)C\gamma^5 S^d_{cc'}(x)\sigma_{\kappa\lambda}C] \\
& - \gamma^\mu\gamma^5 S^u_{aa'}(x)\sigma^{\kappa\lambda}CS^{dT}_{bb'}(x)C\gamma^5 S^u_{cc'}(x)\gamma^\nu\sigma_{\kappa\lambda} \\
& - \beta\gamma^\mu S^u_{cc'}(x)\gamma^\nu\sigma^{\kappa\lambda}\mathrm{Tr}[S^u_{aa'}(x)\sigma_{\kappa\lambda}CS^{dT}_{bb'}(x)C] \\
& - \beta\gamma^\mu S^u_{aa'}(x)\sigma^{\kappa\lambda}CS^{dT}_{bb'}(x)CS^u_{cc'}(x)\gamma^\nu\sigma_{\kappa\lambda} \\
& - \gamma^\mu\gamma^5 S^u_{bb'}(x)\sigma^{\kappa\lambda}CS^{uT}_{aa'}(x)C\gamma^5 S^d_{cc'}(x)\gamma^\nu\sigma_{\kappa\lambda} \\
& - \gamma^\mu\gamma^5 S^u_{aa'}(x)\sigma^{\kappa\lambda}CS^{uT}_{bb'}(x)C\gamma^5 S^d_{cc'}(x)\gamma^\nu\sigma_{\kappa\lambda} \\
& - \beta\gamma^\mu S^u_{bb'}(x)\sigma^{\kappa\lambda}CS^{uT}_{aa'}(x)CS^d_{cc'}(x)\gamma^\nu\sigma_{\kappa\lambda} \\
& - \beta\gamma^\mu S^u_{aa'}(x)\sigma^{\kappa\lambda}CS^{uT}_{bb'}(x)CS^d_{cc'}(x)\gamma^\nu\sigma_{\kappa\lambda}\Big\}
\end{aligned}
\tag{6.5}
$$

From the Lorentz structure of the correlator as indicated in (6.4) we see that there will be Fourier integrals involving $x_\mu x_\nu$ which are handled using

$$
\int d^4x\, e^{iq\cdot x} x_\mu x_\nu f(x) = -\partial_\mu\partial_\nu \int d^4x\, e^{iq\cdot x} f(x) = -\partial_\mu\partial_\nu \hat{f}(q).
$$

The sum rule at the structure $\gamma_\mu\gamma_\nu$ has dimension 7 and its leading term is the quark condensate. The first $\mathcal{O}(m_q)$ terms both account for the growth of the nucleon mass with increasing quark mass. Note that they are analogous to the terms increasing the nucleon mass in the spin-1/2 case.

$$
\begin{aligned}
\tilde{\lambda}^2 M_{\mathrm{N}} e^{-M_{\mathrm{N}}^2/M^2} &= \tilde{\Pi}'_1(q^2) \\
&\equiv -\frac{1}{8\pi^2}\langle\bar{q}q\rangle M^4 E_1 L^{8/27} - \frac{1+3\beta}{96}\langle\bar{q}q\rangle\left\langle\frac{\alpha_s}{\pi}G^2\right\rangle L^{8/27} + m_q\langle\bar{q}q\rangle^2 \\
&+ \frac{3}{64\pi^4}m_q M^6 E_2 - \frac{5}{3}\, m_q\langle\bar{q}q\rangle\langle\bar{q}D^2q\rangle\frac{1}{M^2} + \frac{3-\beta}{24}\, m_q\langle\bar{q}q\rangle\langle g_s\bar{q}\sigma\cdot Gq\rangle\frac{1}{M^2} \\
&+ \frac{1}{128\pi^2}\, m_q\left\langle\frac{\alpha_s}{\pi}G^2\right\rangle M^2\left[12H^2(M^2) - 12H(M^2) + \beta - 3\right] \\
&+ \frac{1}{\pi^2}\, m_q^2\langle\bar{q}D^2q\rangle + \frac{1}{64\pi^2}\, m_q^2\langle g_s\bar{q}\sigma\cdot Gq\rangle\left[H(M^2)(2\beta-8) - (\beta+1)\right] \\
&+ \frac{1}{288}\, m_q^2\langle\bar{q}q\rangle\left\langle\frac{\alpha_s}{\pi}G^2\right\rangle\frac{1}{M^2}\left[(120+24\beta)H(M^2) + 283 + 33\beta\right] \\
&- \frac{1}{64\pi^4}\, m_q^3 M^4\left[6H(M^2) + 13\right] + \frac{5\beta-4}{24}\, m_q^3\langle\bar{q}q\rangle\langle g_s\bar{q}\sigma\cdot Gq\rangle\frac{1}{M^4} \\
&- \frac{5}{2}\, m_q^3\langle\bar{q}q\rangle^2\frac{1}{M^2} + \frac{1}{1536\pi^2}\, m_q^3\left\langle\frac{\alpha_s}{\pi}G^2\right\rangle\big[24(3+\beta)H^2(M^2) \\
&\qquad -(396+108\beta)H(M^2) - (112-24\beta) - 7\pi^2(\beta+3)\big]\,.
\end{aligned}
\tag{6.6}
$$

The dimension 5 sum rule at $\gamma_\mu q_\nu \not{q}$ is given by

$$
\begin{aligned}
-\tilde{\lambda}^2 \frac{4}{M_{\rm N}} e^{-M_{\rm N}^2/M^2} =& -\Pi_2'(q^2) \\
\equiv& \ \frac{1}{2\pi^2}\langle\bar{q}q\rangle M^2 E_0 L^{8/27} - \frac{3}{4\pi^2}\langle\bar{q}D^2q\rangle L^{-2/9} + \frac{\beta+3}{16\pi^2}\langle g_s\bar{q}\sigma\cdot Gq\rangle L^{-2/9} \\
& - \frac{1+\beta}{12}\langle\bar{q}q\rangle\left\langle\frac{\alpha_s}{\pi}G^2\right\rangle\frac{1}{M^2}L^{8/27} + 4m_q\langle\bar{q}q\rangle^2\frac{1}{M^2} - \frac{3}{32\pi^4}\ m_q M^4 E_1 \\
& + \frac{3-\beta}{12}\ m_q\langle\bar{q}q\rangle\langle g_s\bar{q}\sigma\cdot Gq\rangle\frac{1}{M^4} - \frac{10}{3}m_q\langle\bar{q}q\rangle\langle\bar{q}D^2q\rangle\frac{1}{M^4} \\
& + \frac{1}{64\pi^2}\ m_q\left\langle\frac{\alpha_s}{\pi}G^2\right\rangle\left[(6-2\beta)H(M^2)+15+3\beta\right] + \frac{4}{\pi^2}\ m_q^2\langle\bar{q}D^2q\rangle\frac{1}{M^2} \\
& - \frac{9}{2\pi^2}\ m_q^2\langle\bar{q}q\rangle + \frac{1}{16\pi^2}\ m_q^2\langle g_s\bar{q}\sigma\cdot Gq\rangle\frac{1}{M^2}\left[(2\beta-8)H(M^2)+\beta-9\right] \\
& + \frac{1}{48}\ m_q^2\langle\bar{q}q\rangle\left\langle\frac{\alpha_s}{\pi}G^2\right\rangle\frac{1}{M^4}\left[(40+8\beta)H(M^2)+121+15\beta\right] - 5m_q^3\langle\bar{q}q\rangle^2\frac{1}{M^4} \\
& + \frac{3}{48\pi^4}\ m_q^3 M^2\left[6H(M^2)+7\right] + \frac{5\beta-4}{12}\ m_q^3\langle\bar{q}q\rangle\langle g_s\bar{q}\sigma\cdot Gq\rangle\frac{1}{M^6} \\
& + \frac{1}{96\pi^2}\ m_q^3\left\langle\frac{\alpha_s}{\pi}G^2\right\rangle\frac{1}{M^2}\Big[(18+6\beta)H^2(M^2) \\
& \qquad -(63+15\beta)H(M^2)-109+3\beta-\pi^2(\beta+3)\Big]\,.
\end{aligned}
\tag{6.7}
$$

As a result of the lower dimension of this sum rule, the factorial suppression factors of $1/(M^2)^k$ from the Borel transform (see eq. (3.22) resp. App.B) act more efficiently than in most baryonic sum rules. Thus, the OPE convergence of this sum rule is supposed to be good.
Last, the dimension 6 sum rule at $\gamma_\mu\gamma_\nu\not{q}$ resp. $\gamma^\mu q^\nu$ corresponds to the one at $\not{q}$ in the spin-1/2 case:

$$
\begin{aligned}
\tilde{\lambda}^2 e^{-M_{\rm N}^2/M^2} =& \ \Pi_3'(q^2) \\
\equiv& \ \langle\bar{q}q\rangle^2 L^{20/27} - \langle\bar{q}q\rangle\langle\bar{q}D^2q\rangle\frac{1}{M^2}L^{2/9} + \frac{\beta+3}{24}\langle\bar{q}q\rangle\langle g_s\bar{q}\sigma\cdot Gq\rangle\frac{1}{M^2}L^{2/9} \\
& - \frac{3}{4\pi^2}\ m_q\langle\bar{q}q\rangle M^2 E_0 + \frac{1}{32\pi^2}\ m_q\langle g_s\bar{q}\sigma\cdot Gq\rangle\left[(2+2\beta)H(M^2)-(\beta+3)\right] \\
& + \frac{3}{4\pi^2}\ m_q\langle\bar{q}D^2q\rangle + \frac{1}{96}\ m_q\langle\bar{q}q\rangle\left\langle\frac{\alpha_s}{\pi}G^2\right\rangle\frac{1}{M^2}\left[20H(M^2)+59+\beta\right] \\
& - 2m_q^2\langle\bar{q}q\rangle^2\frac{1}{M^2} + \frac{3}{32\pi^4}m_q^2M^4 - \frac{4\beta+3}{24}m_q^2\langle\bar{q}q\rangle\langle g_s\bar{q}\sigma\cdot Gq\rangle\frac{1}{M^4} \\
& - \frac{1}{1536\pi^2}\ m_q^2\left\langle\frac{\alpha_s}{\pi}G^2\right\rangle\Big[(24+24\beta)H^2(M^2)+(216-24\beta)H(M^2) \\
& \qquad +(456+24\beta)-\pi^2(\beta+1)\Big] \\
& + \frac{3}{8\pi^2}\ m_q^3\langle\bar{q}q\rangle\left[4H(M^2)+5\right] - \frac{1}{8\pi^2}\ m_q^3\langle\bar{q}D^2q\rangle\frac{1}{M^2}\left[6H(M^2)+13\right] \\
& + \frac{1}{64\pi^2}\ m_q^3\langle g_s\bar{q}\sigma\cdot Gq\rangle\frac{1}{M^2}\left[(14+12\beta)H(M^2)+23+19\beta\right] \\
& + \frac{1}{96}\ m_q^3\langle\bar{q}q\rangle\left\langle\frac{\alpha_s}{\pi}G^2\right\rangle\frac{1}{M^4}\left[(10+2\beta)H(M^2)-23-\beta\right].
\end{aligned}
\tag{6.8}
$$

Contrary to the spin-1/2 case, this sum rule does not show a purely perturbative term in zeroth order, which should provide an indication of lower perturbative corrections. Also the gluon condensate is missing in the chiral limit. Admittedly, the leading terms in the low mass limit are the two four-quark terms, from which we conclude that this sum rule should be discarded in an analysis due to the poor knowledge about these condensates.

6.2 Results

Given the sum rules for the fields (6.1) and (6.2) we follow the same strategy as in chapter 5 using only the two sum rules at the structures $\gamma_\mu\gamma_\nu$ and $\gamma_\mu q_\nu \not{q}$ which do not contain the four-quark condensate as leading term. The same values for $\left\langle \frac{\alpha_s}{\pi} G^2 \right\rangle$ and λ_q^2 as in eq. (5.7) are used and $\langle \bar{q}q \rangle$ is varied. The first step is once again the determination of valid Borel regimes and corresponding field mixing parameters β dependent on m_q. The analysis of [19] uses $\beta = 0$ for $m_q = 0$ which we adopt. The Borel regimes for the considered quark mass range is shown in fig. 6.1. β is kept 0 for

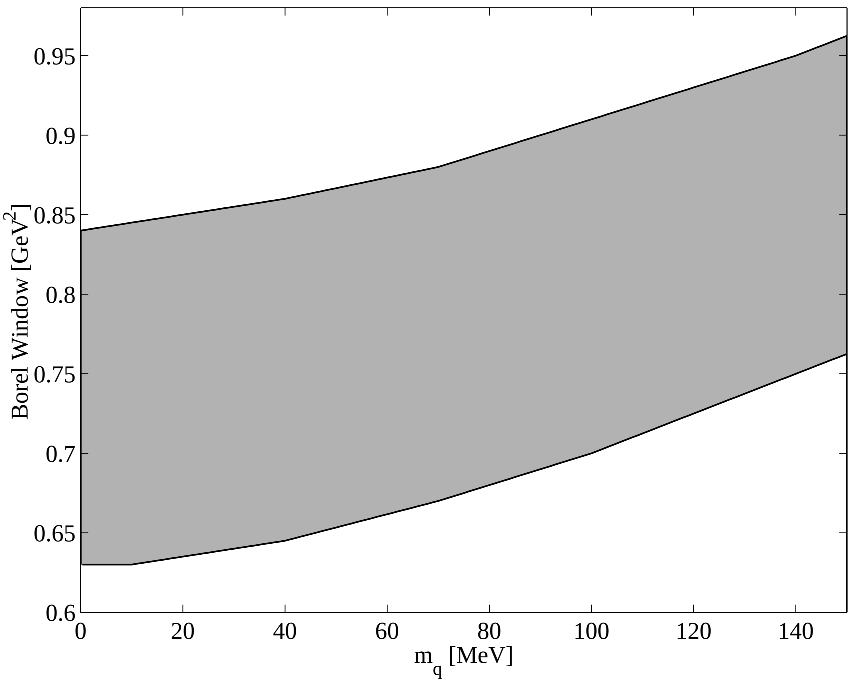

Figure 6.1: The valid Borel window for the tensor sum rules as a function of m_q

$m_q \leq 60$MeV and then raised to -1.2 at $m_q = 150$. It turns out that the convergence in powers of m_q is not satisfactory for quark masses higher than 150 MeV. Additionally, the optimization does not lead to acceptable agreement of the phenomenological side and the two OPE sides of the sum rules with each other. This indicates a breakdown of the $\mathcal{O}(m_q^3)$ expansion. This can in fact already be seen from the Borel windows in fig. 6.1, since lower and upper ends of the Borel regimes do not grow as fast as in the spin-1/2 case. Hence, for higher m_q the Borel parameter M is not large enough to establish convergence of the OPE as a series in m_q. The quotient m_q/M is not sufficiently small. Nevertheless, calculations up to $m_q = 100 - 120$ MeV are reliable.

Results of the analysis for $\langle \bar{q}q \rangle = (-235\,\text{MeV} \pm 20)^3$ and $\langle \bar{q}q \rangle = (-245 \pm 20\,\text{MeV})^3$ as well

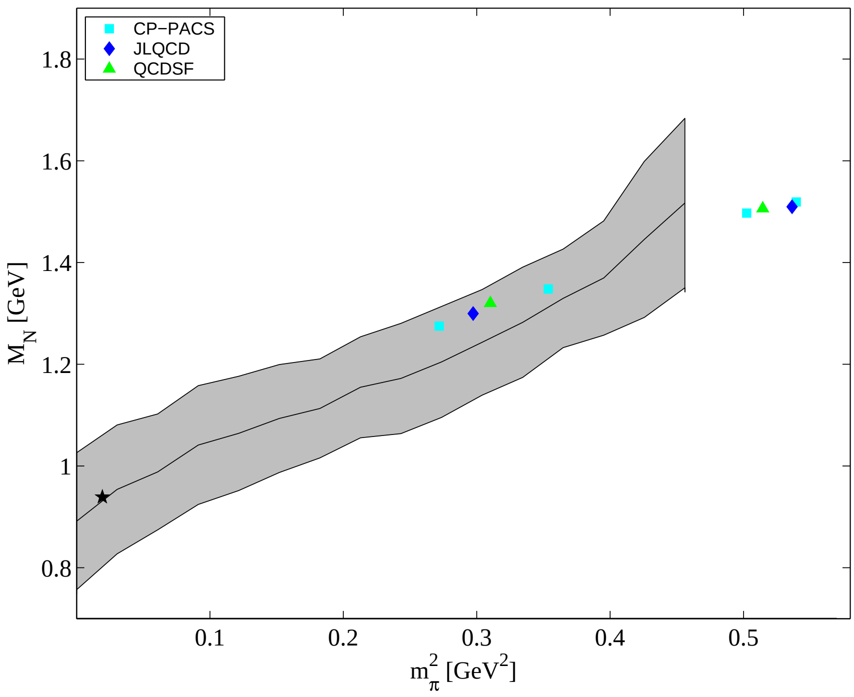

Figure 6.2: Tensor sum rule predictions of $M_{\mathrm{N}}(m_\pi^2)$ using $\langle\bar{q}q\rangle = (-235 \pm 20\,\mathrm{MeV})^3$

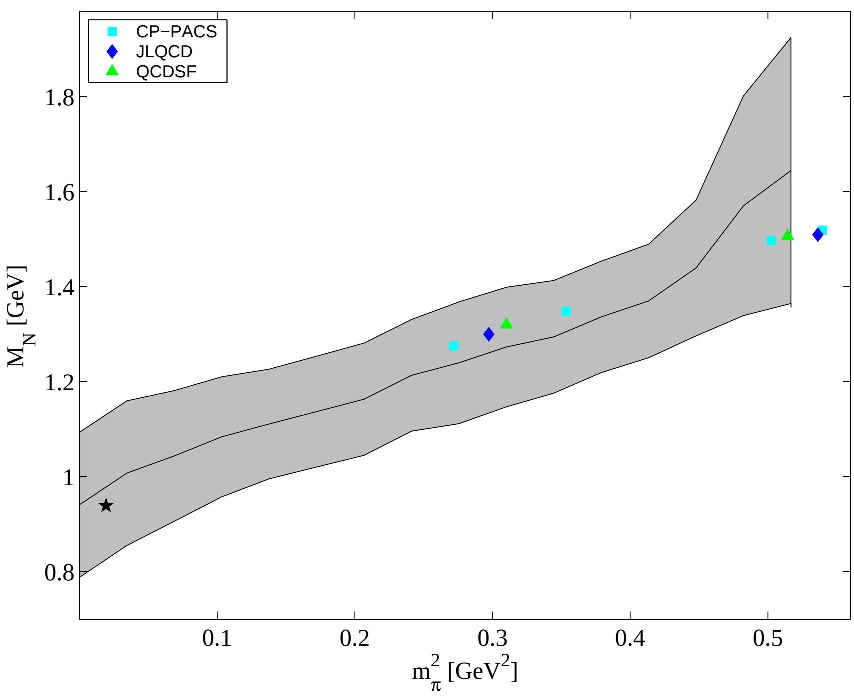

Figure 6.3: Tensor sum rule predictions of $M_{\mathrm{N}}(m_\pi^2)$ using $\langle\bar{q}q\rangle = (-245 \pm 20\,\mathrm{MeV})^3$

as eq. (5.7) for the condensates involving gluons are shown in figs. 6.2 and 6.3. Both figures show a good agreement of the nucleon tensor sum rule predictions for $M_{\mathrm{N}}(m_\pi^2)$ with the Lattice data. Contrary to the spin-1/2 sum rules the low quark mass limit works out fine. The physical point is well included in the error band, see already [19]. The same is true for the four lower Lattice points. The error stays at the $(100-150)\,\mathrm{MeV}$ over most of the m_q-range, implying a relative error around $10-15\%$, which is less than the input uncertainty of the condensates. Up to $m_\pi^2 = 0.4\,\mathrm{GeV}^2$, the relative error declines as the pion mass grows which can be interpreted as a stabilization of the OPE side of the sum rules due to the inclusion of mass terms.
Figs. 6.2 and 6.3 both show a strong rise of the nucleon mass accompanied by a sudden rise of the error at the end of the treated pion mass range, $\approx 0.4\,\mathrm{GeV}^2$ resp $\approx 0.45\,\mathrm{GeV}^2$. These values correspond to quark masses exceeding 130 MeV. This is the region where the convergence of the OPE begins to worsen. Problems can also be read off from the behaviour of the threshold s_0 which does not show the expected monotone growth but an oscillatory behaviour for $m_q > 100\,\mathrm{MeV}$. The mean values of s_0 are not always clearly larger than $M_{\mathrm{N}}(m_\pi^2) + m_\pi^2$ as expected from a valid continuum model. In summary, these kinks at higher quark masses should not be overinterpreted. For a reasonable expansion of the controllable quark mass range the expansion in m_q would have to be extended. Once again, the similarity of figs. 6.2 and 6.3 over a considerably big quark mass range supports the weak dependence of the results on the precise input condensate values, especially $\langle \bar{q}q \rangle$, when the GOR relation is used.

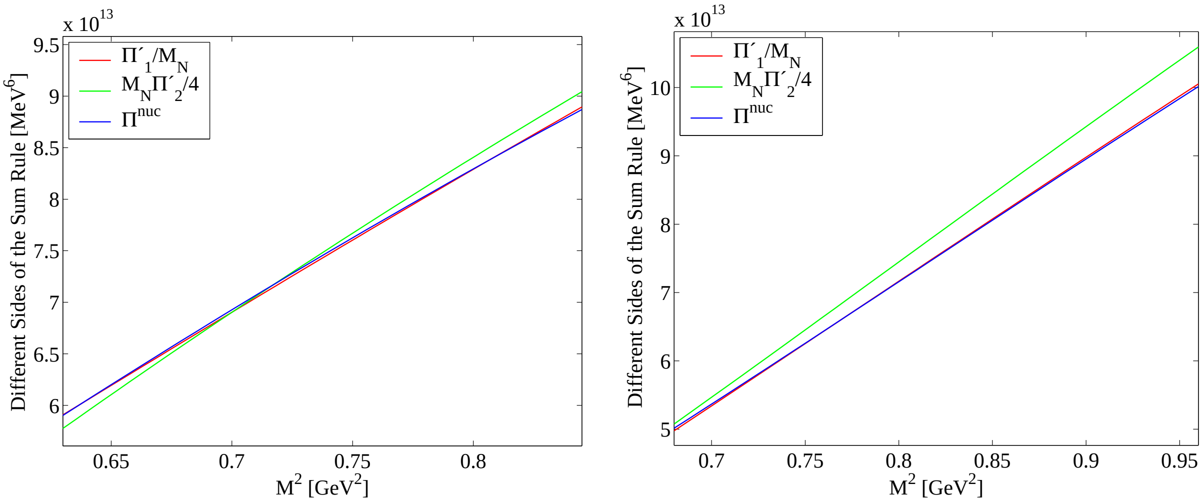

Figure 6.4: Comparison of different sum rule sides at $m_q = 10\,\mathrm{MeV}$ (left) and $m_q = 100\,\mathrm{MeV}$ (right) along the Borel regimes

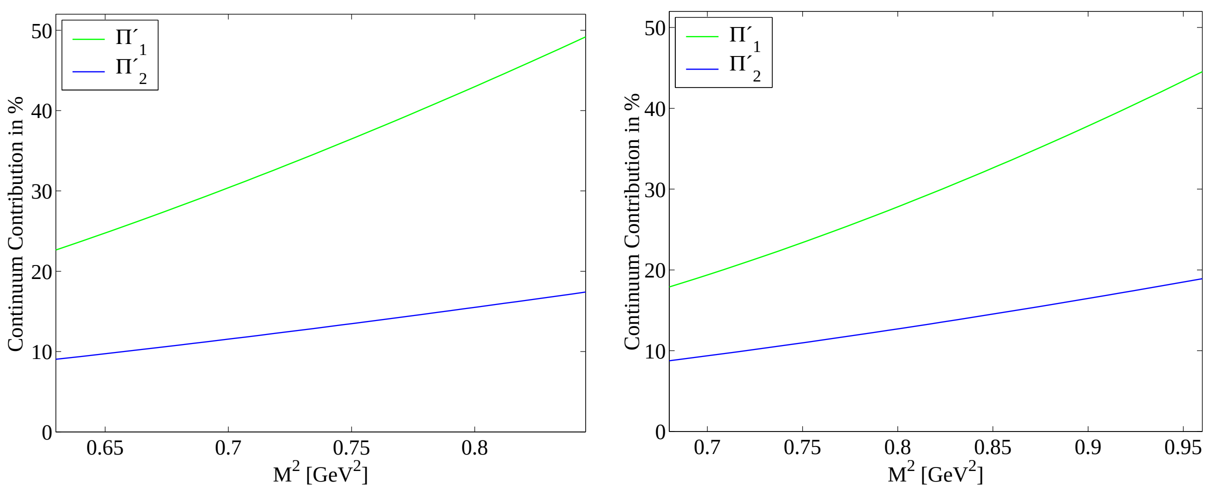

Figure 6.5: Continuum contributions to the OPE sides of the two relevant sum rules at $m_q = 10\,\mathrm{MeV}$ (left) and $m_q = 100\,\mathrm{MeV}$ (right) against the Borel parameter M^2

Again, we proceed with the investigation of important features of the system of equations deduced from (6.6) and (6.7). The degree of agreement of the sum rules with optimized parameters M_{N}, s_0, and $\tilde{\lambda}^2$ for the central condensate values can be evaluated from fig.6.4 where the two OPE sides Π_1' and Π_2' and the nucleon pole side of the sum rules Π^{nuc} are compared. Here, we have defined

$$\Pi^{\mathrm{nuc}}(M^2) = \tilde{\lambda}^2 e^{-M_{\mathrm{N}}^2/M^2}$$

Expecially for $m_q = 10\,\mathrm{MeV}$ the agreement is excellent, such that the continuum at the upper end and the higher dimensional condensate contribution at the lower end (see[19]) are the dominant factors restricting the size of the Borel window. For $m_q \approx 100\,\mathrm{MeV}$ the continuum modified OPE Π_2' starts to systematically deviate from the pole term and Π_1'. For even higher masses the

agreement of the different sides of the sum rules gets even worse. This limits the applicability of the tensor sum rules to quark masses not larger than 100 MeV.
The form of the continuum contributions to the right hand side of the sum rules (6.6) and (6.7) is outlined in fig. 6.5. The continuum contamination is higher in 6.6 because of the factor $M^4 E_1$ relatively including more continuum than $M^2 E_0$ in (6.7).
An estimation of the acceptability of the quark mass expansion is provided by figs. 6.6 and 6.7

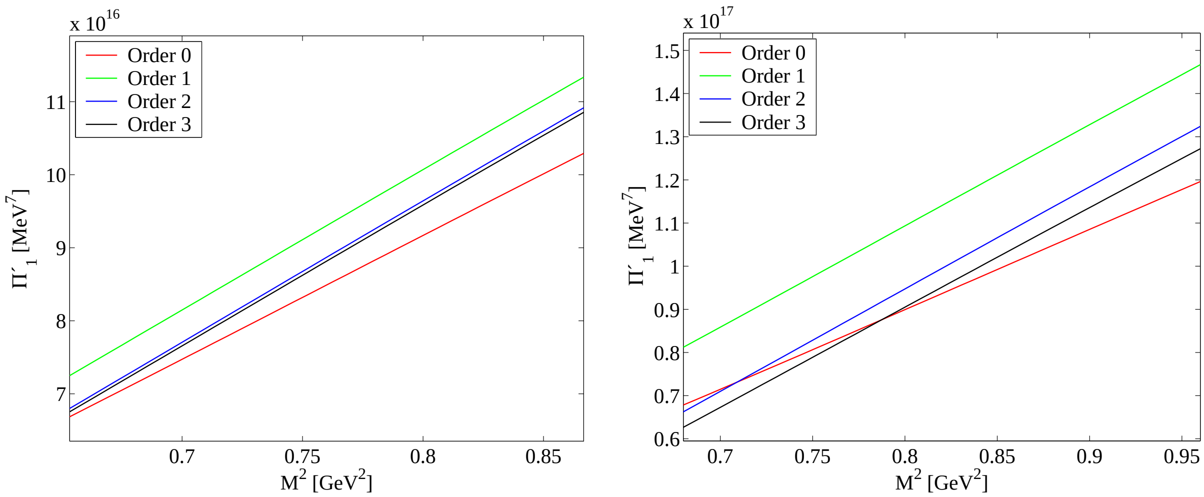

Figure 6.6: Contributions of different orders in m_q in the OPE of (6.6) at $m_q = 50\,\mathrm{MeV}$ (left) and $m_q = 100\,\mathrm{MeV}$ (right) plotted against the Borel parameter M^2

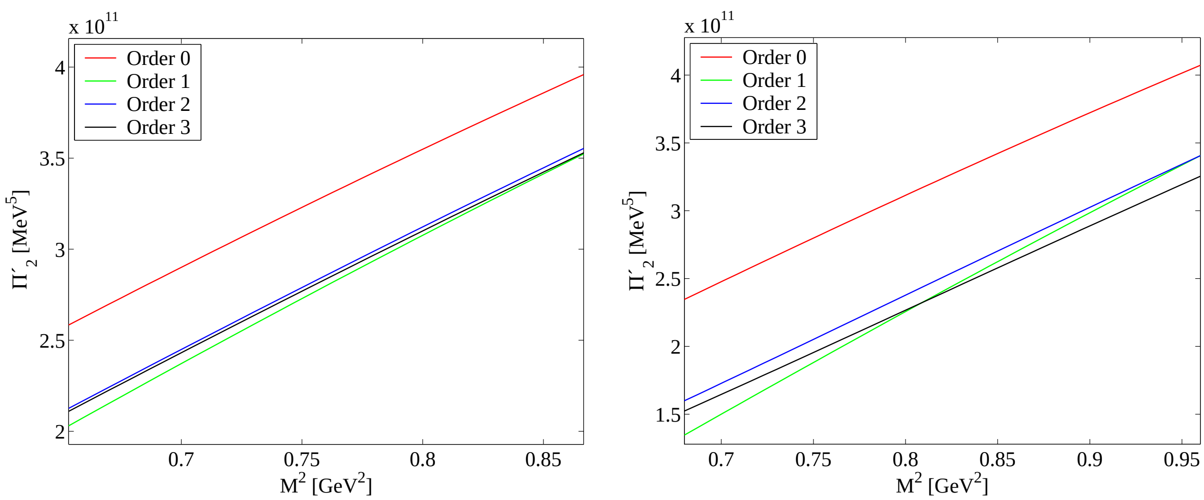

Figure 6.7: Contributions of different orders in m_q in the OPE of (6.7) at $m_q = 50\,\mathrm{MeV}$ (left) and $m_q = 100\,\mathrm{MeV}$ (right) plotted against the Borel parameter M^2

where the contributions of different orders of m_q to the OPE sides of eqs. (6.6) and (6.7) are displayed. In the case of the sum rule (6.6) the third order shows up at $m_q = 100\,\mathrm{MeV}$ due to the term $m^3 M^4$. In the sum rule 6.7 the third order does also have significance due to $m_q^3 M^2$

and the relatively low lying Borel windows.

6.3 Combination of Spin-1/2 and Tensor Sum Rules

Together with the spin-1/2 sum rules we have now gathered a total of 5 sum rules, one of which - eq. (6.8) - was totally ignored in the analysis. It is an interesting perspective to perform a combined analysis of spin-1/2 and tensor sum rules. We restrict ourselves to the three more reliable equations (5.4) (including the α_s-correction (5.9)), (6.6), and (6.7), ignoring also eq. (5.5) because of the known problems with the large continuum contribution from the perturbative term $\sim M^6 E_2$, its large perturbative correction, and the important but badly known four-quark condensate. We assume the same phenomenological model for spin-1/2 and tensor sum rules and equate the thresholds of all three sum rules. The analysis is performed just as before but with four instead of three phenomenological parameters M_N, s_0, λ_N^2, and $\tilde{\lambda}^2$. The combination of the three sum rules works out fine such that Borel regimes can be found for $m_q = 0\,\mathrm{MeV}$ up to $m_q = 200\,\mathrm{MeV}$. The problems with the mass expansion in the tensor sum rules do not show up confirming the conjecture that they arise from the slow growth of the boundaries of the Borel regimes in the tensor only case. Even the agreement of the four sides of the sum rules is excellent. The determined Borel regimes are displayed in fig. 6.8. The following condensate values were used:

$$\begin{aligned} \left\langle \frac{\alpha_s}{\pi} G^2 \right\rangle &= (330 \pm 10\,\mathrm{MeV})^4 \\ \lambda_q^2 &= (0,36 \pm 0.05)\,\mathrm{GeV}^2 \end{aligned}$$

Here, λ_q^2 from eq. (3.19) parametrizes the quark-gluon condensate $\langle g_s \bar{q}\sigma \cdot Gq\rangle$ in terms of the quark condensate $\langle \bar{q}q\rangle$. Results of the calculations with $\langle \bar{q}q\rangle = (-235 \pm 10\,\mathrm{MeV})^3$ resp. $\langle \bar{q}q\rangle = (-245 \pm 10\,\mathrm{MeV})^3$ are depicted in figs. 6.9 and 6.10. Obviously, the agreement with the Lattice calculations is excellent. The error band in fig. 6.9 includes all Lattice points. This almost perfect consistency arises perhaps accidentally for this set of QCD parameters. However, fig. 6.10 does not show a major deviation, which underlines the stability of the sum rule predictions with respect to the input condensate values.

The conclusion of the present chapter is that the alternative use of unconventional interpolating tensor fields for the nucleon provides two additional reliable sum rules not as much affected by the uncertainty in the four quark condensates or perturbative corrections as the second equation coming from the spin-1/2 sum rules (5.5). The analysis of these sum rules leads to a prediction of $M_\mathrm{N}(m_\pi^2)$ for quark masses up to $\approx 100\,\mathrm{MeV}$. A combination with the unproblematic spin-1/2 sum rule (5.4) provides an opportunity to predict $M_\mathrm{N}(m_\pi^2)$ for the quark mass range $0, \ldots, 200\,\mathrm{MeV}$. The agreement with the Lattice data is astonishing.

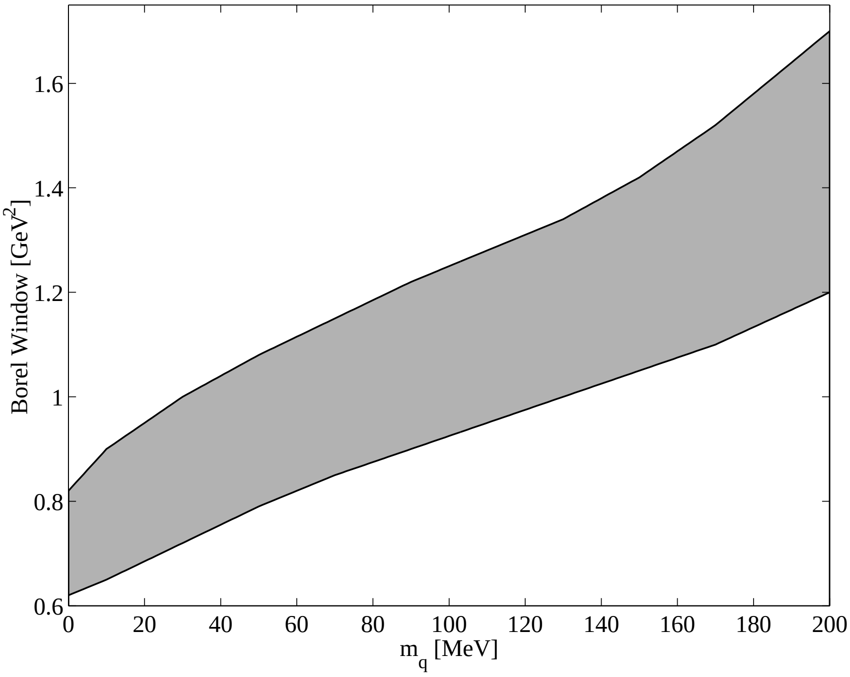

Figure 6.8: The valid Borel window for the joined analysis of spin-1/2 and tensor sum rules as a function of m_q

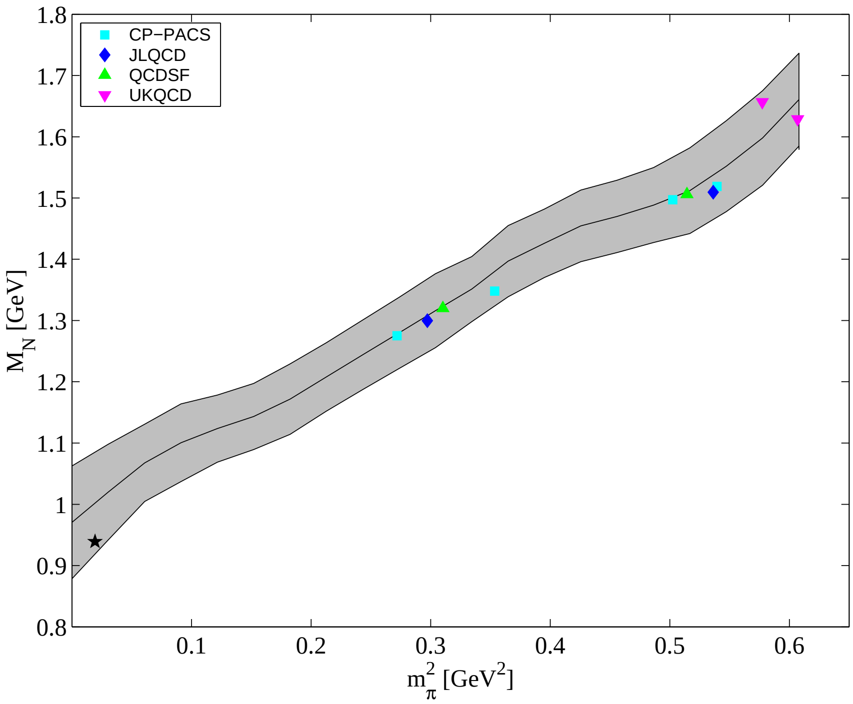

Figure 6.9: Combined analysis of spin-1/2 and tensor sum rules using $\langle \bar{q}q \rangle = (-235 \pm 20\,\mathrm{MeV})^3$

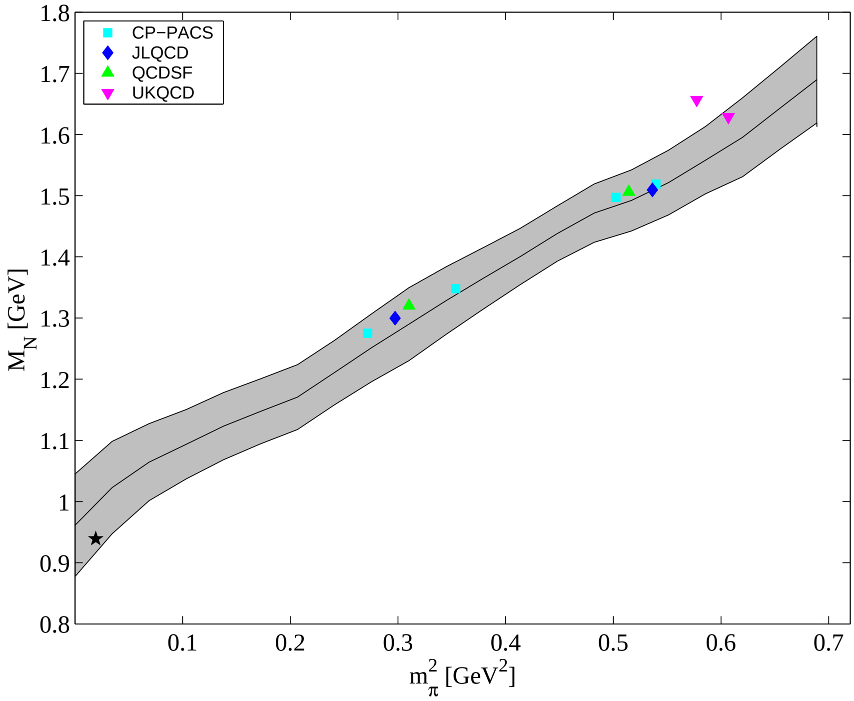

Figure 6.10: Combined analysis of spin-1/2 and tensor sum rules using $\langle \bar{q}q \rangle = (-245 \pm 20\,\mathrm{MeV})^3$

Chapter 7

Detailed Treatment of Four-Quark Condensates

7.1 Estimating the Four-Quark Condensate

As pointed out earlier, the sum rule omitted in the determination of the nucleon mass which carries the four-quark condensate as the dominant term can be used to estimate the value of $\langle \bar{q}q\bar{q}q \rangle$ for every m_q. Of course, this will not lead to a high precision determination but it can give an indication of a value that leads to consistency within the three sum rules coming from the correlator (6.3). To this end, we solve the sum rule (6.8) at $\gamma_\mu \gamma_\nu \not{q}$ for $\langle \bar{q}q \rangle^2$ which we identify with $\langle \bar{q}q\bar{q}q \rangle$:

$$\langle \bar{q}q\bar{q}q \rangle = \frac{1}{1 - 2m_q^2/M^2} \left[\tilde{\lambda}^2 e^{-M_\mathrm{N}^2/M^2} + \langle \bar{q}q \rangle \langle \bar{q}D^2 q \rangle \frac{1}{M^2} + \frac{\beta + 3}{24} \langle \bar{q}q \rangle \langle g_s \bar{q}\sigma \cdot G q \rangle \frac{1}{M^2} + \dots \right] \quad (7.1)$$

The strategy is now rather obvious: For fixed m_q the χ^2-measure of section 5.2 constructed from the two other sum rules (6.6) and (6.7) is optimized for the N_p parameter sets and the macroscopic parameters $M_\mathrm{N}^{(k)}$, $s_0^{(k)}$, and $\tilde{\lambda}^2_{(k)}$ together with the corresponding condensate set $(\langle \bar{q}q \rangle_{(k)}, \left\langle \frac{\alpha_s}{\pi} G^2 \right\rangle_{(k)}, (\lambda_q^2)_k)$ are inserted into eq. (7.1). Eq. (7.1), which depends on the Borel parameter M^2, is then averaged over the corresponding Borel regime yielding $\langle \bar{q}q\bar{q}q \rangle_{(k)}$. Finally, a quark mass dependent estimate of the four-quark condensate is found analogous to eq. (5.6):

$$\overline{\langle \bar{q}q\bar{q}q \rangle}(m_q) = \frac{1}{N_p} \sum_{k=1}^{N_p} \langle \bar{q}q\bar{q}q \rangle_{(k)}$$

Calculations using the tensor sum rules and the combination of spin-1/2 and tensor sum rules as described in chapter 6 produce the four-quark condensate estimates depicted in fig. 7.1. There the factor $\kappa(m_q) \equiv \langle \bar{q}q\bar{q}q \rangle(m_q)/\langle \bar{q}q \rangle^2$ is plotted against the quark mass for reasons of clearness. Fig. 7.1 shows that physically reasonable results for $\langle \bar{q}q\bar{q}q \rangle$ can indeed be obtained through the primitive partial inversion of input and output in the sum rules. All three calculations yield a $\kappa(m_q = 0)$ around 2, which largely deviates from the factorization hypothesis. For quark masses different from zero, the values shown in fig. 7.1 can not be identified with the prefactor of the

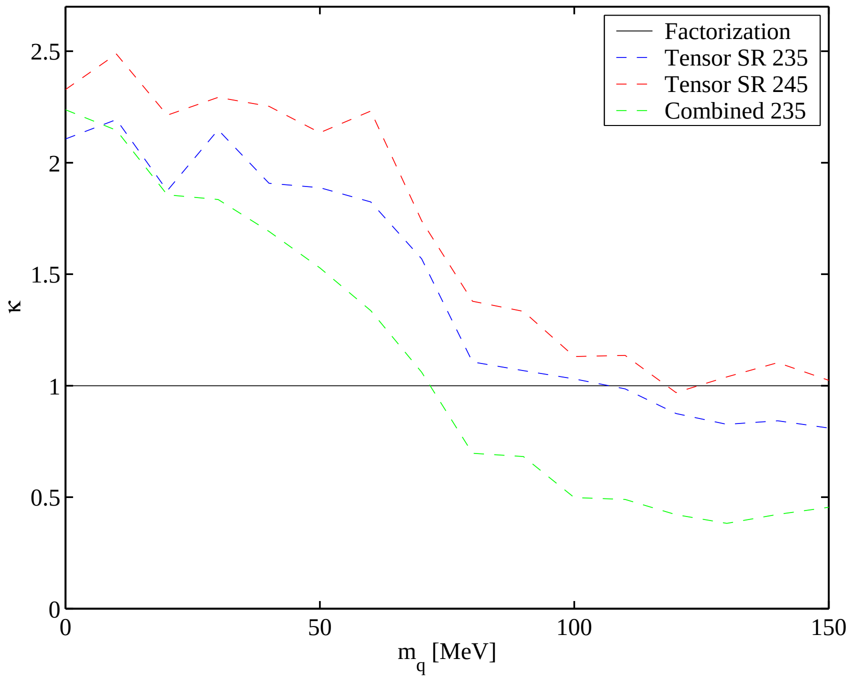

Figure 7.1: Estimates of $\kappa(m_q) \equiv \langle\bar{q}q\bar{q}q\rangle(m_q)/\langle\bar{q}q\rangle^2$ from tensor sum rules (using $\langle\bar{q}q\rangle = (-235\,\mathrm{MeV})^3$ resp. $\langle\bar{q}q\rangle = (-245 \pm 20)^3$) and the combination of spin-1/2 and tensor sum rules (with $\langle\bar{q}q\rangle = (-235\,\mathrm{MeV})^3$)

leading $\langle\bar{q}q\bar{q}q\rangle$ term since the contribution from the $m_q^2\langle\bar{q}q\bar{q}q\rangle$ term is included. The plot thus shows that at least for the tensor sum rules factorization in the discarded sum rule would have been an acceptable approximation whereas it completely fails in the $m_q \to 0$ limit. The strong kink at $m_q = 70\,\mathrm{MeV}$ is mostly due to a variation in the field mixing parameter β and should not be overinterpreted.

The standard deviations are of course quite large (typically more than 50%), especially in the low mass region, and therefore not shown. This can easily be justified by the fact that the four quark condensate carries essentially all responsibility in the $\gamma_\mu\gamma_\nu\not{q}$-sum rule (6.8) such that any variation in the input parameter is directly reflected in $\langle\bar{q}q\bar{q}q\rangle$. For higher quark masses the other terms increase and the importance of the four quark condensate diminishes. An interesting fact is the type of mass dependence that is produced. Since heavier quarks lead to heavier pions, such that the pionic intermediate states ignored in the factorization hypothesis are shifted towards higher energies, one expects that factorization becomes more plausible. The procedure seems to reproduce this expectation at least for the tensor only analysis.

Although the results of fig. 7.1 are quite plausible, the resolution of the desired value $\langle\bar{q}q\bar{q}q\rangle(m_q = 0)$ is not too good because of the inherently large errors of the method. It is therefore interesting to see results obtained when the input uncertainties are reduced strongly. Fig. 7.2 shows the results of tensor sum rule calculations performed for the input parameters $\langle\bar{q}q\rangle = (-235 \pm 3\,\mathrm{MeV})^3$, resp. $\langle\bar{q}q\rangle = (-247 \pm 3\,\mathrm{MeV})^3$ together with $\left\langle\frac{\alpha_s}{\pi}G^2\right\rangle = (330 \pm 5\,\mathrm{MeV})^4$, and $\lambda_q^2 = (0.36 \pm 0.02)\,\mathrm{GeV}^2$. Qualitatively, fig.7.2 shows the same m_q dependence of κ as the tensor parts in fig.7.1. The errors are now of course smaller. The kink is present just as before. From this obvious β dependence of

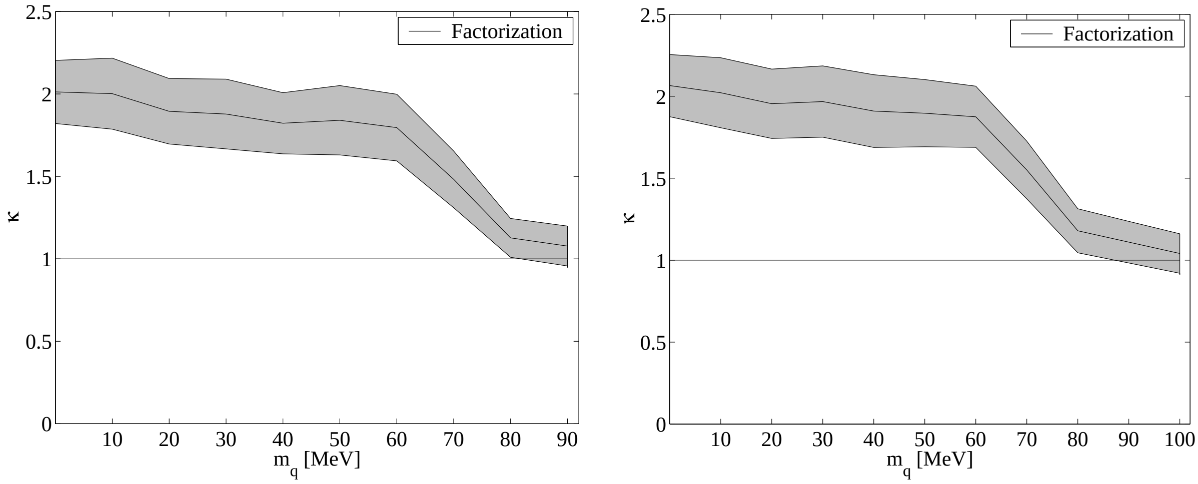

Figure 7.2: Errorbands for the estimates for $\kappa(m_q) \equiv \langle \bar{q}q\bar{q}q\rangle(m_q)/\langle \bar{q}q\rangle^2$ using $\langle \bar{q}q\rangle = (-235 \pm 3\,\mathrm{MeV})^3$ resp. $\langle \bar{q}q\rangle = (-247 \pm 3\,\mathrm{MeV})^3$ in the tensor sum rules.

the estimate for $\langle \bar{q}q\bar{q}q\rangle$ we conclude that there are β-dependent prefactors of $\langle \bar{q}q\rangle^2$ missing in the sum rule (6.8), where the coefficient of $\langle \bar{q}q\rangle^2$ is $(1-2m_q^2/M^2)$. The rest of this chapter is dedicated to the treatment of four-quark condensates beyond the factorization hypothesis, meaning that the contributions from pionic intermediate states are explicitly calculated.

7.2 Preparations

The goal of this chapter is to derive a calculational framework for the treatment of four-quark condensates beyond vacuum saturation. Starting point of the derivation is the general form of a four-quark condensate emerging from the background field method described in sections 3.3 and 3.4

$$\chi^q_{a\alpha}\bar{\chi}^q_{b\beta}\chi^q_{c\gamma}\bar{\chi}^q_{d\delta} = \langle q^a_\alpha \bar{q}^b_\beta q^c_\gamma \bar{q}^d_\delta\rangle. \tag{7.2}$$

In principle, the flavours of the four quark fields are arbitrary. However, from the background field method there arise only four quark condensates of the form $\langle u^a_\alpha \bar{u}^b_\beta u^c_\gamma \bar{u}^d_\delta\rangle$ resp. $\langle u^a_\alpha \bar{u}^b_\beta d^c_\gamma \bar{d}^d_\delta\rangle$. The two pairs of operators $q\bar{q}$ in each expectation value may not be mixed in order not to double count contributions in the Wick contracted time ordered product of eq. (3.1). Hence, it is clear that when inserting a full set of intermediate states in the four quark operator expectation value, for example

$$\sum_n \langle 0|u^a_\alpha \bar{u}^b_\beta|n\rangle\langle n|d^c_\gamma \bar{d}^d_\delta|0\rangle,$$

only flavour diagonal two quark operators emerge although flavour non-diagonal operators could have overlap with pionic intermediate states. To include these operators into the calculation we generalize the concept of the background field propagator by introducing flavour mixing quasi propagators $\hat{S}^{ud}(x)$ and $\hat{S}^{du}(x)$ that arrange for the complete coupling to four quark operators and lack any physical propagation terms, compare eq. (3.14):

$$[\hat{S}^{ud}_{ab}(x)]_{\alpha\beta} = \chi^u_{a\alpha}(x)\bar{\chi}^d_{b\beta}(0) \quad \text{and} \quad [\hat{S}^{du}_{ab}(x)]_{\alpha\beta} = \chi^d_{a\alpha}(x)\bar{\chi}^u_{b\beta}(0). \tag{7.3}$$

It has to be noted that the introduction of the background field propagator is a calculational device to treat the non fully contracted terms in the Wick expansion of the microscopical version of the correlation function. These quasi propagators have to be interpreted likewise. The next steps are rather obvious. Additionally to the Wick contracted products eqs.(5.2) and (6.5) we have to calculate Wick products including flavour mixing two quark operators. Therefore, two u-fields are contracted classically, whereas the remaining fields u, $\bar{u}$, d, $\bar{d}$ are contracted to $\hat{S}^{ud}(x)$ resp. $\hat{S}^{du}(x)$.

$$\begin{aligned}
\underbracket{u^a_\alpha(x)\overline{d}}{}^b_\beta(0) &= [\hat{S}^{ud}_{ab}(x)]_{\alpha\beta} \\
\underbracket{d^a_\alpha(x)\overline{u}}{}^b_\beta(0) &= [\hat{S}^{du}_{ab}(x)]_{\alpha\beta}
\end{aligned}$$

The result for the spin-1/2 correlator of chapter 5 is given by:

$$\begin{aligned}
\Delta\Pi^{\rm OPE}_{\rm 4q}(q^2) &= 4i\varepsilon_{abc}\varepsilon_{a'b'c'} \int d^4x \; e^{iq\cdot x} X_{aa'bb'cc'}(x) \\
X_{aa'bb'cc'}(x) &= S^u_{cc'}\mathrm{Tr}[\hat{S}^{ud}_{bb'}\gamma_5 C\hat{S}^{duT}_{aa'}C\gamma_5] + S^u_{aa'}\gamma_5 C\hat{S}^{udT}_{bb'}C\gamma_5\hat{S}^{du}_{cc'} - \hat{S}^{ud}_{bb'}\gamma_5 C S^{uT}_{aa'}C\gamma_5\hat{S}^{du}_{cc'} \\
&+ \hat{S}^{ud}_{bb'}\gamma_5 C\hat{S}^{duT}_{aa'}C\gamma_5 S^u_{cc'} + \beta S^u_{cc'}\gamma_5\mathrm{Tr}[\hat{S}^{ud}_{bb'}C\hat{S}^{duT}_{aa'}C\gamma_5] + \beta S^u_{aa'}C\hat{S}^{udT}_{bb'}C\gamma_5\hat{S}^{du}_{cc'}\gamma_5 \\
&- \beta\hat{S}^{ud}_{bb'}CS^{uT}_{aa'}C\gamma_5\hat{S}^{du}_{cc'}\gamma_5 + \beta\hat{S}^{ud}_{bb'}C\hat{S}^{duT}_{aa'}C\gamma_5 S^u_{cc'}\gamma_5 + \beta\gamma_5 S^u_{cc'}\mathrm{Tr}[\hat{S}^{ud}_{bb'}\gamma_5 C\hat{S}^{duT}_{aa'}C] \\
&+ \beta\gamma_5 S^u_{aa'}\gamma_5 C\hat{S}^{udT}_{bb'}C\hat{S}^{du}_{cc'} - \beta\gamma_5\hat{S}^{ud}_{bb'}\gamma_5 CS^{uT}_{aa'}C\hat{S}^{du}_{cc'} + \beta\gamma_5\hat{S}^{ud}_{bb'}\gamma_5 C\hat{S}^{duT}_{aa'}CS^u_{cc'} \\
&+ \beta^2\gamma_5 S^u_{cc'}\gamma_5\mathrm{Tr}[\hat{S}^{ud}_{bb'}C\hat{S}^{duT}_{aa'}C] + \beta^2\gamma_5 S^u_{aa'}C\hat{S}^{udT}_{bb'}C\hat{S}^{du}_{cc'}\gamma_5 - \beta^2\gamma_5\hat{S}^{ud}_{bb'}CS^{uT}_{aa'}C\hat{S}^{du}_{cc'}\gamma_5 \\
&+ \beta^2\gamma_5\hat{S}^{ud}_{bb'}C\hat{S}^{duT}_{aa'}CS^u_{cc'}\gamma_5.
\end{aligned}$$

Here, we have skipped the argument x of all propagators. The same procedure applied to the tensor field provides:

$$\begin{aligned}
[\Delta\Pi^{\rm OPE}_{\rm 4q}]^{\mu\nu}(q^2) &= 4i\varepsilon_{abc}\varepsilon_{a'b'c'} \int d^4x \; e^{iq\cdot x} X^{\mu\nu}_{aa'bb'cc'}(x) \\
X^{\mu\nu}_{aa'bb'cc'}(x) &= \gamma^\mu\gamma_5 S^u_{cc'}\gamma^\nu\sigma_{\kappa\lambda}\mathrm{Tr}[\hat{S}^{udT}_{bb'}C\gamma_5\hat{S}^{du}_{aa'}\sigma^{\kappa\lambda}C] + \gamma^\mu\gamma_5 S^u_{aa'}\sigma_{\kappa\lambda}C\hat{S}^{udT}_{bb'}C\gamma_5\hat{S}^{du}_{cc'}\gamma^\nu\sigma^{\kappa\lambda} \\
&- \gamma^\mu\gamma_5\hat{S}^{ud}_{bb'}\sigma_{\kappa\lambda}C\hat{S}^{duT}_{aa'}C\gamma_5 S^u_{cc'}\gamma^\nu\sigma^{\kappa\lambda} + \gamma^\mu\gamma_5\hat{S}^{ud}_{bb'}\sigma_{\kappa\lambda}CS^{uT}_{aa'}C\gamma_5\hat{S}^{du}_{cc'}\gamma^\nu\sigma^{\kappa\lambda} \\
&- \beta\gamma^\mu S^u_{cc'}\gamma^\nu\sigma_{\kappa\lambda}\mathrm{Tr}\hat{S}^{ud}_{bb'}\sigma^{\kappa\lambda}C\hat{S}^{duT}_{aa'}C] - \beta\gamma^\mu\hat{S}^{ud}_{bb'}\sigma_{\kappa\lambda}C\hat{S}^{duT}_{aa'}CS^u_{cc'}\gamma^\nu\sigma^{\kappa\lambda} \\
&+ \beta\gamma^\mu\hat{S}^{ud}_{bb'}\sigma_{\kappa\lambda}CS^{uT}_{aa'}C\hat{S}^{du}_{cc'}\gamma^\nu\sigma^{\kappa\lambda} + \beta\gamma^\mu S^u_{aa'}\sigma_{\kappa\lambda}C\hat{S}^{udT}_{bb'}C\hat{S}^{du}_{cc'}\gamma^\nu\sigma^{\kappa\lambda} \\
&+ \gamma^\mu\gamma_5\hat{S}^{ud}_{cc'}\gamma^\nu\sigma_{\kappa\lambda}\mathrm{Tr}[S^u_{bb'}\sigma^{\kappa\lambda}\hat{S}^{duT}_{aa'}C\gamma_5] + \gamma^\mu\gamma_5 S^u_{bb'}\sigma_{\kappa\lambda}C\hat{S}^{duT}_{aa'}C\gamma_5\hat{S}^{ud}_{cc'}\gamma^\nu\sigma^{\kappa\lambda} \\
&+ \gamma^\mu\gamma_5\hat{S}^{ud}_{cc'}\gamma^\nu\sigma_{\kappa\lambda}\mathrm{Tr}[S^u_{aa'}\sigma^{\kappa\lambda}C\hat{S}^{duT}_{bb'}C\gamma_5] + \gamma^\mu\gamma_5 S^u_{aa'}\sigma_{\kappa\lambda}C\hat{S}^{duT}_{bb'}C\gamma_5\hat{S}^{ud}_{cc'}\gamma^\nu\sigma^{\kappa\lambda} \\
&+ \beta\gamma^\mu\gamma_5\hat{S}^{ud}_{cc'}\gamma^\nu\sigma_{\kappa\lambda}\mathrm{Tr}[S^u_{bb'}\sigma^{\kappa\lambda}C\hat{S}^{duT}_{aa'}C\gamma_5] + \beta\gamma^\mu\gamma_5 S^u_{bb'}\sigma_{\kappa\lambda}C\hat{S}^{duT}_{aa'}C\gamma_5\hat{S}^{ud}_{cc'}\gamma^\nu\sigma^{\kappa\lambda} \\
&+ \beta\gamma^\mu\gamma_5\hat{S}^{ud}_{cc'}\gamma^\nu\sigma_{\kappa\lambda}\mathrm{Tr}[S^u_{aa'}\sigma^{\kappa\lambda}C\hat{S}^{duT}_{bb'}C\gamma_5] + \beta\gamma^\mu\gamma_5 S^u_{aa'}\sigma_{\kappa\lambda}C\hat{S}^{duT}_{bb'}C\gamma_5\hat{S}^{ud}_{cc'}\gamma^\nu\sigma^{\kappa\lambda}.
\end{aligned}$$

The physical interpretation of this proceeding is that the subdiagrams of two quark lines that produce the four quark condensates given in section 4.5 are replaced by a blob representing a variety of processes including pionic dynamics via the various quark operators that emerge from the nonlocal products $q^a_\alpha(x)\bar{q}^b_\beta(0)$.

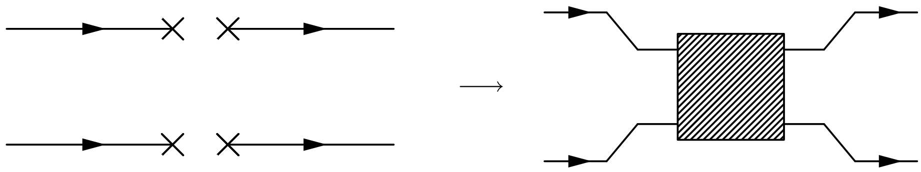

One first step in tackling the four-quark terms in the correlators is the simplification of the color structure making use of the $\delta_{cc'}$ factor provided by the one perturbative line in the four-quark condensate diagrams (the same calculation can be applied to any configuration of flavours):

$$
\begin{aligned}
\varepsilon_{abc}\varepsilon_{a'b'c}\langle u^a_\alpha \bar{u}^{a'}_\beta u^b_\gamma \bar{u}^{b'}_\delta\rangle =& (\delta_{aa'}\delta_{bb'} - \delta_{ab'}\delta_{ba'})\langle 0|u^a_\alpha \bar{u}^{a'}_\beta u^b_\gamma \bar{u}^{b'}_\delta|0\rangle \\
=& \sum_n \left(\langle 0|u^a_\alpha \bar{u}^a_\beta|n\rangle\langle n|u^b_\gamma \bar{u}^b_\delta|0\rangle - \langle 0|u^a_\alpha \bar{u}^b_\beta|n\rangle\langle n|u^b_\gamma \bar{u}^a_\delta|\rangle 0\right) \\
=& \sum_n \left(\langle 0|u_\alpha \bar{u}_\beta|n\rangle\langle n|u_\gamma \bar{u}_\delta|0\rangle - \frac{1}{9}\delta_{ab}\delta_{ab}\langle 0|u_\alpha \bar{u}_\beta|n\rangle\langle n|u_\gamma \bar{u}_\delta|0\rangle\right) \\
=& \frac{2}{3}\langle u^a_\alpha \bar{u}^a_\beta u^b_\gamma \bar{u}^b_\delta\rangle.
\end{aligned}
$$

Here, the irrelevant arguments x and 0 are suppressed and color is implicitly summed over in neighboring operators when no color indices are shown. Next, the Dirac structure of $q^a_\alpha(x)\bar{q}^b_\beta(0)$ is expanded making use of the covariant Talyor expansion (3.11). We restrict ourselves to the leading two terms of this expansion. The first yields

$$
q_\alpha(0)\bar{q}_\beta(0) = -\frac{1}{4}\left[\delta_{\alpha\beta}\;\bar{q}q - i\gamma^5_{\alpha\beta}\;\bar{q}i\gamma_5 q + \gamma^\mu_{\alpha\beta}\;\bar{q}\gamma_\mu q - (\gamma^\mu\gamma_5)_{\alpha\beta}\;\bar{q}\gamma_\mu\gamma_5 q + (\sigma^{\mu\nu})_{\alpha\beta}\;\bar{q}\sigma_{\mu\nu}q\right]. \tag{7.4}
$$

As expected, all different types of operators arise: scalar, pseudoscalar, vector, axialvector and tensor. All of the couple to certain pionic states. The next term in the expansion is given by.

$$
\begin{aligned}
x_\mu\left[D^\mu q_\alpha(x)\bar{q}_\beta(0)\right]_{x=0} =& -\frac{1}{4}\delta_{\alpha\beta}x_\mu\,\bar{q}D^\mu q + \frac{im_q}{16}(\not{x})_{\alpha\beta}\;\bar{q}q + \frac{m_q}{16}(\not{x}\gamma_5)_{\alpha\beta}\;\bar{q}i\gamma_5 q \\
&+ \frac{m_q}{12}x_\mu(\sigma^{\mu\nu})_{\alpha\beta}\;\bar{q}\gamma_\nu q - \frac{i}{12}x_\mu(\sigma^{\mu\nu})_{\alpha\beta}\,\bar{q}D_\nu q \\
&- \frac{m_q}{12}x_\mu(\sigma^{\mu\nu}\gamma_5)_{\alpha\beta}\;\bar{q}\gamma_\nu\gamma_5 q - \frac{i}{12}(\sigma^{\mu\nu}\gamma_5)_{\alpha\beta}\,\bar{q}\gamma_5 D_\nu q.
\end{aligned} \tag{7.5}
$$

Here, we have made use of the Dirac equation $i\not{D}q(x) = m_q q(x)$. Naturally, apart from the known operators, new operators involving the covariant derivative arise. Unfortunately, matrix elements of these operators are not well known, so they are discarded. Nevertheless, many of them vanish for symmetry reasons.

Now, the sum of eqs. (7.4) and (7.5) replaces $\langle u^a_\alpha(x)\bar{u}^a_\beta(0)u^b_\gamma(x)\bar{u}^b_\delta(0)\rangle$ and a complete set of intermediate states can be inserted retaining only states up to two pions [25]. For clarity, only the contribution from eq. (7.4) is shown.

$$
\begin{aligned}
\langle u^a_\alpha \bar{u}^a_\beta u^b_\gamma \bar{u}^b_\delta \rangle = & \sum_n \langle 0 | u^a_\alpha \bar{u}^a_\beta | n \rangle \langle n | u^b_\gamma \bar{u}^b_\delta | 0 \rangle \\
= & \frac{1}{16} \delta_{\alpha\beta} \delta_{\gamma\delta} \langle \bar{u} u \rangle^2 + \frac{1}{16} (\gamma_5)_{\alpha\beta} (\gamma_5)_{\gamma\delta} \int \frac{d^3 p}{(2\pi)^3 2 p_0} | \langle 0 | \bar{u} \gamma_5 u | \pi^0 (\mathbf{p}) \rangle |^2 \\
& + \frac{1}{16} (\gamma_5 \gamma_\mu)_{\alpha\beta} (\gamma_5 \gamma_\nu)_{\gamma\delta} \int \frac{d^3 p}{(2\pi)^3 2 p_0} \langle 0 | \bar{u} \gamma^\mu \gamma_5 u | \pi^0 (\mathbf{p}) \rangle \langle \pi^0 (\mathbf{p}) | \bar{u} \gamma^\nu \gamma_5 u | 0 \rangle \\
& + \frac{1}{16} \delta_{\alpha\beta} \delta_{\gamma\delta} \sum_{\text{charge}} \int \frac{d^3 p_1 d^3 p_2}{(2\pi)^6 4 p_{10} p_{20}} | \langle 0 | \bar{u} u | \pi(\mathbf{p}_1) \pi(\mathbf{p}_2) \rangle |^2 \\
& + \frac{1}{16} (\gamma_\mu)_{\alpha\beta} (\gamma_\nu)_{\gamma\delta} \sum_{\text{charge}} \int \frac{d^3 p_1 d^3 p_2}{(2\pi)^6 4 p_{10} p_{20}} \langle 0 | \bar{u} \gamma^\mu u | \pi(\mathbf{p}_1) \pi(\mathbf{p}_2) \rangle \langle \pi(\mathbf{p}_1) \pi(\mathbf{p}_2) | \bar{u} \gamma^\nu u | 0 \rangle \\
& + \frac{1}{16} (\sigma_{\kappa\lambda})_{\alpha\beta} (\sigma_{\mu\nu})_{\gamma\delta} \sum_{\text{charge}} \int \frac{d^3 p_1 d^3 p_2}{(2\pi)^6 4 p_{10} p_{20}} \langle 0 | \bar{u} \sigma^{\kappa\lambda} u | \pi(\mathbf{p}_1) \pi(\mathbf{p}_2) \rangle \cdot \qquad (7.6) \\
& \cdot \langle \pi(\mathbf{p}_1) \pi(\mathbf{p}_2) | \bar{u} \sigma^{\mu\nu} u | 0 \rangle .
\end{aligned}
$$

In the following, we list matrix elements needed for the evaluation of eq. (7.6) starting with the one-pion contributions. The pseudoscalar operators give

$$
\begin{aligned}
\langle 0 | \bar{u} i \gamma_5 u | \pi^0 \rangle &= - \langle 0 | \bar{d} i \gamma_5 d | \pi^0 \rangle = \frac{G_\pi}{2} \\
\langle 0 | \bar{d} i \gamma_5 u | \pi^+ \rangle &= \langle 0 | \bar{u} i \gamma_5 d | \pi^- \rangle = \frac{G_\pi}{\sqrt{2}}
\end{aligned} \qquad (7.7)
$$

where G_π is defined by

$$
G_\pi = - \frac{2}{f_\pi} \langle \bar{q} q \rangle .
$$

The axialvector operators yield

$$
\begin{aligned}
\langle 0 | \bar{u} \gamma^\mu \gamma_5 u | \pi^0 (p) \rangle &= - \langle 0 | \bar{d} \gamma^\mu \gamma_5 d | \pi^0 (p) \rangle = i f_\pi p^\mu \\
\langle 0 | \bar{d} \gamma^\mu \gamma_5 u | \pi^+ (p) \rangle &= \langle 0 | \bar{u} \gamma^\mu \gamma_5 d | \pi^- (p) \rangle = i \sqrt{2} f_\pi p^\mu .
\end{aligned} \qquad (7.8)
$$

Next, the two-pion states and the corresponding operators are considered. We define $s = (p_1 + p_2)^2$. For the scalar operators we note

$$
\begin{aligned}
\langle 0 | \bar{u} u | \pi^a \pi^b \rangle &= \langle 0 | \bar{d} d | \pi^a \pi^b \rangle = \frac{m_\pi^2}{2 m_q} \delta^{ab} \Gamma_\pi (s) = - \frac{\langle \bar{q} q \rangle}{f_\pi^2} \delta^{ab} \Gamma_\pi (s) \\
\langle 0 | \bar{u} d | \pi^a \pi^b \rangle &= \langle 0 | \bar{d} u | \pi^a \pi^b \rangle = 0
\end{aligned} \qquad (7.9)
$$

where $\Gamma_\pi(0)$ is the normalized pion scalar form factor: $\Gamma_\pi(0) = 1$. Summing over the relevant pionic states provides:

$$
\sum_{\pi^0 \pi^0, \pi^+ \pi^-} | \langle 0 | \bar{u} u | \pi(\mathbf{p}_1) \pi(\mathbf{p}_2) \rangle |^2 = \frac{3}{2} \left| \frac{m_\pi^2}{2 m_q} \Gamma_\pi (s) \right|^2 = \frac{3 \langle \bar{q} q \rangle^2}{2 f_\pi^4} | \Gamma_\pi (s) |^2 .
$$

The general vector-isovector matrix element is

$$\langle 0|\bar{q}\gamma^\mu \frac{\tau^a}{2} q|\pi^b(p_1)\pi^c(p_2)\rangle = i\varepsilon^{abc}(p_1 - p_2)^\mu F_\pi(s). \tag{7.10}$$

After summation over the possible charges, we get

$$\sum_{\text{charges}} \langle 0|\bar{u}\gamma^\mu u|\pi^b(p_1)\pi^c(p_2)\rangle\langle\pi^b(p_1)\pi^c(p_2)|\bar{u}\gamma^\nu u|0\rangle = (p_1 - p_2)^\mu(p_1 - p_2)^\nu |F_\pi(s)|^2.$$

Turning to the tensor operator the following definition is used

$$\langle 0|\bar{q}\sigma^{\mu\nu}(t^a/2)q|\pi^b(p_1)\pi^c(p_2)\rangle = i\varepsilon^{abc}(p_1^\mu p_2^\nu - p_2^\mu p_1^\nu)F_T(s).$$

Here, $F_T(s)$ is the pion tensor form factor, which is unfortunately not well known. When summation over charges is performed, one ends up with:

$$\sum_{\text{charges}} \langle 0|\bar{u}\sigma^\mu\nu u|\pi^b(p_1)\pi^c(p_2)\rangle\langle\pi^b(p_1)\pi^c(p_2)|\bar{u}\sigma^\alpha\beta u|0\rangle = (g^{\mu\alpha}g^{\nu\beta} - g^{\mu\beta}g^{\nu\alpha})\frac{s}{24}(s - 4m_\pi^2)|F_T(s)|^2$$

When putting things together [25], we finally arrive at a convenient representation of the general four-quark condensate (recall, that the contribution from $x_\mu[D_\mu q_\alpha(x)]_{x=0}$ is omitted).

$$\begin{aligned}\langle u_\alpha^a \bar{u}_\beta^a u_\gamma^b \bar{u}_\delta^b\rangle = \frac{\langle\bar{q}q\rangle^2}{16} \big[&\delta_{\alpha\beta}\delta_{\gamma\delta}\big(S_{(\bar{u}u)(\bar{u}u)}(\text{vac}) + S_{(\bar{u}u)(\bar{u}u)}(2\pi)\big) + (\gamma_5)_{\alpha\beta}(\gamma_5)_{\gamma\delta}P_{(\bar{u}u)(\bar{u}u)}(1\pi) \\ &+ (\gamma_\mu\gamma_5)_{\alpha\beta}(\gamma^\mu\gamma_5)_{\gamma\delta}A_{(\bar{u}u)(\bar{u}u)}(1\pi) + (\gamma_\mu)_{\alpha\beta}(\gamma^\mu)_{\gamma\delta}V_{(\bar{u}u)(\bar{u}u)}(2\pi) \\ &+(\sigma_{\mu\nu})_{\alpha\beta}(\sigma^{\mu\nu})_{\gamma\delta}T_{(\bar{u}u)(\bar{u}u)}(2\pi)\big]\end{aligned}$$

All pionic dynamics is absorbed in the parameters $S_{(\bar{u}u)(\bar{u}u)}$, $P_{(\bar{u}u)(\bar{u}u)}$, $A_{(\bar{u}u)(\bar{u}u)}$, $V_{(\bar{u}u)(\bar{u}u)}$, and $T_{(\bar{u}u)(\bar{u}u)}$. Analogous representations can be gained for $\langle u_\alpha^a \bar{u}_\beta^a d_\gamma^b \bar{d}_\delta^b\rangle$ and $\langle u_\alpha^a \bar{d}_\beta^a d_\gamma^b \bar{u}_\delta^b\rangle$. Some of the scalar parts are easily evaluated:

$$S_{(\bar{u}u)(\bar{u}u)}(\text{vac}) = S_{(\bar{u}u)(\bar{d}d)}(\text{vac}) = 1 \quad \text{and surely} \quad S_{(\bar{d}u)(\bar{u}d)}(\text{vac}) = 0.$$

It turns out that the axial vector contributions are suppressed by a factor of $(m_q/m_\pi)^2$ and can thus be neglected

$$A_{(\bar{u}u)(\bar{u}u)}(1\pi) = A_{(\bar{u}u)(\bar{d}d)}(1\pi) = A_{(\bar{d}u)(\bar{u}d)}(1\pi) \approx 0.$$

If we define

$$S_2 = S_{(\bar{u}u)(\bar{u}u)}(2\pi), \quad P_1 = P_{(\bar{u}u)(\bar{u}u)}(1\pi), \quad V_2 = V_{(\bar{u}u)(\bar{u}u)}(2\pi), \quad T_2 = T_{(\bar{u}u)(\bar{u}u)}(2\pi)$$

then from the equations (7.7) - (7.10) one can derive:

$$\begin{aligned}&S_{(\bar{u}u)(\bar{d}d)}(2\pi) = S_2, && P_{(\bar{u}u)(\bar{d}d)}(1\pi) = -P_1, && V_{(\bar{u}u)(\bar{d}d)}(2\pi) = -V_2, && T_{(\bar{u}u)(\bar{d}d)}(2\pi) = -T_2 \\ &S_{(\bar{u}d)(\bar{d}u)}(2\pi) = 0, && P_{(\bar{u}d)(\bar{d}u)}(1\pi) = 2P_1, && V_{(\bar{u}d)(\bar{d}u)}(2\pi) = 2V_2, && T_{(\bar{u}d)(\bar{d}u)}(2\pi) = 2T_2\end{aligned}$$

The results for P_1, S_2, V_2, and T_2 are given by [25]

$$P_1 = \frac{2}{(4\pi f_\pi)^2}\left[\Lambda^2 + m_\pi^2 \log\frac{m_\pi}{2\sqrt{e}\Lambda}\right] \tag{7.11}$$

$$S_2 = \frac{1}{(4\pi)^2}\int\limits_{m_\pi}^{\Lambda/2} d\omega_1 \int\limits_{m_\pi}^{\Lambda/2} d\omega_2 \int\limits_{s_-}^{s_+} ds\ \frac{6}{f_\pi^4}\ |\Gamma_\pi(s)|^2 \tag{7.12}$$

$$V_2 = \frac{1}{(4\pi)^4}\int\limits_{m_\pi}^{\Lambda/2} d\omega_1 \int\limits_{m_\pi}^{\Lambda/2} d\omega_2 \int\limits_{s_-}^{s_+} ds\ \frac{4m_\pi^2 - s}{\langle\bar{q}q\rangle^2}\ |F_\pi(s)|^2 \tag{7.13}$$

$$T_2 = \frac{1}{(4\pi)^4}\int\limits_{m_\pi}^{\Lambda/2} d\omega_1 \int\limits_{m_\pi}^{\Lambda/2} d\omega_2 \int\limits_{s_-}^{s_+} ds\ \frac{s(s-4m_\pi^2)}{6\langle\bar{q}q\rangle^2}\ |F_T(s)|^2 \tag{7.14}$$

where $\Lambda \approx 2\pi f_\pi$ is a momentum cutoff and

$$s_\pm = 2\left[m_\pi^2 + \omega_1\omega_2 \pm \sqrt{(\omega_1^2 - m_\pi^2)(\omega_2^2 - m_\pi^2)}\right].$$

As pointed out above, the tensor form factor is not well known. Hence, the tensor contribution T_2 has to be discarded. However, it is easily seen that $T_2 \geq 0$. The numerical values of S_2, P_1, and V_2 depend on the pion mass and the cutoff Λ and are depicted in figs 7.3, 7.4, and 7.5 for several values of Λ. As expected from eqs. (7.11) - (7.13), the dependence on the cutoff Λ strong for all three parameters. For a rather high cutoff $\Lambda = 3\pi f_\pi$, the one pion corrections P_1 exceed 1 and hence the vacuum contributions. After all, the existence of a value of Λ that reproduces the estimate on violation of factorization of section 7.1 would be preferable.

7.3 Results

7.3.1 Tensor Sum Rules

Using the formalism described in the previous section, we can now calculate the four-quark condensate contributions beyond factorization. The pionic corrections for the tensor sum rule (6.8) related to the structure $\gamma^\mu\gamma^\nu\not{q}$ are given by:

$$\begin{aligned}\langle\bar{q}q\rangle^2\left(1 - \frac{2m_q^2}{M^2}\right) \mapsto{}& (1+S_2)\langle\bar{q}q\rangle^2 - P_1\langle\bar{q}q\rangle^2 + 6(\beta+1)T_2\langle\bar{q}q\rangle^2 + \frac{2(\beta+3)}{3}V_2\langle\bar{q}q\rangle^2 \\ &+ \frac{m_q^2\langle\bar{q}q\rangle^2}{M^2}\left[-2(1+S_2) + \frac{2\beta+9}{3}P_1 - 6(\beta+1)T_2 - \frac{44(\beta+3)}{27}V_2\right]\end{aligned} \tag{7.15}$$

Concentrating on the low mass limit, we can immediately compare the κ as estimated in section 7.1 to the present theoretical result. Eq. (7.15) provides (T_2 being neglected)

$$\kappa(m_q \to 0) = 1 + S_2 - P_1 + \frac{2(\beta+3)}{3}V_2 \tag{7.16}$$

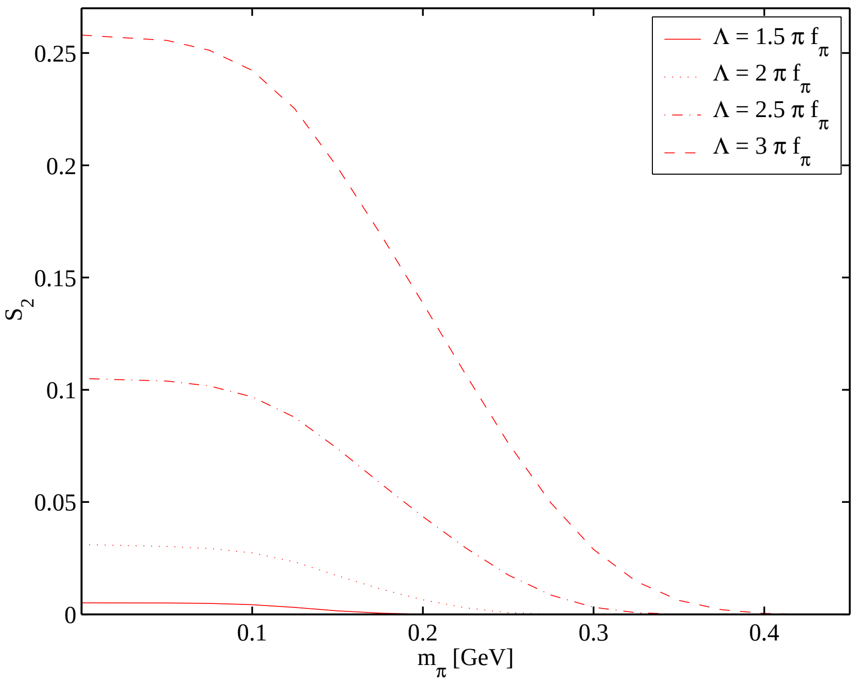

Figure 7.3: The scalar two pion correction $S_2(m_\pi)$ according to eq. (7.12)

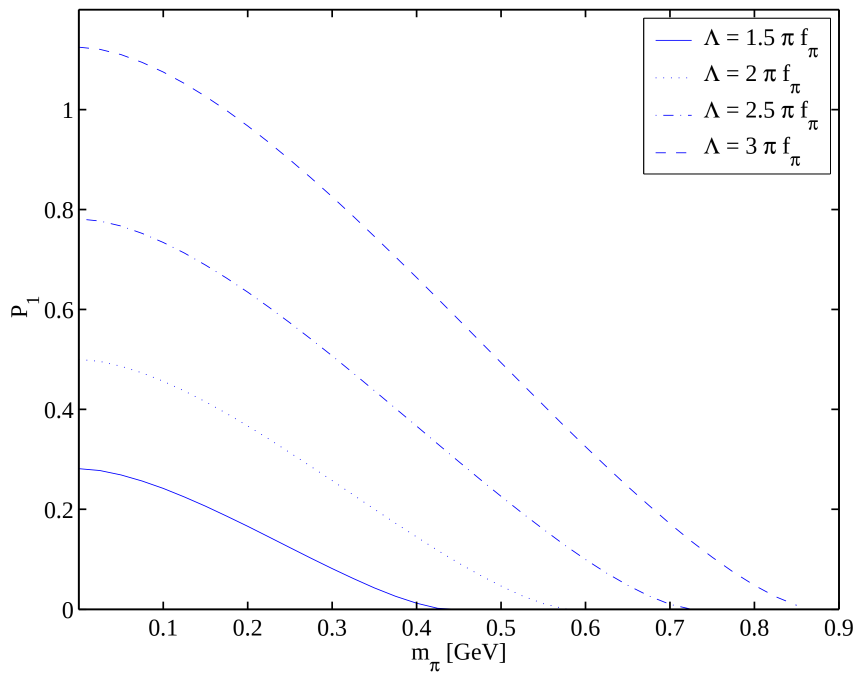

Figure 7.4: The pseudoscalar one pion correction $P_1(m_\pi)$ according to eq. (7.11)

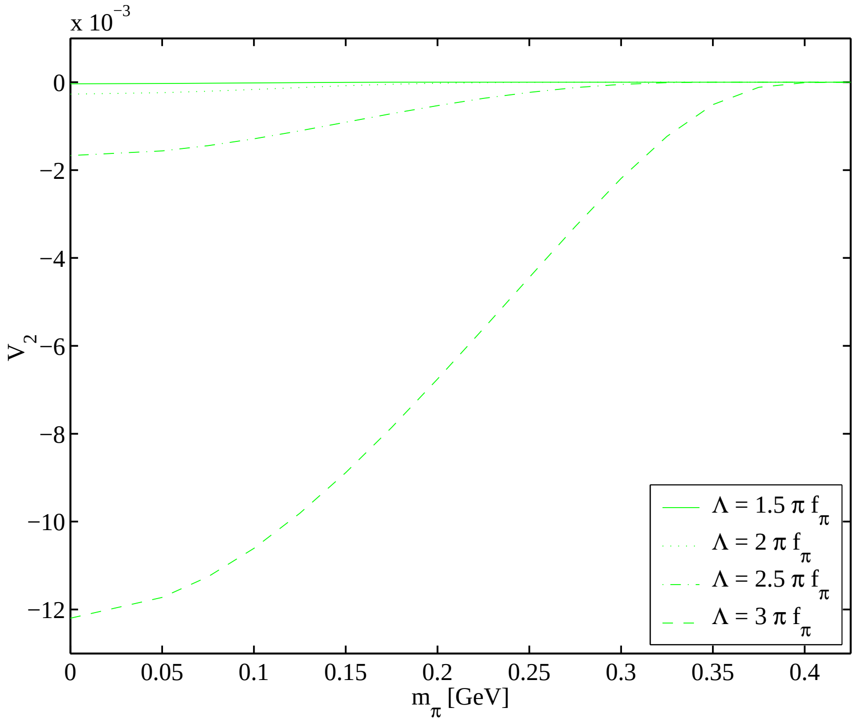

Figure 7.5: The vector two pion correction $V_2(m_\pi)$ according to eq. (7.13)

For different momentum cutoffs Λ we get:

$$\begin{aligned}
\Lambda = 1.5\pi f_\pi : &\quad \kappa(m_q \to 0) = 0.74 \\
\Lambda = 2.0\pi f_\pi : &\quad \kappa(m_q \to 0) = 0.54 \\
\Lambda = 2.5\pi f_\pi : &\quad \kappa(m_q \to 0) = 0.33 \\
\Lambda = 3.0\pi f_\pi : &\quad \kappa(m_q \to 0) = 0.12
\end{aligned}$$

Obviously, all of these values so far disagree with the estimate of $\kappa \approx 2$ from section 7.1, even the sign of the contributions beyond factorization is opposite there. This issue needs a more careful study.
For the four quark condensates in eq. (6.6) we obtain the following corrections

$$\begin{aligned}
m_q \langle \bar{q}q \rangle^2 \left(1 - \frac{5m_q^2}{2M^2}\right) \mapsto m_q \langle \bar{q}q \rangle^2 &\left[1 + S_2 - \frac{2(\beta+3)}{3} P_1 + \frac{14\beta+18}{3} V_2\right] \\
&+ \frac{m_q^3 \langle \bar{q}q \rangle^2}{M^2} \left[-\frac{5}{2}(1+S_2) + \frac{3\beta+9}{2} P_1 - \frac{4(67\beta+93)}{27} V_2\right] \qquad (7.17)
\end{aligned}$$

and finally in eq. (6.7) at $\gamma^\mu q^\nu \not{q}$ the inclusion of intermediate pion states provides

$$
\begin{aligned}
-\frac{m_q\langle\bar{q}q\rangle^2}{M^2}\left(4-\frac{5m_q^2}{M^2}\right) \mapsto \frac{m_q\langle\bar{q}q\rangle^2}{M^2}&\left[-4(1+S_2)+\frac{8(\beta+3)}{3}P_1-\frac{8(27\beta+37)}{9}V_2\right]\\
&+\frac{m_q^3\langle\bar{q}q\rangle^2}{M^4}\left[5(1+S_2)-\frac{8\beta+27}{3}P_1+\frac{8(67\beta+93)}{27}V_2\right] \qquad (7.18)
\end{aligned}
$$

As a result of missing knowledge of Λ and the resulting large uncertainties of the parameters S_2, P_1, and V_2, we refrain from performing an analysis of $M_{\mathrm{N}}(m_\pi^2)$. Regarding figs. 7.3 - 7.5, we conclude that for large pion masses factorization is a reasonable approximation for our purposes. So the results of chapter 5 and 6 do not have to be challenged.

7.3.2 Spin-1/2 Sum Rules

As we saw in chapter 5, the four-quark condensate term in eq. (5.5) is rather important for the quality of the agreement between sum rules and Lattice data. The two four-quark terms in this equation are corrected in the following form

$$
\begin{aligned}
\frac{7-2\beta-5\beta^2}{6}\langle\bar{q}q\rangle^2 \mapsto \langle\bar{q}q\rangle^2&\left[(7-2\beta-5\beta^2)\left(\frac{1+S_2}{6}+\frac{P_1}{2}\right)+72(1-\beta^2)T_2\right.\\
&\left.-\frac{35+22\beta+35\beta^2}{3}V_2\right]\\
-\frac{41-22\beta-55\beta^2}{24}\frac{m_q^2\langle\bar{q}q\rangle^2}{M^2} \mapsto \frac{m_q^2\langle\bar{q}q\rangle^2}{M^2}&\left[-\frac{41-22\beta-55\beta^2}{24}(1+S_2)-\frac{23-10\beta-25\beta^2}{8}P_1\right.\\
&\left.+72(\beta^2-1)T_2+\frac{91+42\beta+143\beta^2}{9}V_2\right] \qquad (7.19)
\end{aligned}
$$

Contrary to the tensor sum rule (6.8), the one pion correction $\sim P_1$ has the same sign as the scalar parts. In fig. 7.6 we show the coefficient κ as defined by

$$
\frac{7-2\beta-5\beta^2}{6}\kappa \equiv (7-2\beta-5\beta^2)\left(\frac{1+S_2}{6}+\frac{P_1}{2}\right)-\frac{35+22\beta+35\beta^2}{3}V_2 \qquad (7.20)
$$

for several cutoff values Λ. As before, the tensor contribution is discarded. At $m_\pi = 0.4\,\mathrm{GeV}$ which is the lower bound of the accessible pion mass range of the spin-1/2 sum rules, the different cutoffs predict values for κ between 1 and 3. This seems to support the results from fig. 5.14, at least at the lower pion mass region.

For the sake of completeness, we list the corrections for the spin-1/2 sum rule at the structure $\mathbb{1}$

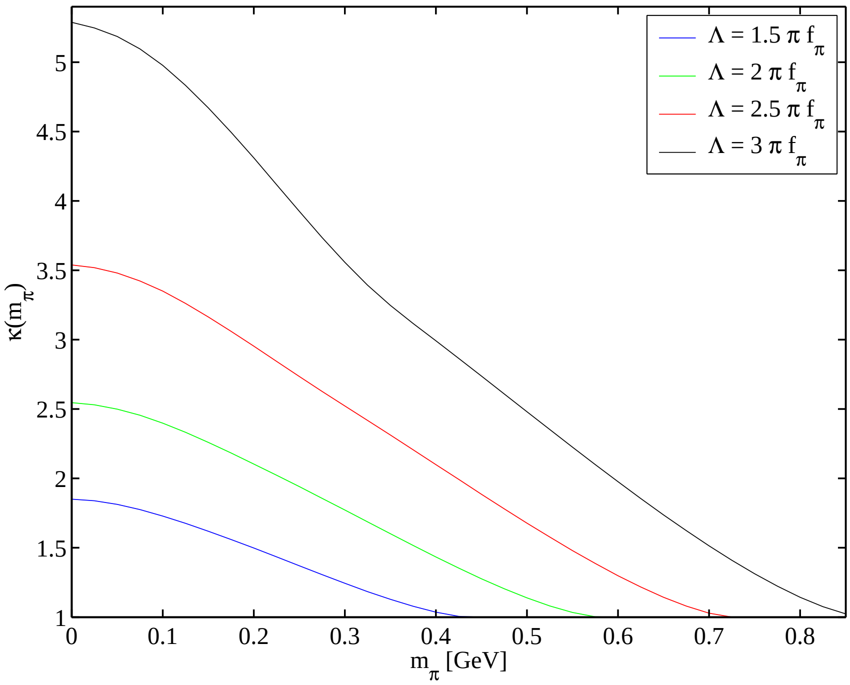

Figure 7.6: κ for the leading four quark term in the $\not{q}$-sum rule (5.5)

(5.4)

$$\frac{2(2+2\beta+5\beta^2)}{3} m_q \langle\bar{q}q\rangle^2 \mapsto m_q \langle\bar{q}q\rangle^2 \Bigg[\frac{2(2+2\beta+5\beta^2)}{3}(1+S_2) + \frac{5+2\beta+5\beta^2}{2} P_1 + 12(7+6\beta+7\beta^2)T_2 - \frac{2(11+8\beta-19\beta^2)}{3} V_2\Bigg] \tag{7.21}$$

$$-\frac{5+2\beta+5\beta^2}{2}\frac{m_q^3\langle\bar{q}q\rangle^2}{M^2} \mapsto \frac{m_q^3\langle\bar{q}q\rangle^2}{M^2}\Bigg[-\frac{(5+2\beta+5\beta^2)}{2}(1+S_2+P_1) - 12(7+6\beta+7\beta^2)T_2 + \frac{26+12\beta-38\beta^2}{3} V_2\Bigg] \tag{7.22}$$

We have listed the results, eqs. (7.15) – (7.22), for completeness and in order to make them available for further investigastions. Further detailed studies are obviously necessary to address the non-factorization issue of the four-quark condensates.

Chapter 8

Summary and Conclusion

In this work, we have extended well known QCD sum rules for the nucleon to higher, i.e. unphysical, quark (resp. pion) masses and compared the results to Lattice QCD determinations of the nucleon mass. The agreement is quite satisfactory. Another issue was the estimate of contributions to the four-quark condensates beyond factorization, which has been an open question for a long time.
The determination of the pion mass dependence of the nucleon mass was performed with two largely independent approaches, which differed by the choice of the interpolating field for the nucleon. On the one hand, the usual, frequently used spin-1/2 conerns the expansion of kinematics in the quark sector. All processes involving propagation of a quark were expanded up to order 3 in the quark mass.
Both mentioned approaches yield feasible results in certain quark mass regions. The advantage of the spin-1/2 case lies in the higher quark mass region, whereas no analysis was possible for quark masses between 0 and $\approx 50\,\mathrm{MeV}$. This failure for low quark masses arises from large continuum contaminations of one of the two sum rules. Another problem is posed by the huge perturbative corrections for the purely perturbative term in the same sum rule. Nevertheless, the trend produced by this sum rule is not extremely off the Lattice predictions.
The primary advantage of the tensor interpolating field is that it provides three sum rules due to the richer Lorentz structure. One of them is rather useless for an analysis and has to be eliminated immediately. The remaining two equations do not suffer from difficulties in the low quark mass region, quite the contrary. The analysis works out fine at the physical point and up to quark masses around $100\,\mathrm{MeV}$. Beyond $100\,\mathrm{MeV}$, several criteria of the analysis (like the agreement of two sum rules and OPE convergence) could not be fulfilled anymore. The errorband obtained from this part of the analysis basically includes all of the Lattice data points. The new combined analysis of the one reliable spin-1/2 sum rule and the two preferable tensor sum rules leads to an almost perfect agreement of QCD sum rules and Lattice QCD predictions. While this success should not be overinterpreted because of remaining sources of uncertainty, it should nevertheless be noted that all results show stability with respect to the input QCD condensate values. This is an important point.
Standard questions raised in the area of QCD sum rules include the uncertainties in the QCD condensates, OPE convergence and factorization. The first point is successfully handled in our method of analysis. We found that the output uncertainty of the nucleon mass is smaller than the input uncertainties. OPE convergence is not a big problem since the Borel regimes move towards

higher energies when increasing the quark mass. Last, the influence of factorization is minimized by disregarding the sum rules involving four-quark condensates as leading terms in the analysis. One open questions concerns the quark mass dependence of QCD condensates. In the analysis we kept the condensates constant for all quark masses, which is simply the idea of an expansion around the physical point where the quark mass is small. This seems meaningful in view of the persisting large uncertainties in the condensate values.

The last part of the thesis was dedicated to a more detailed study of the four-quark condensates. As pointed out above, these terms still pose a problem. We tried to extract information on these quantities from the discarded tensor sum rule by inserting the macroscopical spectral parameters obtained from more reliable sum rules. Next, we explicitly calculated the contributions from intermediate pion states in the four quark operators to all sum rules. So far, the comparison of phenomenological and theoretical results is not successful. It is at this point where forthcoming studies must still yield further substantial progress.

Appendix A

Special Fourier Integrals

A.1 The Wick Rotation.

In calculating the sum rules for the analysis of the m_q dependence of M_N we encounter integrals of the following type

$$\int d^4x \; e^{iq\cdot x} \frac{\log^k(-m_q^2 x^2)}{(x^2)^n}$$

where the logarithms come from the expansion of all parts involving kinematics in the background field propagator (see chapter 4). In fact we have to be more careful and shift the poles away from the real x_0 axis in order to get well-defined integrals. So we are actually concerned about Fourier integrals of the following kind

$$\int d^4x \; e^{iq\cdot x} \frac{\log^k(-m_q^2(x^2 - i\varepsilon))}{(x^2 - i\varepsilon)^n} \tag{A.1}$$

The signs of the infinitesimal shifts (contrary to those appearing in momentum space) appear in accord with the massless scalar propagator (see [26]) and come from the different signs of the Fourier transform and its inverse in the exponential factors $\exp \pm iq\cdot x$:

$$\Delta(x) = \frac{i}{4\pi^2} \frac{1}{x^2 - i\varepsilon}$$

For simplicity the calculation of the Fourier transforms (A.1) is performed in Euclidean space. The translation to Minkowski space will then involve a Wick rotation which we will adress now. In the case of an integral without a logarithm ($k = 0$ in (A.1)) the Wick rotation is not much of a problem, the poles are simply shifted away from the real x_0-axis (see fig. A.1), and the Wick rotation $x_4 = -ix_0$ is well defined, since the contours do not cross a pole. Now considering the case $k \neq 0$ we have to be careful since we now face branch cuts in the x_0-plane, too. Fortunately, the branch cuts are also shifted in a way, that the Wick rotation can easily be carried through, which can be seen in figure A.2. Now the translation from Minkowski to Euclidean space reads as follows. The first step of course being an analytic continuation of the integrand to the whole

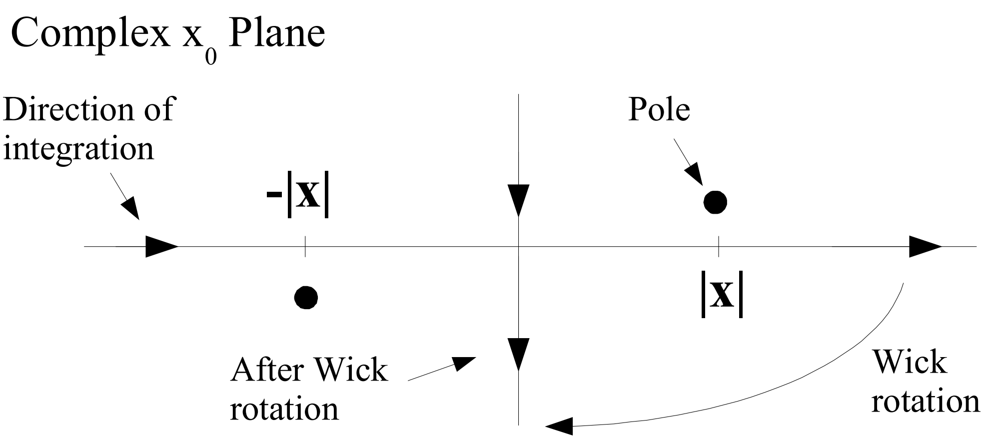

Figure A.1: Positions of poles and the Wick Rotation in the Fourier integral of eq. (A.1) with $k = 0$. The Wick rotation is possible since the contour does not cross a pole during the rotation.

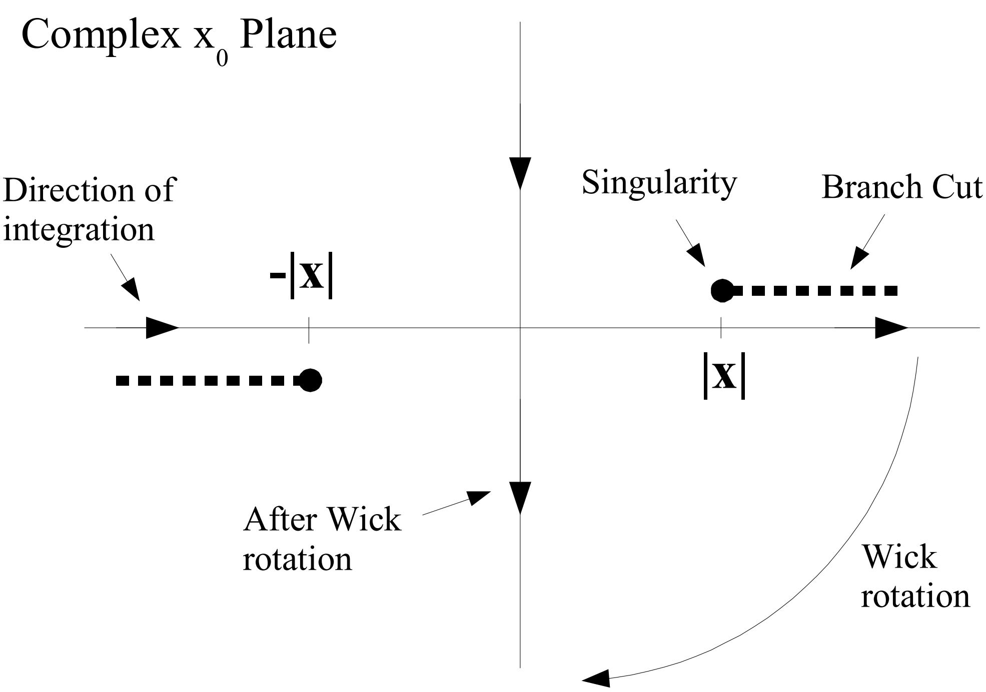

Figure A.2: Positions of poles and branch cuts and the Wick Rotation in the calculation of Fourier transforms (A.1). The Wick rotation does neither cross a pole nor the branch cuts.

x_0-plane (we skip the infinitesimal shifts for clarity)

$$\begin{aligned}\int d^4x\; e^{iq\cdot x}\frac{\log(-m_q^2 x^2)}{(x^2)^n} &= \int d^3\mathbf{x}\int dx_0\; e^{i(q_0x_0-\mathbf{q}\cdot\mathbf{x})}\;\frac{\log(-m_q^2(x_0^2-\mathbf{x}^2))}{(x_0^2-\mathbf{x}^2)^n}\\ &= -i\int d^3\mathbf{x}\int dx_4\; e^{-i(q_4x_4+\mathbf{q}\cdot\mathbf{x})}\;\frac{\log(m_q^2(x_4^2+\mathbf{x}^2))}{(-x_4^2-\mathbf{x}^2)^n}\\ &= -i\int d^4\bar{x}\; e^{-i\bar{q}\cdot\bar{x}}\;\frac{\log(m_q^2\bar{x}^2)}{(-\bar{x}^2)^n}\end{aligned}$$

Here we have set $q_4 = iq_0$, so the integral was also analytically continued to the whole q_0-plane. By rotational invariance of the integral we can skip the minus in the exponential. From this calculation we can conclude some simple translation rules for the step from Minkowski to Euclidean, and - even more important - vice versa: we have to multiply the euclidean result by $-i$ and substitute $\bar{q}^2 \mapsto -q^2$ respectively $\bar{x}^2 \mapsto -x^2$.

A.2 Evaluation of Integrals in Euclidean Space

A.2.1 The Master Formula

Starting point for the calculation of Minkowski integrals of the type

$$\int d^4x\; e^{iq\cdot x}\;\frac{\log^m(-\Lambda^2x^2)}{(x^2)^n}$$

is the Euclidean formula

$$\int \frac{d^4\bar{x}}{4\pi^2}\frac{e^{i\bar{q}\cdot\bar{x}}}{|\bar{x}|^s} = 2^{2-s}|\bar{q}|^{s-4}\frac{\Gamma(2-s/2)}{\Gamma(s/2)}, \qquad 3/2 < s < 4 \tag{A.2}$$

As we will see, differentiating this equation with respect to s creates logarithms under the integral on the right hand side, the left hand side of the resulting equation then gives the Fourier transform. We shall proof eq. (A.2) in the following. Starting with a transformation to spherical coordinates ($r = |\bar{x}|$) and carrying out the two trivial angle integrations we get

$$\begin{aligned}\int \frac{d^4\bar{x}}{4\pi^2}\frac{e^{i\bar{q}\cdot\bar{x}}}{|\bar{x}|^s} &= \frac{1}{\pi}\int_0^\infty dr\; r^{3-s}\int_{-1}^1 d\cos\theta\;\;\sin\theta\; e^{ir|\bar{q}|\cos\theta}\\ (z\equiv\cos\theta,\; y\equiv r|\bar{q}|)\quad &= \frac{1}{\pi}|\bar{q}|^{s-4}\int_0^\infty dy\; y^{3-s}\int_{-1}^1 dz\sqrt{1-z^2}e^{izy}\\ &= |\bar{q}|^{s-4}\int_0^\infty dy y^{2-s}J_1(y) = 2^{2-s}|\bar{q}|^{s-4}\frac{\Gamma(2-s/2)}{\Gamma(s/2)}\end{aligned}$$

Now the integrals with logarithms can be calculated by simply differentiating eq. (A.2) with respect to s, and setting $s = 2n$, since

$$\frac{d^m}{ds^m}\frac{1}{|\bar{x}|^s} = (-1)^m\frac{\log^m(|\bar{x}|)}{|\bar{x}|^s}$$

A.2.2 No Logarithm.

A first application of eq. (A.2) is to calculate the Fourier transforms of $(x^2)^{-n},\ n = 1, 2, 3, \ldots$. Inserting $s = 2$ gives

$$\int d^4\bar{x} \frac{e^{i\bar{q}\cdot\bar{x}}}{\bar{x}^2} = \frac{4\pi^2}{\bar{q}^2}$$

For $s \geq 4$ the situation is slightly more difficult, since the Gamma function has singularities in 0 and all negative integers. We therefore regularize the corresponding expressions on the right hand side of (A.2) by setting $s = 4 + \varepsilon$ (resp. $6 + \varepsilon$, $8 + \varepsilon$, and $10 + \varepsilon$), and expanding around $\varepsilon = 0$. The results are still singular in ε but these singularities accompagny polynomials in $\bar{q}^2$ in the form of negative powers ($\varepsilon^{-1}, \varepsilon^{-2}$, etc.) and are thus most easily identified. For example, for $s = 6 + \varepsilon$ an expansion of the r.h.s. of eq. (A.2) gives:

$$\frac{\pi^2}{4}\bar{q}^2 \log\frac{|\bar{q}|}{2} + \frac{\pi^2}{4}\bar{q}^2\left[\frac{1}{\varepsilon} + \gamma_E - \frac{5}{4}\right]$$

Since polynomials vanish after the Borel Transform, which is to be applied after the Fourier transform the polynomials with divergent coefficients are discarded. In summary, the results without the insignificant polynomials in Q^2 are given by:

$$\begin{aligned}
\int d^4\bar{x}\ \frac{e^{i\bar{q}\cdot\bar{x}}}{(\bar{x}^2)^2} &= -2\pi^2 \log|\bar{q}| + \ldots \\
\int d^4\bar{x}\ \frac{e^{i\bar{q}\cdot\bar{x}}}{(\bar{x}^2)^3} &= \frac{\pi^2}{4}\bar{q}^2 \log|\bar{q}| + \ldots \\
\int d^4\bar{x}\ \frac{e^{i\bar{q}\cdot\bar{x}}}{(\bar{x}^2)^4} &= -\frac{\pi^2}{96}\bar{q}^4 \log|\bar{q}| + \ldots \\
\int d^4\bar{x}\ \frac{e^{i\bar{q}\cdot\bar{x}}}{(\bar{x}^2)^5} &= \frac{\pi^2}{4608}\bar{q}^6 \log|\bar{q}| + \ldots
\end{aligned}$$

Translation to Minkowski space is performed in the way described in section A.1. The results are found in the formulary (Appendix C).

A.2.3 One Logarithm.

Differentiating eq. (A.2) once with respect to s yields:

$$\int d^4\bar{x}\ e^{i\bar{q}\cdot\bar{x}}\frac{\log(|\bar{x}|)}{|\bar{x}|^s} = 2^{3-s}\pi^2|\bar{q}|^{s-4}\left[\psi\Big(2 - \frac{s}{2}\Big) + \psi\Big(\frac{s}{2}\Big) - 2\log\frac{|\bar{q}|}{2}\right]$$

Both the $\psi-$ and the $\Gamma-$Function are divergent for $s = 0$, however the singularities cancel each other, so a series in $s = \varepsilon$ yields a nice result. For $s = 2$ all participants are finite and for $s = 4, 6, 8, \ldots$ the integrals give infinite constants. Again setting $s = 4 + \varepsilon$ (resp. $6 + \varepsilon$ and $8 + \varepsilon$) and expanding in ε yield results where these infinite constants can easily be identified and removed. Infinite constants and polynomials are still ofno relevance for our calculations since the

Borel Transformation annihilates them. The results of this procedure are:

$$\int d^4\bar{x}\; e^{i\bar{q}\cdot\bar{x}}\;\log|\bar{x}| = -\frac{8\pi^2}{(\bar{q}^2)^2}$$
$$\int d^4\bar{x}\; e^{i\bar{q}\cdot\bar{x}}\;\frac{\log|\bar{x}|}{\bar{x}^2} = -\frac{4\pi^2}{\bar{q}^2}\left[\log\frac{|\bar{q}|}{2}+\gamma_E\right]$$
$$\int d^4\bar{x}\; e^{i\bar{q}\cdot\bar{x}}\;\frac{\log|\bar{x}|}{(\bar{x}^2)^2} = \pi^2\left[\log\frac{|\bar{q}|}{2}+\gamma_E-\frac{1}{2}\right]^2$$
$$\int d^4\bar{x}\; e^{i\bar{q}\cdot\bar{x}}\;\frac{\log|\bar{x}|}{(\bar{x}^2)^3} = -\frac{\pi^2\bar{q}^2}{8}\left[\log\frac{|\bar{q}|}{2}+\gamma_E-\frac{5}{4}\right]^2$$
$$\int d^4\bar{x}\; e^{i\bar{q}\cdot\bar{x}}\;\frac{\log|\bar{x}|}{(\bar{x}^2)^4} = \frac{\pi^2(\bar{q}^2)^2}{192}\left[\log\frac{|\bar{q}|}{2}+\gamma_E-\frac{5}{3}\right]^2$$

After the translation to Minkowski space the scale Λ in the logarithms $\log(-\Lambda^2x^2)$ is easily included making use of the standard formulas derived in section A.2.2.

A.2.4 Two Logarithms.

The second derivative of eq. (A.2) with respect to s is:

$$\int d^4x\; e^{i\bar{q}\cdot\bar{x}}\frac{\log^2(|\bar{x}|)}{|\bar{x}|^s} = \frac{\Gamma(2-s/2)|\bar{q}|^{s-4}\pi^2}{2^{s-2}\Gamma(s/2)}\Bigg[\log^2\frac{|\bar{q}|}{2}+\left[\psi\Big(2-\frac{s}{2}\Big)+\psi\Big(\frac{s}{2}\Big)\right]^2$$
$$-4\log\frac{|\bar{q}|}{2}\left[\psi\Big(2-\frac{s}{2}\Big)+\psi\Big(\frac{s}{2}\Big)\right]+\psi'\Big(2-\frac{s}{2}\Big)-\psi'\Big(\frac{s}{2}\Big)\Bigg]$$

As above, certain terms seperately diverge for $s=0$, the singularities however cancel each other. For $s=2$ the expression is well defined and for $s=4$ the situation is the same as in the case of one logarithm, the same steps are applied. This procedure yields the following formulas:

$$\int d^4\bar{x}\; e^{i\bar{q}\cdot\bar{x}}\log^2|\bar{x}| = \frac{16\pi^2}{(\bar{q}^2)^2}\left[\log\frac{|\bar{q}|}{2}+\gamma_E-\frac{1}{2}\right]$$
$$\int d^4\bar{x}\; e^{i\bar{q}\cdot\bar{x}}\frac{\log^2|\bar{x}|}{\bar{x}^2} = \frac{4\pi^2}{\bar{q}^2}\left[\log\frac{|\bar{q}|}{2}+\gamma_E\right]$$
$$\int d^4\bar{x}\; e^{i\bar{q}\cdot\bar{x}}\frac{\log^2|\bar{x}|}{(\bar{x}^2)^2} = \pi^2\Bigg[\left[\log\frac{|\bar{q}|}{2}+\gamma_E\right]^2-\left[\log\frac{|q|}{2}+\gamma_E\right]$$
$$-\frac{2}{3}\left[\log\frac{|\bar{q}|}{2}+\gamma_E\right]^3+\frac{3-2\zeta(3)}{6}\Bigg]$$

Appendix B

The Borel Transform

The Borel transform is defined by the following limiting process:

$$\mathcal{B}\big[f(Q^2)\big] = \lim_{\substack{Q^2,n\to\infty \\ Q^2/n=M^2}} \frac{(Q^2)^{n+1}}{n!}\left(\frac{-d}{dQ^2}\right)^n f(Q^2)$$

From this definition it becomes obvious that polynomials are mapped to zero: $\mathcal{B}[(Q^2)^k] = 0, \forall k$. A somewhat more convenient form for explicit calculations is given by

$$\mathcal{B}\big[f(Q^2)\big] = \lim_{n\to\infty} \frac{M^{2(n+1)}}{(n-1)!}\left(\frac{-d}{dM^2}\right)^n f(nM^2)$$

B.1 Simple Borel Transforms

Well known formulas that are extensively used throughout the QCD sum rule literature are [5]

$$\mathcal{B}\Big[(Q^2)^k\Big] = 0 \qquad\qquad \mathcal{B}\left[\frac{1}{(Q^2)^k}\right] = \frac{1}{(k-1)!}\left(\frac{1}{M^2}\right)^{k-1}$$

$$\mathcal{B}\Big[(Q^2)^k\log(Q^2/\Lambda^2)\Big] = k!(-M^2)^{k+1} \qquad\qquad \mathcal{B}\left[\frac{1}{s+Q^2}\right] = e^{-s/M^2}$$

As for the Fourier transform, the presence of logarithms coming from the mass expansion of kinematical pieces of the background field propagator leads to new types of functions that have to be Borel transformed. These include the following functions, where c is some arbitrary constant.

$$\begin{aligned}
W_1(Q^2) &= Q^2\left[\frac{1}{2}\log\frac{Q^2}{\Lambda^2} + \gamma_E + c\right]^2 \\
W_2(Q^2) &= \left[\frac{1}{2}\log\frac{Q^2}{\Lambda^2} + \gamma_E + c\right]^2 \\
W_3(Q^2) &= \frac{1}{(Q^2)^m}\left[\frac{1}{2}\log\frac{Q^2}{\Lambda^2} + \gamma_E + c\right]
\end{aligned}$$

An especially useful identity for this purpose is

$$\left(-\frac{d}{dx}\right)^n \frac{\log x}{x^m} = \frac{(m+n-1)!}{(m-1)!}\left[\frac{\log x}{x^{m+n}} - \frac{1}{x^{m+n}}\sum_{k=m}^{m+n-1}\frac{1}{k}\right]$$

which is easily proven by induction along n for fixed m. We shall calculate the Borel transform of $W_3(Q^2)$ explicitely, W_1 and W_2 can be treated very similarly.

$$\begin{aligned}
&\mathcal{B}\left[\frac{1}{(Q^2)^m}\left[\frac{1}{2}\log\frac{Q^2}{\Lambda^2}+\gamma_E+c\right]\right] = \\
&= \lim_{n\to\infty}\frac{M^{2(n+1)}}{(n-1)!}\left(\frac{-d}{dM^2}\right)^n\frac{1}{n^m M^{2m}}\left[\frac{1}{2}\log\frac{nM^2}{\Lambda^2}+\gamma_E+c\right]\\
(X\equiv M^2)\quad &= \lim_{n\to\infty}\frac{X^{n+1}}{(n-1)!n^m}\left(\frac{-d}{dX}\right)^n\frac{1}{X^m}\left[\frac{1}{2}\log X+\frac{1}{2}\log n-\frac{1}{2}\log\Lambda^2+\gamma_E+c\right]\\
&= \lim_{n\to\infty}\frac{X^{n+1}}{(n-1)!n^m}\left[\frac{(m+n-1)!}{2(m-1)!}\left[\frac{\log X}{X^{m+n}}-\frac{1}{X^{m+n}}\sum_{k=m}^{m+n-1}\frac{1}{k}\right]\right.\\
&\qquad\left.+\frac{(m+n-1)!}{(m-1)!}\frac{\frac{1}{2}\log n-\frac{1}{2}\log\Lambda^2+\gamma_E+c}{X^{m+n}}\right]\\
&= \frac{1}{2(m-1)!X^{m-1}}\lim_{n\to\infty}\left[\log\frac{X}{\Lambda^2}+\log n-\sum_{k=m}^{m+n-1}\frac{1}{k}+2\gamma_E+2c\right]\\
&= \frac{1}{2(m-1)!(M^2)^{m-1}}\left[\log\frac{M^2}{\Lambda^2}+\psi(m)+2\gamma_E+2c\right]
\end{aligned}$$

Here we observe the same factorial suppression factors as in the case without logarithms:

$$\mathcal{B}\left[\frac{1}{(Q^2)^m}\right] = \frac{1}{(m-1)!}\frac{1}{(M^2)^{m-1}}$$

The results for W_1 and W_2 are

$$\begin{aligned}
\mathcal{B}\left[Q^2\left[\frac{1}{2}\log\frac{Q^2}{\Lambda^2}+\gamma_E+c\right]^2\right] &= \frac{M^4}{2}\left[\log\frac{M^2}{\Lambda^2}+\gamma_E+2c+1\right]\\
\mathcal{B}\left[\left[\frac{1}{2}\log\frac{Q^2}{\Lambda^2}+\gamma_E+c\right]^2\right] &= -\frac{M^2}{2}\left[\log\frac{M^2}{\Lambda^2}+\gamma_E+2c\right]
\end{aligned}$$

B.2 Derivation of the Master Formula

For the calculation of Borel transforms of functions of the type $\log^k(Q^2/\Lambda^2)/(Q^2)^m$ the following Master Formula is of great benefit.

$$\mathcal{B}[F(Q,s)] \equiv \mathcal{B}\left[Q^{s-4}2^{2-s}\frac{\Gamma(2-s/2)}{\Gamma(s/2)}\right] = \frac{2^{2-s}M^{s-2}}{\Gamma(s/2)} \qquad \text{(B.1)}$$

The derivation is as follows.

$$\begin{aligned}
\mathcal{B}[Q^{s-4}] &= \lim_{n\to\infty} \frac{M^{2(n+1)}}{(n-1)!}\left(\frac{-d}{dM^2}\right)^n (nM^2)^{s/2-2} \\
&= \lim_{n\to\infty} \frac{M^{2(n+1)}}{(n-1)!} n^{s/2-2} M^{s-4-2n}(2-s/2)(3-s/2)\cdot\ldots\cdot(n+1-s/2) \\
&= M^{s-2}\lim_{n\to\infty} \frac{n^{s/2-2}}{(n-1)!}(2-s/2)(3-s/2)\cdot\ldots\cdot(n-1+(2-s/2)) \\
(a\equiv 2-s/2) \quad &= M^{s-2}\lim_{n\to\infty} \frac{a(a+1)\cdot\ldots\cdot(n-1+a)}{n^a(n-1)!} \\
&= M^{s-2}\lim_{n\to\infty} \frac{a(a+1)\cdot\ldots\cdot(n+a)}{(n+1)^a n!} \\
&= M^{s-2}\frac{1}{\Gamma(2-s/2)}
\end{aligned}$$

Here we have used a well known representation of the Γ-function:

$$\Gamma(z) = \lim_{n\to\infty} \frac{(n+1)!n^z}{z(z+1)\cdot\ldots\cdot(z+n)}$$

and shifted the index $n-1\mapsto n$ in the fifth line.

B.3 Borel Transform of $\log^2 Q^2/(Q^2)^m$-Functions

At first sight, a canonical way of doing the Borel transform of $\log^2(Q^2/\Lambda^2)/(Q^2)^m$ functions would be to differentiate eq. (B.1) twice with respect to s and set s to the value desired. Unfortunately, for $s=0$ and $s=-2$ when expanding around these values in s the contribution from $\log^2 Q^2$ on the left hand side vanishes. So one has to go one step further and use linear combinations of the function itself up to the third derivative of $F(Q,s)$. The rest of the procedure resembles the one for the Fourier transform explained in sections A.2.3 and A.2.4. In the following we set $c\equiv\log 2-\gamma_E$.

$$\begin{aligned}
\frac{\log^2 Q^2}{Q^2} &= \left[\frac{\partial^2}{\partial s^2}+2c\frac{\partial}{\partial s}+c^2\right]F(Q,s)\bigg|_{s=2} \\
\frac{\log^2 Q^2}{Q^4} &= \left[\frac{1}{6}\frac{\partial^3}{\partial s^3}+\frac{2c+1}{4}\frac{\partial^2}{\partial s^2}+\frac{2c^2+2c+1}{4}\frac{\partial}{\partial s}\right]F(Q,s)\bigg|_{s=0} \\
\frac{\log^2 Q^2}{Q^6} &= \left[-\frac{1}{48}\frac{\partial^3}{\partial s^3}-\frac{4c+5}{64}\frac{\partial^2}{\partial s^2}-\frac{8c^2+20c+17}{128}\frac{\partial}{\partial s}\right]F(Q,s)\bigg|_{s=-2}
\end{aligned}$$

The results are:

$$\begin{aligned}
\mathcal{B}\left[\frac{\log^2 Q^2}{Q^2}\right] &= \frac{1}{4}(\log M^2-\gamma_E)^2-\frac{\pi^2}{24} \\
\mathcal{B}\left[\frac{\log^2 Q^2}{Q^4}\right] &= \frac{1}{4M^2}\left[(\log M^2-\gamma_E+1)^2+1-\frac{\pi^2}{6}\right] \\
\mathcal{B}\left[\frac{\log^2 Q^2}{Q^6}\right] &= \frac{1}{8M^4}\left[(\log M^2-\gamma_E+3/2)^2+\frac{5}{4}-\frac{\pi^2}{6}\right]
\end{aligned}$$

Of course, all logarithms of Q^2 arising from the Fourier transform carry a scale Λ^2. This constant scale can easily be included by the use of known formulas. In principle, this procedure allows the calculation of functions of the type $\log^k(Q^2)/(Q^2)^m$ for arbitrary k and m. Borel transforms of frequently arising polynomials of second order in $\log Q^2/\Lambda^2$ are listed in Appendix C.

Appendix C

Useful Formulae

C.1 Fourier Transforms

The formulas in this section give Fourier Integrals needed throughout the calculation of Sum Rules. Their derivation is given in Appendix A. Polynomials with possibly infinite constants are not displayed, for they are irrelevant due to the subsequent Borel transform. The integrals are sorted by the number of logarithms and the Lorentz structure.

Integrals without a logarithm

Scalar Integrals.

$$\int d^4x \; e^{iq\cdot x}\frac{1}{x^2} = \frac{4\pi^2 i}{Q^2}$$

$$\int d^4x \; e^{iq\cdot x}\frac{1}{(x^2)^2} = i\pi^2 \log Q^2$$

$$\int d^4x \; e^{iq\cdot x}\frac{1}{(x^2)^3} = \frac{i\pi^2}{8}Q^2 \log Q^2$$

$$\int d^4x \; e^{iq\cdot x}\frac{1}{(x^2)^4} = \frac{i\pi^2}{2^6 3}(Q^2)^2 \log Q^2$$

$$\int d^4x \; e^{iq\cdot x}\frac{1}{(x^2)^5} = \frac{i\pi^2}{2^6 3!4!}(Q^2)^3 \log Q^2$$

Vector Integrals.

$$\int d^4x\ e^{iq\cdot x}\frac{\not{x}}{x^2} = \frac{8\pi^2}{(Q^2)^2}\ \not{q}$$

$$\int d^4x\ e^{iq\cdot x}\frac{\not{x}}{(x^2)^2} = \frac{-2\pi^2}{Q^2}\ \not{q}$$

$$\int d^4x\ e^{iq\cdot x}\frac{\not{x}}{(x^2)^3} = -\frac{\pi^2}{4}\log Q^2\ \not{q}$$

$$\int d^4x\ e^{iq\cdot x}\frac{\not{x}}{(x^2)^4} = -\frac{\pi^2}{2^4 3}Q^2\log Q^2\ \not{q}$$

$$\int d^4x\ e^{iq\cdot x}\frac{\not{x}}{(x^2)^5} = -\frac{\pi^2}{2^5 3!4!}(Q^2)^2(3\log Q^2+1)\ \not{q}$$

Tensor Integrals.

$$\int d^4x\ e^{iq\cdot x}\frac{x_\mu x_\nu}{x^2} = -\frac{32\pi^2 i}{(Q^2)^3}q_\mu q_\nu - \frac{8\pi^2 i}{(Q^2)^2}g_{\mu\nu}$$

$$\int d^4x\ e^{iq\cdot x}\frac{x_\mu x_\nu}{(x^2)^2} = \frac{4\pi^2 i}{(Q^2)^2}q_\mu q_\nu + \frac{2\pi^2 i}{Q^2}g_{\mu\nu}$$

$$\int d^4x\ e^{iq\cdot x}\frac{x_\mu x_\nu}{(x^2)^3} = -\frac{\pi^2 i}{2Q^2}q_\mu q_\nu + \frac{\pi^2 i}{4}\log Q^2 g_{\mu\nu}$$

$$\int d^4x\ e^{iq\cdot x}\frac{x_\mu x_\nu}{(x^2)^4} = -\frac{\pi^2 i}{24}(\log Q^2+1)q_\mu q_\nu + \frac{\pi^2 i}{48}Q^2\log Q^2 g_{\mu\nu}$$

$$\int d^4x\ e^{iq\cdot x}\frac{x_\mu x_\nu}{(x^2)^5} = -\frac{\pi^2 i}{2^4 4!}Q^2(\log Q^2+5/6) - \frac{\pi^2}{2^5 3!4!}(Q^2)^2(3\log Q^2+1)g_{\mu\nu}$$

Integrals with one logarithm

Throughout this section Λ is an arbitrary scale.

Scalar Integrals.

$$\int d^4x\ e^{iq\cdot x}\log(-\Lambda^2x^2)=\frac{16\pi^2 i}{(Q^2)^2}$$

$$\int d^4x\ e^{iq\cdot x}\frac{\log(-\Lambda^2x^2)}{x^2}=-\frac{8\pi^2 i}{Q^2}\left[\frac{1}{2}\log\left(\frac{Q^2}{4\Lambda^2}\right)+\gamma_E\right]$$

$$\int d^4x\ e^{iq\cdot x}\frac{\log(-\Lambda^2x^2)}{(x^2)^2}=-2\pi^2 i\left[\frac{1}{2}\log\left(\frac{Q^2}{4\Lambda^2}\right)+\gamma_E-\frac{1}{2}\right]^2$$

$$\int d^4x\ e^{iq\cdot x}\frac{\log(-\Lambda^2x^2)}{(x^2)^3}=-\frac{\pi^2 i}{4}Q^2\left[\frac{1}{2}\log\left(\frac{Q^2}{4\Lambda^2}\right)+\gamma_E-\frac{5}{4}\right]^2$$

$$\int d^4x\ e^{iq\cdot x}\frac{\log(-\Lambda^2x^2)}{(x^2)^4}=-\frac{\pi^2 i}{96}(Q^2)^2\left[\frac{1}{2}\log\left(\frac{Q^2}{4\Lambda^2}\right)+\gamma_E-\frac{5}{3}\right]^2$$

Vector Integrals.

$$\int d^4x\ e^{iq\cdot x}\log(-\Lambda^2x^2)\ \not{x}=\frac{64\pi^2}{(Q^2)^3}\ \not{q}$$

$$\int d^4x\ e^{iq\cdot x}\frac{\log(-\Lambda^2x^2)}{x^2}\ \not{x}=\frac{8\pi^2}{(Q^2)^2}\left[1-2\gamma_E-\log\left(\frac{Q^2}{4\Lambda^2}\right)\right]\not{q}$$

$$\int d^4x\ e^{iq\cdot x}\frac{\log(-\Lambda^2x^2)}{(x^2)^2}\ \not{x}=\frac{4\pi^2}{Q^2}\left[\frac{1}{2}\log\frac{Q^2}{4\Lambda^2}+\gamma_E-\frac{1}{2}\right]\not{q}$$

$$\int d^4x\ e^{iq\cdot x}\frac{\log(-\Lambda^2x^2)}{(x^2)^3}\ \not{x}=\frac{\pi^2}{2}\left[\left[\frac{1}{2}\log\frac{Q^2}{4\Lambda^2}+\gamma_E-\frac{5}{4}\right]^2+\left[\frac{1}{2}\log\frac{Q^2}{4\Lambda^2}+\gamma_E-\frac{5}{4}\right]\right]\not{q}$$

$$\int d^4x\ e^{iq\cdot x}\frac{\log(-\Lambda^2x^2)}{(x^2)^4}\ \not{x}=\frac{\pi^2}{48}Q^2\left[\left[\frac{1}{2}\log\frac{Q^2}{4\Lambda^2}+\gamma_E-\frac{5}{3}\right]+2\left[\frac{1}{2}\log\frac{Q^2}{4\Lambda^2}+\gamma_E-\frac{5}{3}\right]^2\right]\ \not{q}$$

Tensor Integrals.

$$\int d^4x\ e^{iq\cdot x}\log(-\Lambda^2x^2)\ x_\mu x_\nu = -\frac{384\pi^2 i}{(Q^2)^4}q_\mu q_\nu - \frac{64\pi^2 i}{(Q^2)^3}g_{\mu\nu}$$

$$\int d^4x\ e^{iq\cdot x}\frac{\log(-\Lambda^2x^2)}{x^2}\ x_\mu x_\nu = \frac{64\pi^2 i}{(Q^2)^3}\left[\frac{1}{2}\log\frac{Q^2}{4\Lambda^2}+\gamma_E-\frac{3}{4}\right]q_\mu q_\nu - \frac{8\pi^2 i}{(Q^2)^2}\left[1-2\gamma_E-\log\frac{Q^2}{4\Lambda^2}\right]g_{\mu\nu}$$

$$\int d^4x\ e^{iq\cdot x}\frac{\log(-\Lambda^2x^2)}{(x^2)^2}\ x_\mu x_\nu = -\frac{8\pi^2 i}{(Q^2)^2}\left[\frac{1}{2}\log\frac{Q^2}{4\Lambda^2}+\gamma_E-1\right]q_\mu q_\nu - \frac{4\pi^2 i}{Q^2}\left[\frac{1}{2}\log\frac{Q^2}{4\Lambda^2}+\gamma_E-\frac{1}{2}\right]g_{\mu\nu}$$

$$\int d^4x\ e^{iq\cdot x}\frac{\log(-\Lambda^2x^2)}{(x^2)^3}\ x_\mu x_\nu = \frac{\pi^2 i}{Q^2}\left[\frac{1}{2}\log\frac{Q^2}{4\Lambda^2}+\gamma_E-\frac{3}{4}\right]q_\mu q_\nu - \frac{\pi^2 i}{2}\left[\left[\frac{1}{2}\log\frac{Q^2}{4\Lambda^2}+\gamma_E-\frac{5}{4}\right]^2+\left[\frac{1}{2}\log\frac{Q^2}{4\Lambda^2}+\gamma_E-\frac{5}{4}\right]\right]g_{\mu\nu}$$

$$\int d^4x\ e^{iq\cdot x}\frac{\log(-\Lambda^2x^2)}{(x^2)^4}\ x_\mu x_\nu = \frac{\pi^2 i}{24}\left[3\left[\frac{1}{2}\log\frac{Q^2}{4\Lambda^2}+\gamma_E-\frac{3}{2}\right]+2\left[\frac{1}{2}\log\frac{Q^2}{4\Lambda^2}+\gamma_E-\frac{5}{3}\right]^2\right]q_\mu q_\nu - \frac{\pi^2 i}{48}Q^2\left[\left[\frac{1}{2}\log\frac{Q^2}{4\Lambda^2}+\gamma_E-\frac{5}{3}\right]+2\left[\frac{1}{2}\log\frac{Q^2}{4\Lambda^2}+\gamma_E-\frac{5}{3}\right]^2\right]g_{\mu\nu}$$

Integrals with two logarithms

Throughout this section Λ_1 and Λ_2 are arbitrary scales.

Scalar Integrals.

$$\int d^4x\ e^{iq\cdot x}\log(-\Lambda_1^2x^2)\log(-\Lambda_2^2x^2) = -\frac{64\pi^2 i}{Q^4}\left[\frac{1}{4}\log\frac{Q^2}{4\Lambda_1^2}+\frac{1}{4}\log\frac{Q^2}{4\Lambda_2^2}+\gamma_E-\frac{1}{2}\right]$$

$$\int d^4x\ e^{iq\cdot x}\frac{\log(-\Lambda_1^2x^2)\log(-\Lambda_2^2x^2)}{x^2} = \frac{16\pi^2 i}{Q^2}\left[\frac{1}{2}\log\frac{Q^2}{4\Lambda_1^2}+\gamma_E\right]\left[\frac{1}{2}\log\frac{Q^2}{4\Lambda_2^2}+\gamma_E\right]$$

$$\int d^4x\ e^{iq\cdot x}\frac{\log(-\Lambda_1^2x^2)\log(-\Lambda_2^2x^2)}{(x^2)^2} =$$
$$-4\pi^2 i\left\{\left[\frac{1}{2}\log\frac{Q^2}{4\Lambda_1^2}+\gamma_E\right]\left[\frac{1}{2}\log\frac{Q^2}{4\Lambda_2^2}+\gamma_E\right]-\left[\frac{1}{4}\log\frac{Q^2}{4\Lambda_1^2}+\frac{1}{4}\log\frac{Q^2}{4\Lambda_2^2}+\gamma_E\right]\right.$$
$$\left.-\frac{2}{3}\left[\frac{1}{2}\log\frac{Q^2}{4\Lambda_1^2}+\gamma_E\right]\left[\frac{1}{2}\log\frac{Q^2}{4\Lambda_2^2}+\gamma_E\right]\left[\frac{1}{4}\log\frac{Q^2}{4\Lambda_1^2}+\frac{1}{4}\log\frac{Q^2}{4\Lambda_2^2}+\gamma_E\right]+\frac{3-2\zeta(3)}{6}\right\}$$

Vector Integrals.

$$\int d^4x\ e^{iq\cdot x}\log(-\Lambda_1^2x^2)\log(-\Lambda_2^2x^2)\ \not{x} = -\frac{256\pi^2}{(Q^2)^3}\left[\frac{1}{4}\log\frac{Q^2}{4\Lambda_1^2}+\frac{1}{4}\log\frac{Q^2}{4\Lambda_1^2}+\gamma_E-\frac{3}{4}\right]\ \not{q}$$

$$\int d^4x\ e^{iq\cdot x}\frac{\log(-\Lambda_1^2x^2)\log(-\Lambda_2^2x^2)}{x^2}\ \not{x} = \frac{32\pi^2}{(Q^2)^2}\left\{\left[\frac{1}{2}\log\frac{Q^2}{4\Lambda_1^2}+\gamma_E\right]\left[\frac{1}{2}\log\frac{Q^2}{4\Lambda_2^2}+\gamma_E\right]\right.$$
$$\left.-\left[\frac{1}{4}\log\frac{Q^2}{4\Lambda_1^2}+\frac{1}{4}\log\frac{Q^2}{4\Lambda_2^2}+\gamma_E\right]\right\}\ \not{q}$$

$$\int d^4x\ e^{iq\cdot x}\frac{\log(-\Lambda_1^2x^2)\log(-\Lambda_2^2x^2)}{(x^2)^2}\ \not{x} = \frac{8\pi^2}{Q^2}\left\{\left[\frac{1}{4}\log\frac{Q^2}{4\Lambda_1^2}+\frac{1}{4}\log\frac{Q^2}{4\Lambda_1^2}+\gamma_E\right]\right.$$
$$\left.-\left[\frac{1}{2}\log\frac{Q^2}{4\Lambda_1^2}+\gamma_E\right]\left[\frac{1}{2}\log\frac{Q^2}{4\Lambda_2^2}+\gamma_E\right]-\frac{1}{2}\right\}\ \not{q}$$

Tensor Integrals.

$$\int d^4x\ e^{iq\cdot x}\log(-\Lambda_1^2x^2)\log(-\Lambda_2^2x^2)\ x_\mu x_\nu =$$
$$\frac{1536\pi^2 i}{(Q^2)^4}\left[\frac{1}{4}\log\frac{Q^2}{4\Lambda_1^2}+\frac{1}{4}\log\frac{Q^2}{4\Lambda_2^2}+\gamma_E-\frac{11}{12}\right]q_\mu q_\nu$$
$$+\frac{256\pi^2 i}{(Q^2)^3}\left[\frac{1}{4}\log\frac{Q^2}{4\Lambda_1^2}+\frac{1}{4}\log\frac{Q^2}{4\Lambda_2^2}+\gamma_E-\frac{3}{4}\right]g_{\mu\nu}$$

$$\int d^4x\ e^{iq\cdot x}\frac{\log(-\Lambda_1^2x^2)\log(-\Lambda_2^2x^2)}{x^2}\ x_\mu x_\nu = -\frac{16\pi^2 i}{(Q^2)^3}\left[8\left[\frac{1}{2}\log\frac{Q^2}{4\Lambda_1^2}+\gamma_E\right]\left[\frac{1}{2}\log\frac{Q^2}{4\Lambda_2^2}+\gamma_E\right]\right.$$
$$\left.-12\left[\frac{1}{4}\log\frac{Q^2}{4\Lambda_1^2}+\frac{1}{4}\log\frac{Q^2}{4\Lambda_2^2}+\gamma_E-\frac{1}{6}\right]\right]q_\mu q_\nu$$
$$-\frac{32\pi^2 i}{(Q^2)^2}\left[\left[\frac{1}{2}\log\frac{Q^2}{4\Lambda_1^2}+\gamma_E\right]\left[\frac{1}{2}\log\frac{Q^2}{4\Lambda_2^2}+\gamma_E\right]\right.$$
$$\left.-\left[\frac{1}{4}\log\frac{Q^2}{4\Lambda_1^2}+\frac{1}{4}\log\frac{Q^2}{4\Lambda_2^2}+\gamma_E\right]\right]g_{\mu\nu}$$

$$\int d^4x\; e^{iq\cdot x}\frac{\log(-\Lambda_1^2 x^2)\log(-\Lambda_2^2 x^2)}{(x^2)^2}\; x_\mu x_\nu =$$

$$\begin{aligned} &\frac{16\pi^2 i}{(Q^2)^2}\left[\frac{1}{2}\log\frac{Q^2}{4\Lambda_1^2}+\gamma_E-1\right]\left[\frac{1}{2}\log\frac{Q^2}{4\Lambda_2^2}+\gamma_E-1\right] q_\mu q_\nu \\ &-\frac{8\pi^2 i}{Q^2}\left[\left[\frac{1}{4}\log\frac{Q^2}{4\Lambda_1^2}+\frac{1}{4}\log\frac{Q^2}{4\Lambda_2^2}+\gamma_E\right]\right. \\ &\qquad\left.-\left[\frac{1}{2}\log\frac{Q^2}{4\Lambda_1^2}+\gamma_E\right]\left[\frac{1}{2}\log\frac{Q^2}{4\Lambda_2^2}+\gamma_E\right]-\frac{1}{2}\right] g_{\mu\nu} \end{aligned}$$

C.2 Borel Transforms

Basic Transforms

$$\mathcal{B}\left[\frac{1}{Q^2}\right] = 1 \qquad \mathcal{B}\left[\log(Q^2/\Lambda^2)\right] = -M^2$$

$$\mathcal{B}\left[\frac{1}{(Q^2)^2}\right] = \frac{1}{M^2} \qquad \mathcal{B}\left[Q^2\log(Q^2/\Lambda^2)\right] = M^4$$

$$\mathcal{B}\left[\frac{1}{(Q^2)^3}\right] = \frac{1}{2M^4} \qquad \mathcal{B}\left[(Q^2)^2\log(Q^2/\Lambda^2)\right] = -2M^6$$

$$\mathcal{B}\left[\frac{1}{(Q^2)^k}\right] = \frac{1}{(k-1)!}\left(\frac{1}{M^2}\right)^{k-1} \qquad \mathcal{B}\left[(Q^2)^k\log(Q^2/\Lambda^2)\right] = k!(-M^2)^{k+1}$$

Terms with $(Q^2)^{-n}\log Q^2$

$$\mathcal{B}\left[\frac{1}{Q^2}\left[\frac{1}{2}\log\left(\frac{Q^2}{4\Lambda^2}\right) + \gamma_E\right]\right] = \frac{1}{2}\left[\log\left(\frac{M^2}{4\Lambda^2}\right) + \gamma_E\right]$$

$$\mathcal{B}\left[\frac{1}{Q^2}\left[\frac{1}{2}\log\left(\frac{Q^2}{4\Lambda^2}\right) + \gamma_E - \frac{1}{2}\right]\right] = \frac{1}{2}\left[\log\left(\frac{M^2}{4\Lambda^2}\right) + \gamma_E - 1\right]$$

$$\mathcal{B}\left[\frac{1}{Q^2}\left[\frac{1}{2}\log\frac{Q^2}{\Lambda^2} + \gamma_E + c\right]\right] = \frac{1}{2}\left[\log\frac{M^2}{\Lambda^2} + \gamma_E + 2c\right]$$

$$\mathcal{B}\left[\frac{1}{(Q^2)^2}\left[1 - 2\gamma_E - \log\left(\frac{Q^2}{4\Lambda^2}\right)\right]\right] = -\frac{1}{M^2}\left[\log\left(\frac{M^2}{4\Lambda^2}\right) + \gamma_E\right]$$

$$\mathcal{B}\left[\frac{1}{(Q^2)^2}\left[\frac{1}{2}\log\frac{Q^2}{\Lambda^2} + \gamma_E + c\right]\right] = \frac{1}{2M^2}\left[\log\frac{M^2}{\Lambda^2} + \gamma_E + 1 + 2c\right]$$

$$\mathcal{B}\left[\frac{1}{(Q^2)^3}\left[\frac{1}{2}\log\frac{Q^2}{\Lambda^2} + \gamma_E + c\right]\right] = \frac{1}{4M^4}\left[\log\frac{M^2}{\Lambda^2} + \gamma_E + \frac{3}{2} + 2c\right]$$

$$\mathcal{B}\left[\frac{1}{(Q^2)^4}\left[\frac{1}{2}\log\frac{Q^2}{\Lambda^2} + \gamma_E + c\right]\right] = \frac{1}{12M^6}\left[\log\frac{M^2}{\Lambda^2} + \gamma_E + \frac{11}{6} + 2c\right]$$

$$\mathcal{B}\left[\frac{1}{(Q^2)^m}\left[\frac{1}{2}\log\frac{Q^2}{\Lambda^2} + \gamma_E + c\right]\right] = \frac{1}{2(m-1)!M^{2m-2}}\left[\log\frac{M^2}{\Lambda^2} + \psi(m) + 2\gamma_E + 2c\right]$$

Terms with $\log^2 Q^2$

$$\mathcal{B}\left[Q^2\left[\frac{1}{2}\log\left(\frac{Q^2}{4\Lambda^2}\right)+\gamma_E-\frac{5}{4}\right]^2\right]=\frac{M^4}{2}\left[\log\left(\frac{M^2}{4\Lambda^2}\right)+\gamma_E-\frac{3}{2}\right]$$

$$\mathcal{B}\left[\left[\frac{1}{2}\log\left(\frac{Q^2}{4\Lambda^2}\right)+\gamma_E-\frac{1}{2}\right]^2\right]=-\frac{M^2}{2}\left[\log\left(\frac{M^2}{4\Lambda^2}\right)+\gamma_E-1\right]$$

$$\mathcal{B}\left[\frac{1}{Q^2}\left[\frac{1}{2}\log\frac{Q^2}{4\Lambda_1^2}+\gamma_E\right]\cdot\left[\frac{1}{2}\log\frac{Q^2}{4\Lambda_2^2}+\gamma_E\right]\right]=$$
$$\frac{1}{4}\left[\log\frac{M^2}{4\Lambda_1^2}+\gamma_E\right]\left[\log\frac{M^2}{4\Lambda_2^2}+\gamma_E\right]-\frac{\pi^2}{24}$$

$$\mathcal{B}\left[\frac{1}{(Q^2)^2}\left[\frac{1}{2}\log\frac{Q^2}{4\Lambda_1^2}+\gamma_E\right]\cdot\left[\frac{1}{2}\log\frac{Q^2}{4\Lambda_2^2}+\gamma_E\right]\right]=$$
$$\frac{1}{4M^2}\left[\left[\log\frac{M^2}{4\Lambda_1^2}+\gamma_E+1\right]\left[\log\frac{M^2}{4\Lambda_2^2}+\gamma_E+1\right]+1-\frac{\pi^2}{6}\right]$$

$$\mathcal{B}\left[\frac{1}{(Q^2)^3}\left[\frac{1}{2}\log\frac{Q^2}{4\Lambda_1^2}+\gamma_E\right]\cdot\left[\frac{1}{2}\log\frac{Q^2}{4\Lambda_2^2}+\gamma_E\right]\right]=$$
$$\frac{1}{8M^4}\left[\left[\log\frac{M^2}{4\Lambda_1^2}+\gamma_E+\frac{3}{2}\right]\left[\log\frac{M^2}{4\Lambda_2^2}+\gamma_E+\frac{3}{2}\right]+\frac{5}{4}-\frac{\pi^2}{6}\right]$$

Bibliography

[1] M. Procura, T.R. Hemmert, and W. Weise, *Phys. Rev.* **D69** (2004) 034505.

[2] B. Orth, Th. Lippert, and K. Schilling, [arXiv:hep-lat/0503016].

[3] M. Gell-Mann, R. Oakes, and B. Renner, *Phys. Rev.* **122** (1968) 2195.

[4] M.A. Shifman, A.I. Vainshtein, and V.I. Zakharov, *Nucl. Phys.* **B147** (1979) 385 ; **B147** (1979) 448.

[5] B.L. Ioffe, *Nucl. Phys.* **B188** (1981) 317, **B191** (1981) 591(E).

[6] T.D. Cohen, R.J. Furnstahl, D.K. Griegel, and X. Jin, *Prog. Part. Nucl. Phys.* **35** (1995) 221.

[7] V.A. Fock, Sow. Phys. **12** (1937) 404.

[8] J. Schwinger, *Particles, Sources and Fields, Vol. 1*, Addison-Wesley, Reading (1970).

[9] C. Cronström, *Phys. Lett.* **90B** (1980) 267.

[10] L.J. Reinders, H. Rubinstein, and S. Yazaki, *Phys. Rep.* **127** (1985) 1.

[11] V.A. Novikov, M.A. Shifman, A.I. Vainshtein, and V.I. Zakharov, *Fortschr. Phys.* **32** (1984) 585.

[12] K.G. Wilson, *Phys. Rev.* **179** (1969) 1499.

[13] V.A. Novikov, M.A. Shifman, A.I. Vainshtein, and V.I. Zakharov, *Nucl. Phys.* **B174** (1980) 378.

[14] V.A. Novikov, M.A. Shifman, A.I. Vainshtein, and V.I. Zakharov, *Nucl. Phys.* **B249** (1985) 445.

[15] B.L. Ioffe, *Phys. Atom. Nucl.* **66** (2003) 30.

[16] A. Ali Khan et al., *Nucl. Phys.* **B689** (2004) 175.

[17] K.-C. Yang, W.Y.P. Hwang, E.M. Henley, and L.S. Kisslinger, *Phys. Rev.* **D47** (1993) 3001.

[18] D.B. Leinweber, *Ann. Phys.* **198** (1990) 203.

[19] D.B. Leinweber, *Ann. Phys.* **254** (1997) 328.

[20] M. L"uscher, Plenary talk given at the 23rd International Symposium on Lattice Field Theory, Dublin 25-30 July 2005, [arXiv:hep-lat/0509152].

[21] Y. Chung, H.G. Dosch, M. Kremer, and D. Schall, *Nucl. Phys.* **B197** (1982) 55.

[22] D.B. Leinweber, *Phys. Rev.* **D51** (1995) 6383.

[23] H. Shiomi and T. Hatsuda, *Nucl. Phys.* **A594** (1995) 294, [arXiv:hep-ph/9504354].

[24] V.M. Belyaev and B.L. Ioffe, *Sov. Phys. JETP* **57** (1983) 716.

[25] N. Kaiser, private communication/ to be published.

[26] T.-P. Cheng and L.-F. Li, *Gauge theory of elementary particle physics*, Oxford University Press, Oxford (1984).

Danksagung

An dieser Stelle möchte ich einigen Menschen danken, die, jeder auf seine Art, zu dieser Diplomarbeit beigetragen haben:

- Prof. Dr. Wolfram Weise, der mir die Möglichkeit gab, an seinem Lehrstuhl die Diplomarbeit zu schreiben, und mir dieses interessante Thema vorschlug. Er zeigte stets großes Interesse an meiner Arbeit. Unsere Besprechungen waren immer hilfreich und motivierend.
- Norbert Kaiser für ausführliche Diskussionen über physikalische Fragen und seine maßgebliche Unterstützung bei mathematischen Problemen.
- Bernhard Musch und Simon Rößner für die gute Atmosphäre in unserem Büro und interessante Gespräche physikalischer und nicht-physikalischer Art.
- Allen T39-Mitarbeitern für das lockere und nette Klima am Lehrstuhl, insbesondere bei Aktivitäten außerhalb der Universität.
- Meinen Freunden und Kollegen in München und zuhause für die nötigen Ablenkungen diverser Art.
- Mein größter Dank gilt natürlich meinen Eltern Anneliese und Helmut Langwallner und meiner Schwester Verena, die mich während des ganzen Studiums und besonders in den anstrengenden Zeiten unterstützt haben.